working paper
2604

Legacies of the Reformation: How Religious Identity Shapes Political Preferences in Germany

Erik Ortiz-Covarrubias

March 2026

CENTRO DE ESTUDIOS
MONETARIOS Y FINANCIEROS
Casado del Alisal 5, 28014 Madrid, Spain
www.cemfi.es

CEMFI Working Paper No. 2604
March 2026

Legacies of the Reformation: How Religious Identity Shapes Political Preferences in Germany

Abstract

This paper investigates whether Germany's historical confessional divides continue to influence contemporary political behavior by exploiting persistent geographic variation between historically Catholic and Protestant areas through a Geographic Regression Discontinuity Design. Integrating historical and geospatial data with modern electoral and census sources, I find that historically Catholic municipalities show systematically higher support for the center-right Union parties than their counterparts in every federal election from 1990 to 2025, while historically Protestant areas are more likely to support parties on the center-left and left of the political spectrum. Individual-level survey data covering all Federal Elections since 1953 and the German General Social Survey provide suggestive evidence that voting behavior is shaped by confessional affiliation.

JEL Codes: O18, N33, D72, Z12, Z13.

Keywords: Religion, voting behavior, Germany.

Erik Ortiz-Covarrubias
CEMFI
erik.ortiz@cemfi.edu.es

Acknowledgement

I am indebted to Dean Yang and Giulia Buccione for continued guidance on this project. I am thankful to Agustín Casas, Tom Zohar, Daniela Solá, Dmitry Arkhangelsky and Manuel Arellano for helpful comments and discussions. I am especially grateful to Luciana Manuali for valuable comments. I also thank participants at seminars at CEMFI for their insights. I gratefully acknowledge financial support from the Maria de Maeztu Unit of Excellence CEX2020-001104-M, funded by MCIN/AEI/10.13039/501100011033, CEMFI and the Ramón Areces Foundation. All errors and omissions are my own.

1 Introduction

Religion has historically shaped individual thought and preferences, social norms, and political power. Yet, despite growing attention to the topic, the role of religion in molding our societies is not fully understood. Religious environments often evolve slowly and are deeply embedded in historical and institutional settings, which complicates the identification of meaningful counterfactuals on which to test competing hypotheses. The German context provides rare quasi-experimental variation that can be leveraged for empirical analysis: within its modern-day territory, the Protestant Reformation created lasting confessional divides between neighboring communities, leaving behind geographic boundaries between predominantly Catholic and Protestant areas that persist to this day.

In this paper, I exploit this precise geographic variation through a Regression Discontinuity Design (RDD), leveraging historical religious boundaries set by sixteenth- and seventeenth-century conflicts following the Reformation to examine how these divides shape political outcomes in contemporary Germany. Integrating historical and geospatial data with contemporary electoral and census sources, I find that historically Catholic municipalities in Germany have shown higher support for the center-right *Union*, i.e. Christian Democratic Union of Germany (CDU) and Christian Social Union (CSU) (between 1.0 and 2.0 percentage points higher at the discontinuity) than their counterparts in every Federal Election between 1990 and 2025, while historically Protestant municipalities lean to the left and center-left of the political spectrum.

No differences are identifiable in terms of average income and within-municipality levels of inequality. Further, I find no evidence of a discontinuity in terms geographic features or pre-reformation indicators of economic development at the historical confessional border. Results are robust to the exclusion of municipalities within a 0.5 and 1 km radius of the historical confessional border. To further complement the analysis, I conduct a two dimensional Geographic Regression Discontinuity Design (GRDD) (Cattaneo et al., 2025) on high-resolution (1 km^2) grid data for the 2017 federal election in the region of North-West

Germany (Breidenbach & Eilers, 2018). This approach exploits variation in both the perpendicular distance to, and position along, the historical confessional border for identification. My findings for this exercise reinforce the main patterns documented in this work.

Present-day differences in electoral behavior across historical confessional lines may in principle reflect not only religion itself, but also other enduring legacies of the Reformation such as differences in institutional development, governance capacity, or economic structure. Moreover, the confessionalization of Germany was itself a product of the strategic choices of the territorial princes of fragmented Holy Roman Empire that was influenced by extant regional conditions and the rulers' personal characteristics (Ozment, 1982; Scribner & Dixon, 2003; Whaley, 2012a). To address this, I present survey evidence from post election surveys between 1953 and 2005 (Institut für Demoskopie et al., 2007), the German Longitudinal Election Study (GLES) between 2009 and 2025 (GLES, 2024, 2025), and the German General Social Survey that shows that historical and present present-day political preferences are correlated to religious affiliation.

This paper speaks to several strands of literature. First, it contributes to the work on historical persistence (see, e.g. Nunn (2020); Abad et al. (2021); Cantoni & Yuchtman (2021); Cirone & Pepinsky (2022)). More particularly, I contribute to the literature on the consequences of the Protestant Reformation (see Becker et al. (2016, 2021, 2024) for thorough reviews on the subject). While evidence for Max Weber's (1930) Protestant work ethic hypothesis has been mixed (see, e.g. Becker & Woessmann (2009) and Spenkuch (2017)), recent work has shown that the Protestant doctrine historically fostered economic development through human capital accumulation and institutional reform (Becker & Woessmann, 2009, 2010, 2011; Boppart et al., 2013, 2014; Cantoni et al., 2018; Dittmar & Meisenzahl, 2020). Further, recent studies have shown how the confessional divides that formed following the Reformation shape political preferences. For example, Spenkuch & Tillmann (2018) documented reduced support for the Nazi party in historically Catholic regions of Germany, while Basten & Betz (2013) showed an enduring influence of Reformed Protestantism on

attitudes toward redistribution and state intervention in Switzerland. My contribution to this literature is twofold: first, while extant work has largely focused on historical contexts, I conduct a thorough analysis on the impact of the Reformation on current electoral behavior in a large modern democracy. Second, although previous research has often relied on geographical variation for the identification of effects, the use of GRDD in this setting remains uncommon, and, to the extent of my knowledge has not yet been applied at the scale and scope of the present analysis.

This work also relates to the research on the relationship between culture and preferences (McCleary & Barro, 2006; Scheve et al., 2006; Campante & Yanagizawa-Drott, 2015; Iyer, 2016; Carvalho et al., 2019; Montero & Yang, 2022; Lowes et al., 2025; Becker et al., 2025b). In particular, recent studies have shown how religiosity shapes political alignment and vote choice in a variety of settings. For instance, Gerber et al. (2016) showed that declines in church attendance led to lower voter turnout in Britain, while Lanzara et al. (2024) and Pulejo (2024) investigated how Catholic bishops increased candidate support and vote shares for Christian Democrats in post-war Italy. Research has also delved into to the rise of Pentecostal Evangelicals and growing support for far-right politics in Brasil and the United States (Mello & Buccione, 2023; Buccione & Knight, 2024; Solá, 2024). However, much of this literature emphasizes short-run shocks and mobilization episodes, with less attention to whether historically inherited religious cleavages continue to structure partisan alignment today. I leverage a historically predetermined cleavage to study contemporary partisan alignment by exploiting confessional borders in Germany and by validating the aggregate discontinuities with individual-level survey evidence on religion and vote choice.

The rest of this paper proceeds as follows. Section 2 introduces Germany's religious landscape, and provides historical context on the origins and persistence of the confessional divisions. A brief overview of the German political system and its main players is also provided in this section. Next, Section 3 describes the broad range of data utilized in this analysis, and Section 4 details the main empirical strategy utilized for this work. Section 5 presents

the main empirical findings along with robustness checks. Section 6 then explores preliminary evidence regarding the mechanisms behind the identified effects. Finally, I present the conclusions of the present work and emphasize avenues for further research.

2 Germany, the Protestant Reformation, Religion and Politics

Germany's distinct bi-confessional religious landscape provides unique advantages for the study of religion's lasting societal impact. As of 2022, the German population was comprised of approximately 23.1% Protestants[1], 21.5% Catholics, and 51.8% individuals who are non-religious or affiliated with other religious traditions (Statistisches Bundesamt, 2022). The spatial distribution of confessional affiliation in the country still largely reflects the religious boundaries established by the Reformation, and the institutional settlements it triggered (Figure 1). This persistent religious geography provides a rare opportunity to systematically compare communities shaped by Catholic and Protestant traditions within otherwise similar cultural and economic contexts.

An important exception is the territory of the former German Democratic Republic, which, due to decades of state-enforced secularism under communist rule, is today overwhelmingly irreligious. Because religious disaffiliation in the East reflects more recent political and institutional dynamics and fundamentally differs from the historical confessional cleavages central to this study, I exclude East Germany from the rest of the analysis. However, across the rest of the country, the present-day religious landscape continues to reflect historical divisions shaped by centuries of religious conflict and coexistence.

[1]The Protestant Churches in Germany comprise only three closely related traditions: Lutheran, Reformed, and United, that have shared clergy, sacraments, and administration under the Evangelical Church in Germany since 1948.

2.1 From the Protestant Reformation to the Peace of Westphalia

At the dawn of the sixteenth century, the lands now known as Germany consisted of many fragmented, quasi-independent principalities and city-states, bound together under the nominal authority of the Holy Roman Empire. Indeed, while the Emperor wielded considerable prestige and symbolic authority, effective sway over internal (and occasionally imperial) matters predominantly rested with the territorial lords and the imperial estates [2].

While the Roman Catholic Church's religious dominance in the Empire remained largely uncontested, the Pope faced growing calls for reform amid demands for greater regional autonomy, widespread outrage over fiscal exploitation, and a desire among many to restore the Church to its original, divinely ordained state of spiritual purity. Martin Luther's public challenge to the Church in 1517 in the form of the publication of his 95 theses provided a vehicle for the growing discontent, marking the beginning of the Protestant Reformation. The growing dissidence was challenged by Emperor Charles V, a staunch Catholic, and brewing tensions soon erupted into military conflicts.

In an attempt to restore peace, the princes of the Empire met at the Diet of Augsburg in 1555. The compromises achieved there formally legalized the nascent Lutheran confession by granting territorial rulers *ius reformandi*, the constitutional right to determine the official religion of their territories. The settlement also codified the principle of *cuius regio, eius religio* ("whose realm, whose religion"), whereby the religion of a prince became the official faith of his domain and, by extension, of its inhabitants.

Yet, religious tensions continued to mount, eventually reaching a boiling point with the Defenestration of Prague in 1618, which ignited the Thirty Years' War (1618–1648). What began as a religious conflict within the Empire soon escalated into a broader political and military struggle drawing in Europe's major hegemonic powers. As the war drew to a close, delegations from across the continent convened in the Westphalian cities of Münster and Osnabrück to negotiate a comprehensive settlement. The Peace of Westphalia concluded

[2] The following summary largely follows the accounts of Whaley (2012a).

in 1648, confirmed the agreements reached at Augsburg in 1555, and extended religious toleration to the Reformed Church. Territorial reallocations and confirmations of sovereignty were part of the settlement, but the religious compromises reached were ultimately of greater historical consequence. Confessional status was fixed based on the situation as of the "normal year" of 1624, which served as the reference point for assigning each territory to either Roman Catholic or Protestant control. Rulers were barred from altering their state's official religion through personal conversion, which stabilized the Empire's religious and political structure and formalized the coexistence of its major confessions (Figure 2).

2.2 Determinants of the Spread of Protestantism

The adoption of the Reformation by the princes of the Empire was shaped the geopolitical landscape of the realm, local power structures and personal beliefs and networks. Princely endorsement of the Reformation was frequently contingent on prior developments, including local reform movements in the towns, the penetration of Protestant ideas into rural communities, and the alignment of influential nobles and officials (Whaley, 2012a). For instance, the religious movement tended to take root in regions far away from the imperial seats of power in Vienna and Brussels (Whaley, 2012a) and in those closer to the center of the Reformation at Wittenberg (Becker & Woessmann, 2009; Cantoni, 2012; Kim & Pfaff, 2012). Further, ecclesiastical status often led to the preservation of the old religion (Cantoni, 2012; Whaley, 2012a).

The popularity of the Protestant movement among the urban classes made towns and the imperial cities in particular fertile ground for the spread of the Reformation (Ozment, 1982; Scribner & Dixon, 2003), where the diffusion of the movement was further accelerated by the spread of the printing press (Whaley, 2012a; Rubin, 2014) and particularly so in local media markets with more competing prints (Dittmar & Seabold, 2015). Moreover, the spread of Luther's personal network itself aided in spreading the Reformation (Becker et al., 2020, 2025a)

2.3 The Continuity of Confessional Geography

Most territories in the Holy Roman Empire remained religiously homogeneous until the early nineteenth century. The ideas of the French Revolution and the Napoleonic Wars set forth the largest redistribution of property in German history prior to 1945 in the form of the *Reichsdeputationshauptschluss* (the principal conclusion of the extraordinary imperial commission) of 1803. This agreement led to the widespread secularization of ecclesiastical territories and the mediatization of smaller secular entities, consolidating the political landscape into just over thirty states and fewer than fifty Imperial Cities. As a result, Protestants and Catholics began living under the same political jurisdictions for the first time in centuries (Whaley, 2012b).

Nevertheless, at the local level, religious homogeneity persisted well into the twentieth century. This continuity was ultimately broken by the massive population displacements that followed World War II. By 1947, official statistics counted more than 10 million displaced persons and expellees within Germany's borders - the largest such movement in Europe since late antiquity. This demographic shock significantly diluted regional religious majorities: the number of counties in which a single confession accounted for over 90 percent of residents dropped from 247 in 1939 to just 82 in 1946 (Nowak, 1995).

Despite this upheaval, the regional distribution of religious affiliation in contemporary Germany still largely mirrors the confessional boundaries established by the Peace of Westphalia in 1648. Figures 3 and 4 overlay present-day religious distributions with the historically Catholic and Protestant territories as of the Westphalian settlement. The spatial alignment is striking: regions that were officially Catholic or Protestant in 1648 continue to display disproportionately high shares of those respective denominations today. Indeed, the correlation between a municipality's historical Catholic status and its present-day Catholic population share is 0.77. As I will show throughout the paper, these persistent confessional patterns continue to shape the structure of political competition in Germany.

2.4 The Current Political Landscape in Germany

Germany is a federal parliamentary democracy with a mixed electoral system combining plurality and proportional representation. Federal elections to the *Bundestag* occur every four years, with all citizens aged 18 and older eligible to vote. Half of the *Bundestag*'s members are elected to represent single-seat constituencies, and half are elected through proportional representation. Voters exercise two distinct votes: one for a constituency candidate (*Erststimme*), which determines local representation via plurality, and another for a party list (*Zweitstimme*), which governs the proportional distribution of seats in the *Bundestag*[3].

Germany's political landscape is dominated by two major political forces, the center-right *Union*, comprised of Christian Democratic Union of Germany (CDU) and its Bavarian sister party Christian Social Union (CSU), and the center-left Social Democratic Party of Germany (SPD). Neither party typically secures a parliamentary majority on its own, making coalition governments the norm. Recent years have seen the rise of the far-right Alternative for Germany (AfD), which entered the *Bundestag* in 2017 on an anti-immigration and populist platform. Although now the third-largest parliamentary group, the AfD remains politically isolated, as mainstream parties refuse to enter coalitions with it.

Among the smaller but influential parties, the pro-market Free Democratic Party (FDP) has frequently acted as a coalition partner and kingmaker, often shaping policy beyond its modest electoral base. The Alliance 90/The Greens, initially rooted in environmental and pacifist activism, has evolved into a key progressive force with strong support in urban areas and among younger voters. The Left, formed from the remnants of East Germany's ruling Socialist Unity Party of Germany (SED) and western leftist movements, retains regional strength in the east and advocates for redistributive policies, though it remains largely excluded from federal coalitions.

[3]The following summary borrows heavily from Schleunes et al. (2025).

3 Data

The empirical analysis in this paper integrates diverse historical, geospatial, and micro-level datasets. Historical administrative and religious boundaries of Germany as of 1648 are obtained from the Digital Atlas on the History of Europe since 1500 elaborated by Kunz (2014) at the Leibniz Institute of European History, in Mainz, Germany. Historical population estimates and land development data, with a spatial resolution of approximately 85 km^2 at the equator (5 arc minutes), are sourced from the History Database of the Global Environment (HYDE) (Goldewijk, 2001).

Geospatial characteristics are derived from several contemporary sources. German administrative borders, along with detailed data on slope and elevation at a spatial granularity of 1 km^2, are drawn from the Federal Agency for Cartography and Geodesy (BKG, 2021a,b). Additionally, spatial data on the main[4] German waterways are taken from the HydroRivers dataset, offering spatial resolution at 15 arc seconds, equivalent to approximately 500 m^2 at the equator (Lehner & Grill, 2013).

For the micro-level analysis, I utilize detailed electoral and demographic data. Election outcomes at the municipality level for federal elections from 1990 through 2025 are obtained from the German Election Database (GERDA) (Heddesheimer et al., 2025). Additionally, the RWI-GEO-VOTE data set from the Leibniz Institute for Economic Research provides granular electoral results for the 2017 federal election at a grid resolution of 1 km^2 (Fremerey et al., 2021). Both data sets contain information solely on the distribution of *Zweitstimmen* (Section 2.4). Broad survey data capturing voter behavior and preferences from repeated cross-sectional surveys conducted after federal elections from 2009 to 2025 come from the German Longitudinal Election Study (GLES) (GLES, 2024, 2025), the cumulated post-election surveys covering all elections between 1953 and 2005 (Institut für Demoskopie et al., 2007), and the German General Social Survey (1980 -2021) (GESIS, 2024).

[4] I define main rivers as those classified in HydroRIVERS as Strahler order 1 and with an upstream catchment area of at least 5,000 km^2 (see Lehner & Grill (2013) for details).

Moreover, contemporary municipal religious and demographic data are sourced from the German Census of 2022 (Statistisches Bundesamt, 2022), which includes data at the municipality level and (for a select number of variables) at a spatial resolution of 1 km^2. Finally, municipality-level data on income and within-municipality inequality, constructed from administrative records, are taken from data provided by Frieden et al. (2023).

3.1 Sample Construction

The main sample of geographical units consists of West-German municipalities that lie within historically Catholic or historically Protestant regions as per Kunz (2014). Municipalities classified as historically multi-confessional or those for which no historical designation is available are excluded from the analysis[5].

4 Empirical Strategy

Geographic and administrative borders can generate sharp variations in institutional environments, cultural heritage, or religious composition. Research leveraging such spatial discontinuities to identify causal effects frequently relies on Geographic Regression Discontinuity Designs (GRDDs) (see e.g. Keele & Titiunik (2015, 2016); Keele et al. (2017); Cattaneo et al. (2024) for an overview on methodology). Indeed, works in fields ranging from labor (Jardim et al., 2024) to historical (Dell, 2010) and cultural economics (Brügger et al., 2009; Basten & Betz, 2013) have all exploited this method to uncover localized effects of institutional, social, or cultural differences.

In Germany, the settlements of the peace of Westphalia induced long-standing sharp religious and institutional variation between neighboring communities (Section 2). Because historically Catholic and historically Protestant regions in Germany may have generally

[5]Due to gaps and spatial mismatches in the historical mapping procedure used to vectorize the confessional territories in Kunz (2014), a small number of municipalities cannot be reliably assigned to either the Catholic or Protestant side. These municipalities are therefore excluded from the main sample.

exhibited largely different idiosyncrasies even prior to the Reformation, a localized analysis within the proximity of the confessional border allows for a cleaner empirical exercise. Further, as the border's precise placement often resulted from contingent historical events rather than systematic sorting, municipalities nearby on either side can be considered as if randomly assigned to either confessional legacy. Hence, this paper employs a GRDD strategy to estimate the contemporary political consequences of historical confessional divisions in Germany.

4.1 Setup and Notation

Let $\mathcal{A}^C$ denote the set of municipalities historically assigned to Catholic polities, and $\mathcal{A}^P$ those assigned to Protestant polities. Potential outcomes for municipality i, Y_{i1} and Y_{i0}, correspond to treatments $T_i = 1$ if $i \in \mathcal{A}^C$ and $T_i = 0$ otherwise, so the observed outcome is given by $Y_i = T_i Y_{i1} + (1 - T_i) Y_{i0}$.

Further, each unit i has a bivariate score $\mathbf{S}_i = (S_{i1}, S_{i2}) \in \mathbb{R}^2$, which is given by the longitude and latitude of the geographic center of the administrative seat of each municipality. For my main approach, I calculate a one-dimensional running variable $D_i \in \mathbb{R}$ form $\mathbf{S}_i$ as the shortest perpendicular distance from $\mathbf{S}_i$ to the confessional border $\mathcal{B} = \text{bd}\left(\mathcal{A}^C\right) \cap \text{bd}\left(\mathcal{A}^P\right)$. D_i is then normalized and signed so that $T_i = \mathbf{1}(D_i > 0)$, and all units are pooled for estimation (Figure 5 provides an illustration of the definitions of T_i and D_i as used for the estimation process). Under this setup, identification and inference are identical to the standard one-dimensional RDD (Cattaneo et al., 2024).

Assumption 1 (Positive and Continuous Density of the Running Variable) *The running variable D_i has a density $f_D(d)$ that is continuous in an open neighborhood of $d = 0$ and bounded away from zero.*

Assumption 2 (Continuity of Potential Outcome Means) *The conditional expectations*

of potential outcomes are continuous at the threshold $D_i = 0$:

$$\lim_{d\uparrow 0} \mathbb{E}\big[Y_{i0} \mid D_i = d\big] = \lim_{d\downarrow 0} \mathbb{E}\big[Y_{i0} \mid D_i = d\big], \quad \lim_{d\uparrow 0} \mathbb{E}\big[Y_{i1} \mid D_i = d\big] = \lim_{d\downarrow 0} \mathbb{E}\big[Y_{i1} \mid D_i = d\big].$$

Consider covariates $\mathbf{X}_i \in \mathbb{R}^K$, with $\mathbf{X}_i = T_i\mathbf{X}_{i1} + (1 - T_i)\mathbf{X}_{i0}$, where $\mathbf{X}_{i1}$ and $\mathbf{X}_{i0}$ denote the potential covariates on either side of the historical border.

Assumption 3 (Continuity of Potential Covariate Means) *For every component X_{ik} of the covariate vector $\mathbf{X}_i$, the conditional expectations of the potential covariates are continuous at the cutoff $D_i = 0$:*

$$\lim_{d\uparrow 0} \mathbb{E}\big[X_{i0k} \mid D_i = d\big] = \lim_{d\downarrow 0} \mathbb{E}\big[X_{i0k} \mid D_i = d\big], \qquad \lim_{d\uparrow 0} \mathbb{E}\big[X_{i1k} \mid D_i = d\big] = \lim_{d\downarrow 0} \mathbb{E}\big[X_{i1k} \mid D_i = d\big].$$

Under assumptions 1–3, together with a series of standard regularity conditions (see, e.g. Calonico et al. (2019)), the discontinuity in the conditional mean of the observed outcome identifies the average treatment effect at the cutoff:

$$\tau \;=\; \lim_{d\downarrow 0} \mathbb{E}\big[Y_i \mid D_i = d\big] \;-\; \lim_{d\uparrow 0} \mathbb{E}\big[Y_i \mid D_i = d\big]. \tag{1}$$

4.2 Estimation Framework

To estimate τ in (1), I implement the following specification:

$$Y_i = \alpha + \tau T_i + \gamma_{(0)} \min\{D_i, 0\} + \gamma_{(1)} \max\{D_i, 0\} + \boldsymbol{\eta}^\top \mathbf{X}_i + \varepsilon_i. \tag{2}$$

Here, Y_i denotes the observed outcome of interest (religious composition in 2022, party vote shares in federal elections from 1990 to 2025, and average income and within-municipality inequality between 1998 and 2016). The running variable $D_i \in \mathbb{R}$ represents the signed distance from the administrative seat of municipality i to the historical confessional border $\mathcal{B}$. Treatment status is defined as $T_i = \mathbf{1}(D_i > 0)$, indicating historical assignment to a Catholic

polity.

The covariate vector $\mathbf{X}_i$ includes pre-treatment controls related to historical demography and geography, such as 16th-century rural and urban population counts, land devoted to urban development and croplands, topographic features (average elevation and slope)[6], proximity to major rivers, and a full set of federal-state fixed effects. Covariate adjustment in (2) achieves efficiency gains by reducing residual variance in estimations (Calonico et al., 2019). This enhancement also allows for formal tests on whether municipalities on either side of the border differ systematically in predetermined characteristics, thereby offering empirical support for the validity of treating municipalities near the threshold as counterfactuals for one another.

4.3 Two dimensional Geographic Regression Discontinuity Design

While the main approach provides an effective summary of treatment effects, by construction, the pooled estimate does not convey information of heterogeneity *along* the border (Cattaneo et al., 2024). Although equidistant from the border $\mathcal{B}$ two municipalities may lie far apart along the frontier, potentially experiencing different local contexts that a pooled design cannot distinguish (Keele & Titiunik, 2015).

A second concern is the Modifiable Areal Unit Problem (MAUP), whereby statistical inference can depend on the arbitrary spatial aggregation of data. When individual-level behavior is summarized within administrative units such as municipalities, meaningful variation may be lost or distorted. This can lead to misleading inferences, particularly in cases where the underlying phenomena vary at finer spatial resolutions or where the chosen administrative boundaries do not align with the relevant social or institutional structures (Openshaw, 1984).

To mitigate these concerns, I supplement the main analysis with a high-resolution (1 km^2 grid) examination of the 2017 federal election results in northwestern Germany (Fremerey

[6]All values of historical and topological features are normalized by the total area of a given municipality.

et al., 2021), using a novel two-dimensional GRDD method developed by Cattaneo et al. (2025). While the method's requirement of a continuous boundary $\mathcal{B}$ limits its applicability at the national level, the region surrounding the former Prince-Bishopric of Münster[7] offers a particularly suitable setting. Here, the historical confessional boundary is relatively regular and intersects areas with detailed electoral data[8]. This area encompasses parts of present-day Lower Saxony, Bremen, and Hamburg.

To implement the two-dimensional GRDD method, I sample six evenly spaced coordinates $\mathbf{b}_j = (b_{j1}, b_{j2})$ (50 km apart) along the historical Catholic-Protestant frontier $\mathcal{B}$ and estimate treatment effects locally around each sampled point. Formally, for each grid cell i located at coordinates $\mathbf{S}_i$ and point $\mathbf{b}_j \in \mathcal{B}$ I estimate the following regression:

$$Y_i = \alpha + \tau(\mathbf{b}_j)T_i + \boldsymbol{\gamma}_{(0)}^{\top}(\mathbf{S}_i - \mathbf{b}_j)_- + \boldsymbol{\gamma}_{(1)}^{\top}(\mathbf{S}_i - \mathbf{b}_j)_+ + \varepsilon_i, \tag{3}$$

where Y_i once again denotes the outcome of interest (religious composition in 2022 and party vote shares for the 2017 federal election for grid i) and T_i is an indicator equal to one whenever grid i lies within a historically Catholic region. Conditional average treatment effects are identifiable under a set of conditions analogous to the standard RDD framework and a series of regularity requirements for the Kernel function (Cattaneo et al., 2025).

5 Results

The confessional divisions fixed by the Peace of Westphalia helped shape regional patterns that endured beyond religious practice alone. Here, I examine whether those divisions remain visible in Germany's political landscape, centuries after their institutional origin.

[7]For a general historical and geographic background on the Prince-Bishopric of Münster, see the corresponding Wikipedia entry: https://en.wikipedia.org/wiki/Prince-Bishopric_of_M%C3%BCnster .

[8]The dataset provides 1 km^2 grid-level election results, generally imputed from municipality-level vote shares and population distributions. In the region of interest, however, the data are based on aggregations from geo-referenced polling districts (Wahlbezirke), allowing for greater spatial precision (see Fremerey et al. (2021) for details).

5.1 Main Analysis

5.1.1 Historically Catholic Municipalities Remain Largely Catholic

Religious affiliation in Germany remains closely tied to historical patterns established by the Peace of Westphalia in 1648 (Section 2). As shown in the first three rows of Table 1, there are clear differences in the religious composition of historically Catholic and Protestant municipalities. On average, 57% of the population in historically Catholic areas identify as Catholic, compared to only 16% in historically Protestant ones. Additionally, historically Protestant municipalities exhibit a higher proportion of individuals who are either non-religious or affiliated with other belief systems (39%) than their Catholic counterparts (29%). This difference may reflect varying degrees of persistence in religious adherence, with Catholic identity potentially being more enduring than its Protestant counterpart (Pew Research Center, 2019).

Despite the already documented strong correlation between contemporary religious affiliation and historical geography, identifying a discontinuity at the historical confessional border may help illuminate potential pathways by which historical religious institutions continue to influence present-day outcomes. Figure 6 displays a binned scatter plot of the share of Catholics in 2022 against the distance to the historical confessional border, with negative values in the horizontal axis indicating locations on the Protestant side and positive values on the Catholic side. The plot reveals a sharp discontinuity at the border, with the Catholic share increasing abruptly when crossing from the historically Protestant to the historically Catholic side. Indeed, point estimates from regression (2) indicate a jump of approximately 3.3 percentage points at the border which is significant at the 1% level (Table 2).

5.1.2 Historically Catholic Municipalities Vote *Union*

Cleavages along historical confessional lines are also evident in political behavior. Tables 3 and 4 summarize average party vote shares in all federal elections from 1990 to 2025,

distinguishing between historically Catholic and Protestant municipalities. Across all election years, *Union* consistently receives a markedly higher vote share in Catholic areas than in Protestant ones, reinforcing its traditional alignment with Catholic constituencies. In contrast, the SPD exhibits the opposite pattern, with systematically stronger support in Protestant regions, although its overall vote share has declined steadily over time. A similar though less pronounced dynamic is visible for the Far-Left parties[9] (mainly the Left) , which tends to perform slightly better in Protestant areas. For other parties such as the Greens, FDP, and the Far-Right[10] (mainly AfD and National Democratic Party of Germany (NPD) prior to 2013), the denominational divide is less consistent, with smaller and more variable differences across regions and over time.

Visual evidence once again reinforces these overarching patterns and points to a clear and consistent discontinuity in vote shares for *Union* (Figures 7 and 8). In contrast, the plots for the SPD do not exhibit a similarly sharp break at the border (Figures 9 and 10). Instead, the observed variation appears more gradual, and a broader spatial trend or change in slope cannot be ruled out. In a similar vein, bin-scatter plots on the vote share for the Far-Left provide mixed evidence for the existence of a discontinuity (Figures 11 and 12). For other parties, such as the Greens (Figures 15 and 16), the FDP (Figures 17 and 18), and the Far-Right (Figures 13 and 14), the graphical evidence does not suggest the presence of any consistent discontinuities aligned with the historical confessional divide.

Estimates from the regression discontinuity design (2) further develop the already established motif (Table 6). The *Union* parties have been consistently more successful on the historically Catholic side of the border in every election considered, with vote shares

[9]Far-left parties include BSA (*Bund Sozialistischer Arbeiter*), BWK (*Bund Westdeutscher Kommunisten*), DKP (*Deutsche Kommunistische Partei*), KBW (*Kommunistischer Bund Westdeutschland*), KPD (*Kommunistische Partei Deutschlands*), SGP (*Sozialistische Gleichheitspartei*, formerly PSG), SpAD (*Spartakist-Arbeiterpartei Deutschlands*), V (*Volksfront gegen Reaktion, Faschismus und Krieg*), and the Left.

[10]Far-right parties include AfD, BF_B (*Bund Freier Bürger*), DDD (*Bund der Deutschen Demokraten*), DG (*Deutsche Gemeinschaft*), *Die Rechte*, DNS (*Dachverband der Nationalen Sammlung*), DRP (*Deutsche Reichspartei*), DSU (*Deutsche Soziale Union*), DVU (*Deutsche Volksunion*), FAP (*Freiheitliche Deutsche Arbeiterpartei*), NPD (*Nationaldemokratische Partei Deutschlands*), REP (*Die Republikaner*), and *III. Weg*.

between one and two percentage points higher at the discontinuity. Effects are statistically significant at the 1% level throughout. Point estimates for the SPD also indicate statistically meaningful differences, broadly in line with the earlier descriptive observations. Yet, in light of the lack of clear visual evidence, the overall case remains mixed. Regression results for other political forces do not point to the existence of discontinuities at the historical border.

5.1.3 Results Survive Robustness Checks

To account for potential measurement error in the exact location of the historical confessional boundary, Tables 7 and 8 report estimates from *donut hole* regressions that exclude observations within 0.5 km and 1 km of the border, respectively. For the *Union* parties, the estimated discontinuities increase substantially in magnitude—rising to between 3.4 and 4.6 percentage points—while remaining statistically significant at the 1% level across all years. Similarly, the SPD shows consistently negative and statistically significant estimates, with larger magnitudes of up to 4.3 percentage points, particularly in the earlier election cycles (Figure 25).

Estimates for the remaining political forces present a more heterogeneous picture. The Far-Right and Far-Left occasionally exhibit statistically significant discontinuities, but the direction and magnitude of these effects vary across election years and show no consistent pattern. Similarly, negative and sometimes significant estimates emerge for the Greens and FDP in select elections, yet these results appear sporadic and lack a stable cross-time structure.

Covariate-balance tests further validate the results of the main analysis. While some underlying geographic variation exists between historically Catholic and Protestant municipalities, it does not translate into discontinuities at the historical border. Table 1 reports average differences in elevation, slope, and distance to major rivers, with Catholic areas generally located at higher altitudes, on steeper terrain—likely due to the Bavarian Alps—and closer to major rivers, potentially reflecting proximity to the Elbe. Despite these differences

in levels, graphical analysis in Figure 23 reveals no evidence of sharp breaks at the border. Furthermore, while the main specification indicates marginally statistically significant differences in urban population, built-up area, and cropland share, these imbalances diminish substantially and become statistically insignificant when excluding observations within 0.5 km and 1 km of the boundary (Table 12).

As a further check on the validity of the identification strategy, a McCrary density test is conducted. The estimated discontinuity in the density of observations at the cutoff is small and statistically insignificant (Table 13). This is also visually confirmed in the density plot, which shows no detectable jump in the distribution of municipalities around the threshold (Figure 24).

5.1.4 No Differences in Income Related Variables across Historic Boundaries

Descriptive statistics show no systematic differences in income-related outcomes between historically Catholic and Protestant municipalities across the observed years (Table 5). Likewise, graphical evidence reveals no apparent discontinuities at the historical border for any of the variables considered (Figures 19 - 22). Formal estimates from the regression discontinuity design reinforce this impression: point estimates for (log) average income, (log) income adjusted for capital tax, and both inequality measures (Gini and Theil indices) are consistently small in magnitude and statistically indistinguishable from zero across specifications. These findings remain robust to the exclusion of observations within 0.5 km or 1 km of the border (Tables 9–11).

5.2 Localized Two-Dimensional High-Resolution Analysis

To complement the main analysis, I implement a two-dimensional GRDD design (Cattaneo et al., 2025) on high-resolution (1 km^2) grid data for the 2017 election in the region of North-West Germany. This approach allows for spatially localized estimation that can uncover variation *along* the border, and mitigates concerns due to aggregation problems (Section 4).

An overview of the spatial distribution of religious affiliation and voting patterns reinforces the broader empirical themes developed throughout this study. Figures 26 and 27 overlay the historical confessional boundary of the former Prince-Bishopric of Münster onto grid-level data (1 km² resolution) on Catholic population shares and vote shares for the CDU, SPD, and the Left. The CDU exhibits visibly stronger support in historically Catholic areas (inside the *hook*), with its spatial distribution closely mirroring that of Catholic affiliation. In contrast, the SPD and the Left demonstrate greater electoral strength in Protestant regions. Descriptive statistics reported in Table 14 echo these visual patterns. In grid cells classified as historically Catholic, CDU support reaches an average of 56%, compared to 38% in Protestant cells. In contrast, the SPD and the Left register higher vote shares in Protestant municipalities, 26%, and 6.3%, respectively, relative to 17% and 3.8% in Catholic areas.

Table 15 reports estimates from regression (3) for each of the six sampled locations along the historical border (the corresponding evaluation points are visualized in Figures 26 and 27). The results once again indicate substantial discontinuities in religious affiliation. Leveraging high-resolution data and two-dimensional spatial variation, the estimated effects are considerably larger than in the main analysis: crossing the historical confessional border increases the share of Catholics by between 23.3 and 58.7 percentage points, with statistically significant effects (at the 5% level or better) at four out of six locations. For points $b3$, $b4$, and $b6$, effects are either imprecisely estimated or not statistically significant, reflecting limited numbers of treated observations and reduced power in those segments—a limitation that also affects several of the political outcomes.

Further, CDU support increases significantly at all six border points, with estimated discontinuities ranging from 3.3 to 24.0 percentage points. In contrast, the SPD exhibits negative and statistically significant discontinuities at four locations, ranging from –3.8 to –21.9 percentage points. The Left also shows negative effects across most segments, with magnitudes between –1.4 and –6.7 percentage points where significant. Among the remaining

parties, patterns are more mixed. The Greens exhibits significant negative effects in four locations, with discontinuities between –1.7 and –4.8 percentage points, suggesting slightly weaker support in Catholic areas, although the effect is not uniformly estimated. For the FDP, effects are modest and inconsistent: while some positive or negative estimates are significant at conventional levels, the pattern is not stable across space and includes null results.

The two southernmost points ($b5$ and $b6$) fall within the district of Osnabrück, a historically multi-confessional area that was excluded from earlier analyses. In this localized setting, however, the grid cells closest to the historical border are predominantly Catholic (Figure 26). This pattern suggests that religion may be one of the underlying factors contributing to the observed discontinuities in voting behavior at the border.

6 Channels and Mechanisms

Historical confessional boundaries settled almost four hundred years ago may influence modern-day outcomes through a variety of mechanisms, not limited to religious affiliation alone. The Reformation itself, followed by centuries of territorially fragmented administration, likely created distinct institutional and cultural trajectories, with implications for public authority, civic norms, and state capacity. Further, the roots of regional divergence likely extend beyond religious change, with important differences already present in the pre-Reformation era.

A growing body of literature indeed documents substantial heterogeneity in cultural, institutional, and geographic characteristics across regions during this period. For instance, variation in military power, proximity to Wittenberg, latitude, ecclesiastical status, and the early presence of the printing press all shaped the initial diffusion of the Reformation and may correlate with later socio-political developments (Cantoni, 2012; Rubin, 2014; Becker et al., 2016). Cultural and intellectual factors, such as the presence of humanist scholars and

Luther's personal following in local churches and universities, or proximity to imperial centers like Vienna and Brussels, also played an important role in mediating regional trajectories during and after the Reformation (Whaley, 2012a; Becker et al., 2025a).

Beyond initial regional differences, the confessional divide itself may have contributed to persistent institutional divergence. In Protestant areas, rulers often reallocated ecclesiastical wealth to secular purposes, particularly where they faced limited political constraints (Cantoni et al., 2018). Separately, local movements in a number of Protestant cities pushed for legal and administrative reforms that expanded public goods provision and built a civic infrastructure around education and welfare (Dittmar & Meisenzahl, 2020). These institutional developments likely reinforced long-term differences in governance capacity and civic life across regions.

Yet among the various historical legacies of the Reformation, religious affiliation remains the most salient and enduring feature in contemporary Germany. To assess the plausibility of religion as a channel shaping modern political behavior, I turn to individual-level survey data that allow for a direct comparison between Catholic and non-Catholic voters.

6.1 How are Catholic voters different from the rest?

To examine differences in individual voting behavior by religious affiliation, I estimate a series of logit models using post-election cross-sectional survey data from the German Longitudinal Election Study (GLES) for Bundestag elections between 2009 and 2025 (GLES, 2024, 2025). I restrict the sample to voting-age respondents residing in West Germany at the time of each election (Table 16 reports the distribution of religious affiliation in the analysis sample). Formally, for respondent i in state g at election t, I estimate:

$$\log \frac{\Pr(Y_{igt}=1)}{\Pr(Y_{igt}=0)} = \alpha + \sum_k \delta_k \, \text{Confession}_{ik} + \gamma \, R_{it} + X_{igt}^{\top}\theta + \lambda_t + \xi_g + \varepsilon_{igt}, \tag{4}$$

where Y_{igt} denotes the outcome of interest (vote choice for a given party, reported close-

ness to the *Union*, parental *Union* identification, or right-wing self-placement). Confession_{ik} is a set of indicators for denomination k (Catholic, Protestant, non-religious, other), R_{it} captures self-reported religiosity (somewhat or very religious), and X_{igt} includes gender, education, marital status, age group, and household income. All specifications include election fixed effects λ_t and state fixed effects ξ_g.

6.1.1 Catholic voters *do* lean towards *Union*

Figure 28 plots the results of pairwise comparisons in predicted vote probabilities across religious groups. In line with the spatial patterns uncovered in Section 5, Catholics are significantly more likely to vote for the *Union* parties than Protestants (by 11.3 percentage points), the non-religious (14.9 pp), and respondents of other denominations (10.3 pp). Importantly, these comparisons hold conditional on individuals' self-reported religiosity, suggesting that Catholic affiliation itself, rather than religiosity per se, is associated with stronger support for the *Union*.

The pattern observed for the *Union* is mirrored in reduced support for the SPD among Catholics, with predicted voting probabilities 2.8–8.2 percentage points lower than for other groups. A similar, though smaller, negative relationship emerges for the Left. By contrast, differences in vote probabilities among Protestants, the non-religious, and other groups are less pronounced and largely statistically insignificant (Table 18 contains the full set of estimates for all major German political parties).

The association is far from new. I re-estimate model (4) on cumulated post-election surveys covering all Bundestag elections between 1953 and 2005 (Institut für Demoskopie et al., 2007).[11] Figure 29 shows that the Catholic–*Union* link was, if anything, even stronger in earlier decades. Between 1953 and 2005, Catholics were 12.6 percentage points more likely to vote for the *Union* than Protestants, 20.3 pp more likely than the non-religious,

[11] Two features of this earlier data source require minor adjustments to the specification: religiosity is proxied by church attendance frequency rather than self-reported religiosity; the control vector X_{igt} includes gender, education, age, and occupational class; and consistent state identifiers are not available throughout the period, so state fixed effects ξ_g are not included. Table 17 reports sample characteristics.

and 24.5 pp more likely than respondents of other denominations. The corresponding gaps for the SPD were similarly pronounced: Catholics were 9.1 pp less likely to vote SPD than Protestants and 13.0 pp less likely than the non-religious (Table 19 contains the full set of estimates). Catholic distinctiveness appears to have attenuated over time, but the Catholic–Protestant gap in *Union* support has persisted throughout (Figure 30).

6.1.2 Why do Catholics lean towards *Union*?

The alignment between Catholic voters' political preferences and the patterns observed in earlier analyses is consistent with a role for religion in contemporary partisan alignment. This raises a further question: why might Catholic affiliation be associated with stronger support for the *Union* today?

Policy Preferences A preference-based account is that denomination is correlated with differences in moral and social-policy views. Catholic doctrine and practice are more tightly linked to a unified teaching authority and a clear hierarchy, together with a stronger emphasis on tradition. This is often associated with more restrictive positions on salient values issues such as family policy, sexuality, and bioethics, and with a stronger preference for social order and gradual change. By contrast, the mainline Protestant churches are more decentralized and doctrinally pluralistic, which tends to allow greater variation in interpretation and, in some domains, more permissive attitudes.

I test for differences in values, attitudes and policy position across confessions using data from the German General Social Survey (GESIS, 2024) (1980–2021). To do so, I estimate the same logit specification[12] as in equation (4) for 51 outcomes spanning family norms, moral judgments, abortion attitudes, gender roles, general policy issues, institutional trust, welfare preferences, and democratic satisfaction.

[12]The specification is adapted to the structure of the German General Social Survey. Denomination enters as a set of indicators (Catholic, Protestant, no affiliation, other), with religiosity proxied by church attendance frequency rather than self-reported religiosity, and the control vector includes gender, education, marital status, and age group; household income is not available consistently across waves and is therefore excluded.

Figures 31 and 32 report the Catholic–Protestant contrast (in percentage points) for each outcome. Differences cluster overwhelmingly in the domains of morality and abortion, Catholics are 8.2 percentage points less likely than Protestants to find abortion morally permissible, and 6.9 pp more likely to support an outright ban. Across all specific abortion scenarios – financial hardship (-4.1 pp), no more children wanted (-5.2 pp), any reason (-3.8 pp), single motherhood (-2.8 pp), rape (-2.0 pp), and fetal health concerns (-1.6 pp) – Catholics are consistently less approving. Catholics are also less permissive regarding euthanasia (-3.6 pp). Beyond morality and abortion, Catholics are more supportive of restricting Islamic religious practice (+3.4 pp) and of state monitoring of Islamic organizations (+3.2 pp), and are less supportive of expanding social benefits (-3.3 pp). A small but significant gap also emerges on political efficacy, with Catholics slightly less likely to agree that ordinary people have no influence on government (-1.2 pp). These attitude gaps generally coincide with a broader ideological shift: Catholics are 3.9 percentage points more likely to place themselves on the right of the ideological spectrum.

Identity & Political Socialization Another possibility could center on identity and political socialization. Regardless of policy preferences, political support for the *Union* parties may be driven by a distinct Catholic political identity transmitted across generations and sustained through social ties.

To evaluate this mechanism, I return to the GLES and re-estimate the baseline logit specification for two measures of partisan identification. Figure 33 shows that Catholic respondents are more likely to report feeling close to the *Union* parties (+10.2 pp v.s. Protestants), and to indicate that their parents felt similarly (+16.0 pp v.s. Protestants) (Table 20 contains the full set of estimates). Moreover, restricting attention to respondents who report closeness to the *Union* parties, Catholics display systematically stronger and more deeply rooted partisan attachment: the share reporting a strong party identification ("very strong") is 13.1% among Catholics versus 8.8% among Protestants, Catholics are more likely to report

having identified with the party "since they can remember" (30.9% vs. 20.6%), and they are substantially more likely to describe this attachment in explicitly affective terms ("this party means a lot to me," 67.2% vs. 50.2%) (Figure 34).

The historical roots of Catholic political identity run deep. Bismarck's *Kulturkampf* of the 1870s, a sustained campaign to curtail Catholic institutional influence in the newly unified German state, consolidated a distinct Catholic political consciousness. In response, the Center Party emerged as the political voice of Germany's Catholic minority and maintained a remarkably stable electoral base for over six decades. When the CDU was founded in 1945 as a deliberately cross-confessional party, it nonetheless drew heavily, both in personnel and in ideology, from the former Center Party (Conradt, 2025). This institutional continuity could have helped entrench pre-existing partisan loyalties in Catholic communities.

7 Conclusion

This paper has examined whether the confessional divisions established by the Peace of Westphalia in 1648 continue to shape political behavior in contemporary Germany. Exploiting the geographic variation between historically Catholic and Protestant municipalities through a Geographic Regression Discontinuity Design, I document that historically Catholic areas exhibit systematically higher vote shares for the center-right *Union* parties, on the order of one to two percentage points at the discontinuity in the baseline specification, and larger still in donut hole designs, across every federal election from 1990 to 2025. Historically Protestant municipalities, by contrast, lean toward the SPD and, to a lesser extent, the far-left. These patterns are not accompanied by detectable differences in income or within-municipality inequality at the historical confessional border. A complementary two-dimensional GRDD on high-resolution grid data for northwestern Germany reinforces these findings.

Individual-level survey evidence spanning all federal elections since 1953 suggests that confessional affiliation itself, rather than religiosity alone, is a key driver of these patterns.

Catholic respondents are significantly more likely to vote for the *Union* even after conditioning on self-reported religiosity, and this association, while attenuated over time, has persisted for over seven decades. Two complementary mechanisms appear to sustain this alignment. First, Catholics hold distinctively conservative positions on moral and social-policy issues, particularly abortion and euthanasia, that align with the *Union*'s platform. Second, Catholic political identity appears to be transmitted across generations: Catholic respondents are substantially more likely to report parental identification with the *Union*, to describe their own partisan attachment as longstanding, and to express affective ties to the party.

Several limitations and avenues for further research deserve emphasis. The aggregate discontinuity design cannot fully disentangle the role of religion from other enduring legacies of the Reformation, including differences in institutional development, governance capacity, and civic norms. While the individual-level evidence points toward confessional affiliation as a proximate channel, the deeper question of how Catholic and Protestant regions diverged institutionally and culturally over centuries remains open. Future work might exploit within-denomination variation or exogenous shocks to religious practice to isolate the causal contribution of faith more precisely. The absence of economic differences at the historical border is itself a puzzle that merits further investigation, particularly in light of the extensive literature linking the Reformation to differential human capital accumulation and economic growth.

References

Abad, L. A., Maurer, N., et al. (2021). History never really says goodbye: A critical review of the persistence literature. *Journal of Historical Political Economy*, *1*(1), 31–68.

Basten, C., & Betz, F. (2013). Beyond work ethic: Religion, individual, and political preferences. *American Economic Journal: Economic Policy*, *5*(3), 67–91.
URL https://www.aeaweb.org/articles?id=10.1257/pol.5.3.67

Becker, S., Hsiao, Y., Pfaff, S., & Rubin, J. (2025a). Competing social influence in contested diffusion: contention and the spread of the early reformation. *Social Forces*, (p. soaf079).

Becker, S. O., Bentzen, J., & Kok, C. C. (2025b). Gender and religion: A survey.

Becker, S. O., Hsiao, Y., Pfaff, S., & Rubin, J. (2020). Multiplex network ties and the spatial diffusion of radical innovations: Martin luther's leadership in the early reformation. *American Sociological Review*, *85*(5), 857–894.

Becker, S. O., Pfaff, S., & Rubin, J. (2016). Causes and consequences of the protestant reformation. *Explorations in Economic History*, *62*, 1–25.

Becker, S. O., Rubin, J., & Woessmann, L. (2021). Religion in economic history: A survey. *The handbook of historical economics*, (pp. 585–639).

Becker, S. O., Rubin, J., & Woessmann, L. (2024). Religion and growth. *Journal of Economic Literature*, *62*(3), 1094–1142.

Becker, S. O., & Woessmann, L. (2009). Was weber wrong? a human capital theory of protestant economic history. *The quarterly journal of economics*, *124*(2), 531–596.

Becker, S. O., & Woessmann, L. (2010). The effect of protestantism on education before the industrialization: Evidence from 1816 prussia. *Economics Letters*, *107*(2), 224–228.

Becker, S. O., & Woessmann, L. (2011). The effects of the protestant reformation on human capital. *The Oxford Handbook of the Economics of Religion*, (pp. 93–110).

BKG (2021a). Administrative areas 1:250,000 - vg250 and vg250-ew documentation. URL https://www.bkg.bund.de

BKG (2021b). Digitales Geländemodell Gitterweite 200 m (DGM200). URL https://www.bkg.bund.de

Boppart, T., Falkinger, J., & Grossmann, V. (2014). Protestantism and education: Reading (the bible) and other skills. *Economic Inquiry*, *52*(2), 874–895.

Boppart, T., Falkinger, J., Grossmann, V., Woitek, U., & Wüthrich, G. (2013). Under which conditions does religion affect educational outcomes? *Explorations in Economic History*, *50*(2), 242–266.

Breidenbach, P., & Eilers, L. (2018). Rwi-geo-grid: Socio-economic data on grid level. *Jahrbücher für Nationalökonomie und Statistik*, *238*(6), 609–616. URL https://doi.org/10.1515/jbnst-2017-0171

Brügger, B., Lalive, R., & Zweimüller, J. (2009). Does culture affect unemployment?: evidence from the röstigraben. Tech. rep., CESifo Working Paper.

Buccione, G., & Knight, B. G. (2024). The rise of the religious right: Evidence from the moral majority and the jimmy carter presidency. Tech. rep., National Bureau of Economic Research.

Calonico, S., Cattaneo, M. D., Farrell, M. H., & Titiunik, R. (2019). Regression discontinuity designs using covariates. *Review of Economics and Statistics*, *101*(3), 442–451.

Campante, F., & Yanagizawa-Drott, D. (2015). Does religion affect economic growth and happiness? evidence from ramadan. *The Quarterly Journal of Economics*, *130*(2), 615–658.

Cantoni, D. (2012). Adopting a new religion: the case of protestantism in 16th century germany. *The Economic Journal*, *122*(560), 502–531.

Cantoni, D., Dittmar, J., & Yuchtman, N. (2018). Religious competition and reallocation: The political economy of secularization in the protestant reformation. *The Quarterly Journal of Economics*, *133*(4), 2037–2096.

Cantoni, D., & Yuchtman, N. (2021). Historical natural experiments: Bridging economics and economic history. In *The handbook of historical economics*, (pp. 213–241). Elsevier.

Carvalho, J.-P., Iyer, S., & Rubin, J. (2019). *Advances in the Economics of Religion*. Springer.

Cattaneo, M. D., Idrobo, N., & Titiunik, R. (2024). *A practical introduction to regression discontinuity designs: Extensions*. Cambridge University Press.

Cattaneo, M. D., Titiunik, R., & Yu, R. R. (2025). Estimation and inference in boundary discontinuity designs: Location-based methods.

Cirone, A., & Pepinsky, T. B. (2022). Historical persistence. *Annual Review of Political Science*, *25*(1), 241–259.

Conradt, D. P. (2025). Christian democratic union. https://www.britannica.com/topic/Christian-Democratic-Union-political-party-Germany. Accessed 18 June 2025.

Dell, M. (2010). The persistent effects of peru's mining mita. *Econometrica*, *78*(6), 1863–1903.

Dittmar, J., & Seabold, S. (2015). Media, markets and institutional change: evidence from the protestant reformation. Tech. rep., London School of Economics and Political Science, LSE Library.

Dittmar, J. E., & Meisenzahl, R. R. (2020). Public goods institutions, human capital, and growth: Evidence from german history. *The Review of Economic Studies*, *87*(2), 959–996.

Fremerey, M., Hörnig, L., & Schaffner, S. (2021). RWI-GEO-VOTE: Vote Share of the German Federal Election 2017 on grid level. Data set, In RWI-GEO.
URL https://doi.org/10.7807/vote:share:2017:v1

Frieden, I., Peichl, A., & Schüle, P. (2023). Regional income inequality in germany. In *EconPol Forum*, vol. 24, (pp. 50–55). Munich: CESifo GmbH.

Gerber, A. S., Gruber, J., & Hungerman, D. M. (2016). Does church attendance cause people to vote? using blue laws' repeal to estimate the effect of religiosity on voter turnout. *British Journal of Political Science*, *46*(3), 481–500.

GESIS (2024). German general social survey allbus - cumulation 1980-2021. (ZA5284; Version 1.1.0) [Data set]. GESIS, Cologne. https://doi.org/10.4232/1.14333.

GLES (2024). Gles cross-section 2009-2021, cumulation. (ZA6835; Version 2.0.0) [Data set]. GESIS, Cologne. https://doi.org/10.4232/1.14389.

GLES (2025). Gles cross-section 2025, post-election. (ZA10100; Version 2.0.0) [Data set]. GESIS, Cologne. https://doi.org/10.4232/5.ZA10100.2.0.0.

Goldewijk, K. K. (2001). Estimating global land use change over the past 300 years: the hyde database. *Global biogeochemical cycles*, *15*(2), 417–433.

Heddesheimer, V., Hilbig, H., Sichart, F., & Wiedemann, A. (2025). Gerda: The german election database. *Scientific Data*, *12*, 618.
URL https://www.nature.com/articles/s41597-025-04811-5

Institut für Demoskopie, A., Reigrotzki, E., Scheuch, E. K., Wildenmann, R., Baumert, G., Berger, M., Kaase, M., Schleth, U., Fuchs, D., Klingemann, H.-D., Pappi, F. U., Küchler, M., Forschungsgruppe Wahlen, M., Semetko, H. A., Mannheimer Zentrum für Europäische Sozialforschung (MZES), M., Wissenschaftszentrum Berlin für Sozialforschung (WZB), B., Jung, M., Zentralarchiv für Empirische Sozialforschung, U. z. K., Falter, J. W., Gabriel,

O. W., Rattinger, H., Kühnel, S., Niedermayer, O., Westle, B., Roth, D., Gibowski, W. G., Gruber, E., & Schulte, W. (2007). Post-election surveys on federal parliament election 1949-2005 (cumulated variable selection). (ZA4519; Version 1.0.0) [Data set]. GESIS, Cologne. https://doi.org/10.4232/1.4519.

Iyer, S. (2016). The new economics of religion. *Journal of Economic Literature*, *54*(2), 395–441.

Jardim, E., Long, M. C., Plotnick, R., Vigdor, J., & Wiles, E. (2024). Local minimum wage laws, boundary discontinuity methods, and policy spillovers. *Journal of Public Economics*, *234*, 105131.

Keele, L., Lorch, S., Passarella, M., Small, D., & Titiunik, R. (2017). An overview of geographically discontinuous treatment assignments with an application to children's health insurance. *Regression discontinuity designs: Theory and applications*, (pp. 147–194).

Keele, L., & Titiunik, R. (2016). Natural experiments based on geography. *Political Science Research and Methods*, *4*(1), 65–95.

Keele, L. J., & Titiunik, R. (2015). Geographic boundaries as regression discontinuities. *Political Analysis*, *23*(1), 127–155.

Kim, H., & Pfaff, S. (2012). Structure and dynamics of religious insurgency: Students and the spread of the reformation. *American Sociological Review*, *77*(2), 188–215.

Kunz, A. (2014). Digitaler atlas zur geschichte europas seit 1500. Accessed: 2025-02-22. URL https://www.atlas-europa.de/intern/project.htm

Lanzara, G., Lazzaroni, S., Masella, P., & Squicciarini, M. P. (2024). Do bishops matter for politics? evidence from italy. *Journal of Public Economics*, *238*, 105177.

Lehner, B., & Grill, G. (2013). Global river hydrography and network routing: baseline

data and new approaches to study the world's large river systems. *Hydrological Processes*, *27*(15), 2171–2186.

Lowes, S., Marx, B., & Montero, E. (2025). Religion in emerging and developing regions. Tech. rep., National Bureau of Economic Research.

McCleary, R. M., & Barro, R. J. (2006). Religion and economy. *Journal of Economic perspectives*, *20*(2), 49–72.

Mello, M., & Buccione, G. (2023). Religious media, conversion, and the socioeconomic consequences: The rise of pentecostals in brazil.

Montero, E., & Yang, D. (2022). Religious festivals and economic development: Evidence from the timing of mexican saint day festivals. *American Economic Review*, *112*(10), 3176–3214.

Nowak, K. (1995). *Geschichte des Christentums in Deutschland: Religion, Politik und Gesellschaft vom Ende der Aufklärung bis zur Mitte des 20. Jahrhunderts;[mit 11 Tabellen]*. Beck.

Nunn, N. (2020). The historical roots of economic development. *Science*, *367*(6485), eaaz9986.

Openshaw, S. (1984). The modifiable areal unit problem. *Concepts and techniques in modern geography*.

Ozment, S. (Ed.) (1982). *Reformation Europe: A Guide to Research*. St. Louis: Center for Reformation Research.

Pew Research Center (2019). Once a majority, protestants now account for fewer than a third of germans. Accessed June 17, 2025.
URL https://www.pewresearch.org/short-reads/2019/02/12/once-a-majority-protestants-now-account-for-fewer-than-a-third-of-germans/

Pulejo, M. (2024). Religious mobilization and the selection of political elites: Evidence from postwar italy. *American Journal of Political Science*, *68*(4), 1498–1513.

Rubin, J. (2014). Printing and protestants: an empirical test of the role of printing in the reformation. *Review of Economics and Statistics*, *96*(2), 270–286.

Scheve, K., Stasavage, D., et al. (2006). Religion and preferences for social insurance. *Quarterly Journal of Political Science*, *1*(3), 255–286.

Schleunes, K. A., Hamerow, T. S., Kirby, G. H., Strauss, G., Duggan, L. G., Bayley, C. C., Barkin, K., Geary, P. J., Elkins, T. H., Berentsen, W. H., Turner, H. A., Sheehan, J. J., Wallace-Hadrill, J. M., Leyser, K. J., & Heather, P. J. (2025). Germany. *Encyclopædia Britannica*, 12 Jun. 2025. Accessed 13 June 2025.
URL https://www.britannica.com/place/Germany

Scribner, R. W., & Dixon, C. S. (2003). *The German Reformation*. Studies in European History. Basingstoke: Palgrave Macmillan, 2 ed.

Solá, D. (2024). Brother votes for brother: The effects of pentecostal political influence in brazil.

Spenkuch, J. L. (2017). Religion and work: Micro evidence from contemporary germany. *Journal of Economic Behavior & Organization*, *135*, 193–214.

Spenkuch, J. L., & Tillmann, P. (2018). Elite influence? religion and the electoral success of the nazis. *American Journal of Political Science*, *62*(1), 19–36.

Statistisches Bundesamt (2022). Zensus 2022 - germany: Online database. Accessed: 2024-11-21.
URL https://ergebnisse.zensus2022.de/datenbank/online

Weber, M. (1930). *The Protestant Ethic and the Spirit of Capitalism*. London: Allen and Unwin.

Whaley, J. (2012a). *Germany and the Holy Roman Empire: Volume I: Maximilian I to the Peace of Westphalia, 1493-1648*, vol. 1. Oxford University Press.

Whaley, J. (2012b). *Germany and the Holy Roman Empire: Volume II: The Peace of Westphalia to the Dissolution of the Reich, 1648-1806*, vol. 2. Oxford University Press, USA.

A Figures

Figure 1: Distribution of religious affiliation in Germany

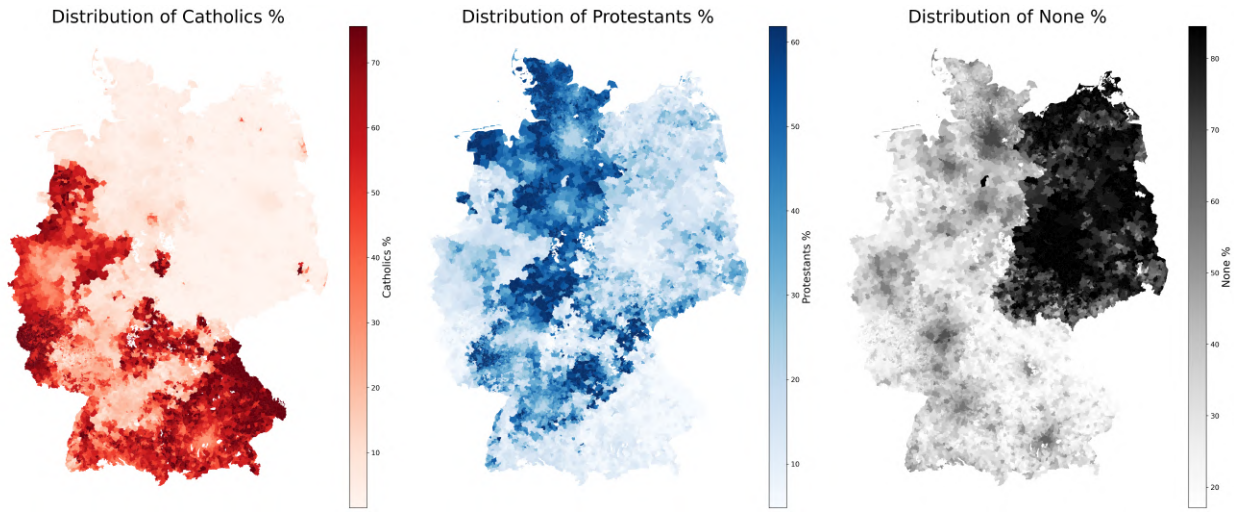

Note: Own elaboration with data from Statistisches Bundesamt (2022)

Figure 2: The Holy Roman Empire in 1648 and the Peace of Westphalia

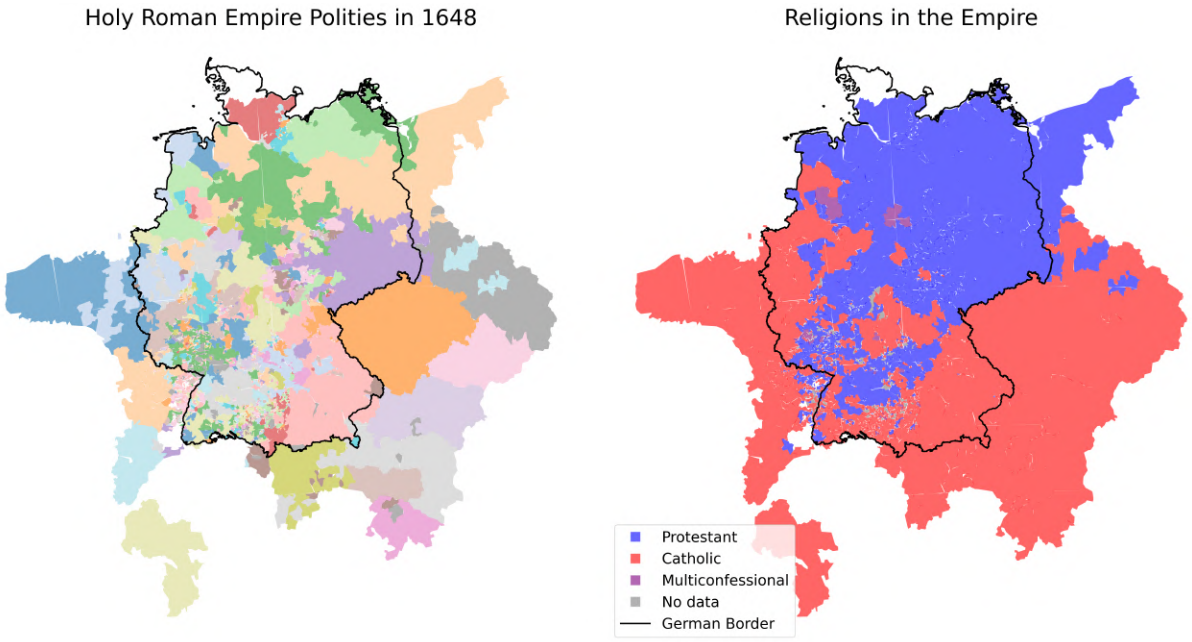

Note: Own elaboration with data from Statistisches Bundesamt (2022)Kunz (2014)

Figure 3: Historically Catholic Regions and Confession Today

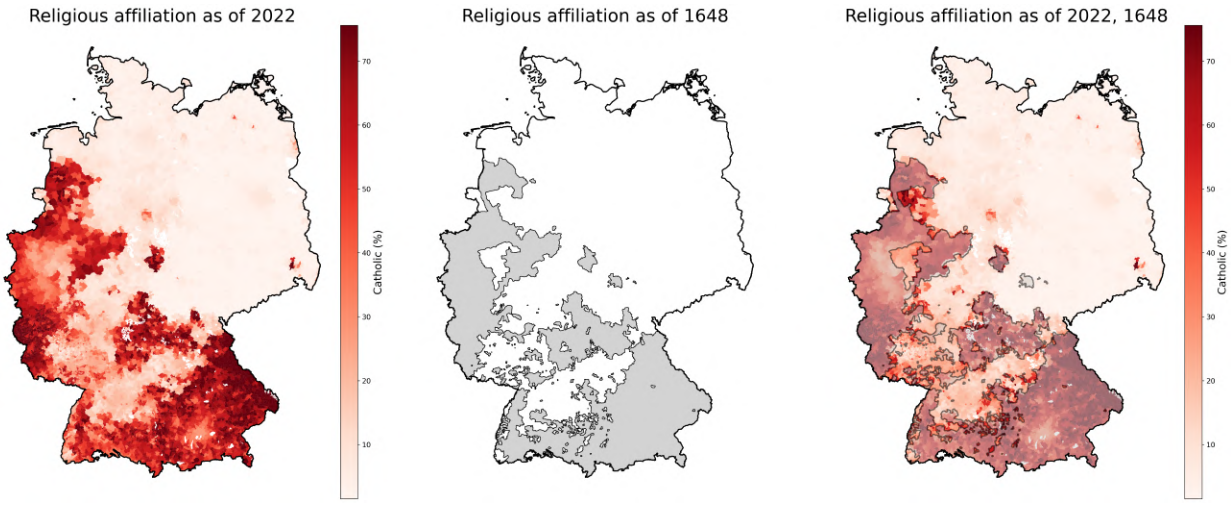

Note: Own elaboration with data from Kunz (2014); Statistisches Bundesamt (2022)

Figure 4: Historically Protestant Regions and Confession Today

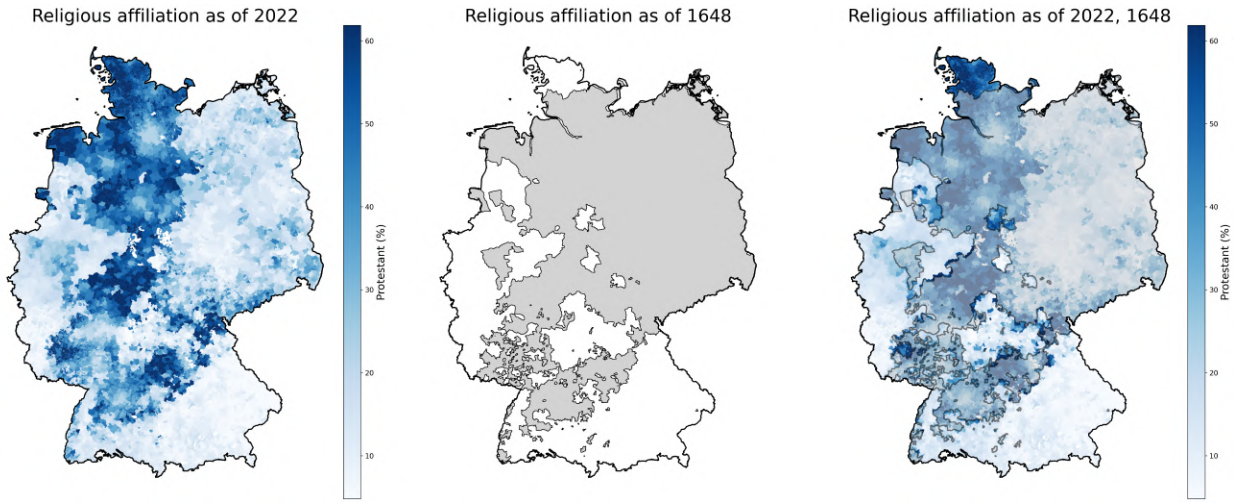

Note: Own elaboration with data from Kunz (2014); Statistisches Bundesamt (2022)

Figure 5: Visualization of the Empirical Strategy

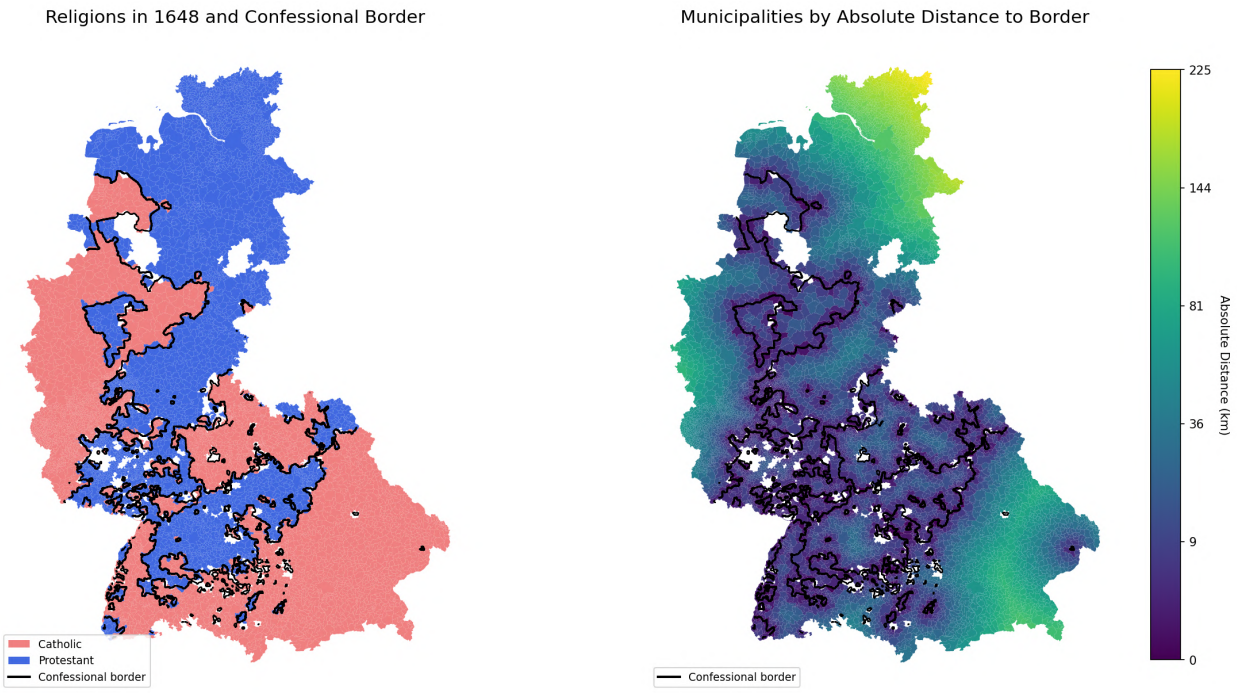

Note: Own elaboration with data from Kunz (2014)

Figure 6: Share of Catholics as of 2022 and Distance to the Confessional Border

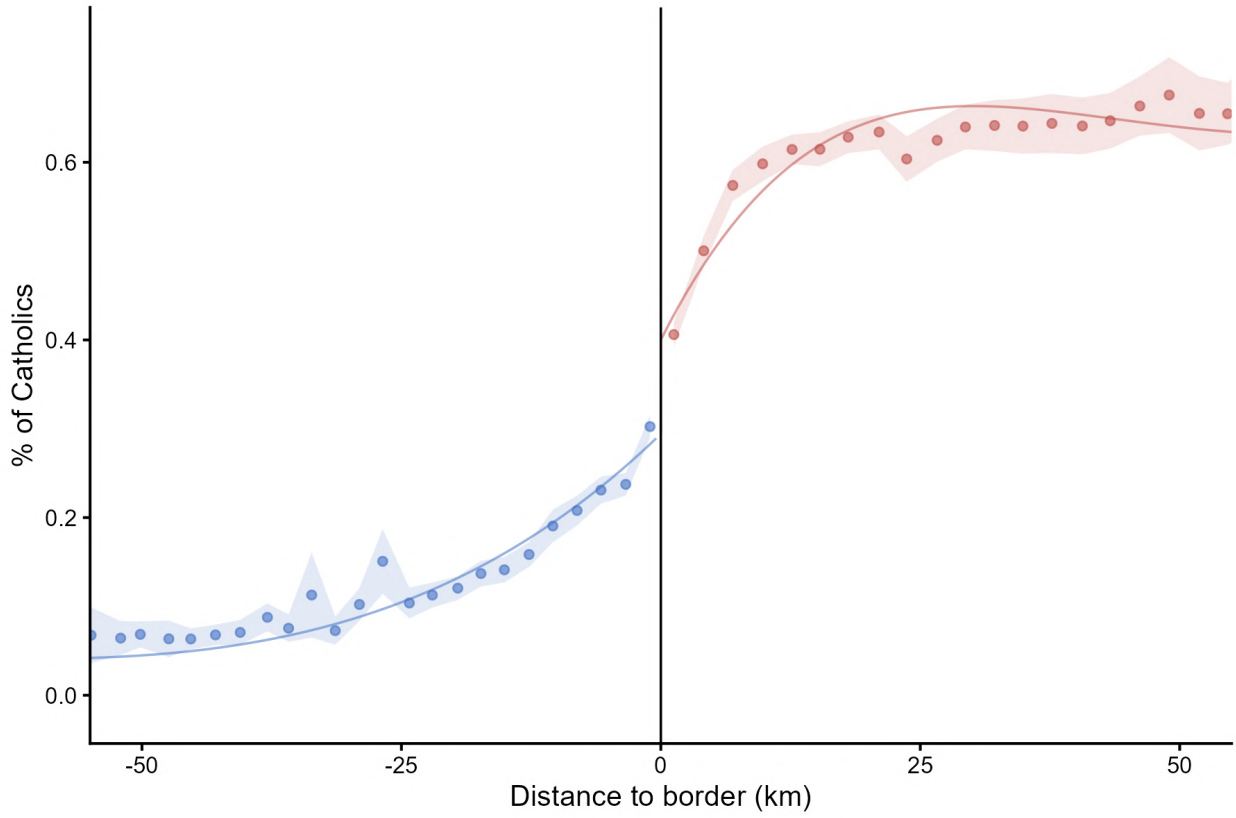

Note: Each dot represents the mean outcome within an evenly spaced bin of the running variable on either side of the cutoff (negative values on the horizontal axis denote historically Protestant municipalities while positive values refer to historically Catholic municipalities). Ribbons indicate 95% confidence intervals. The solid red line shows a fourth-order polynomial fit estimated using a uniform kernel. Bandwidths are selected separately on each side of the threshold using the MSE-optimal two-bandwidth selector.

Figure 7: CDU/CSU Vote Share (1990 - 2009) and Distance to the Confessional Border

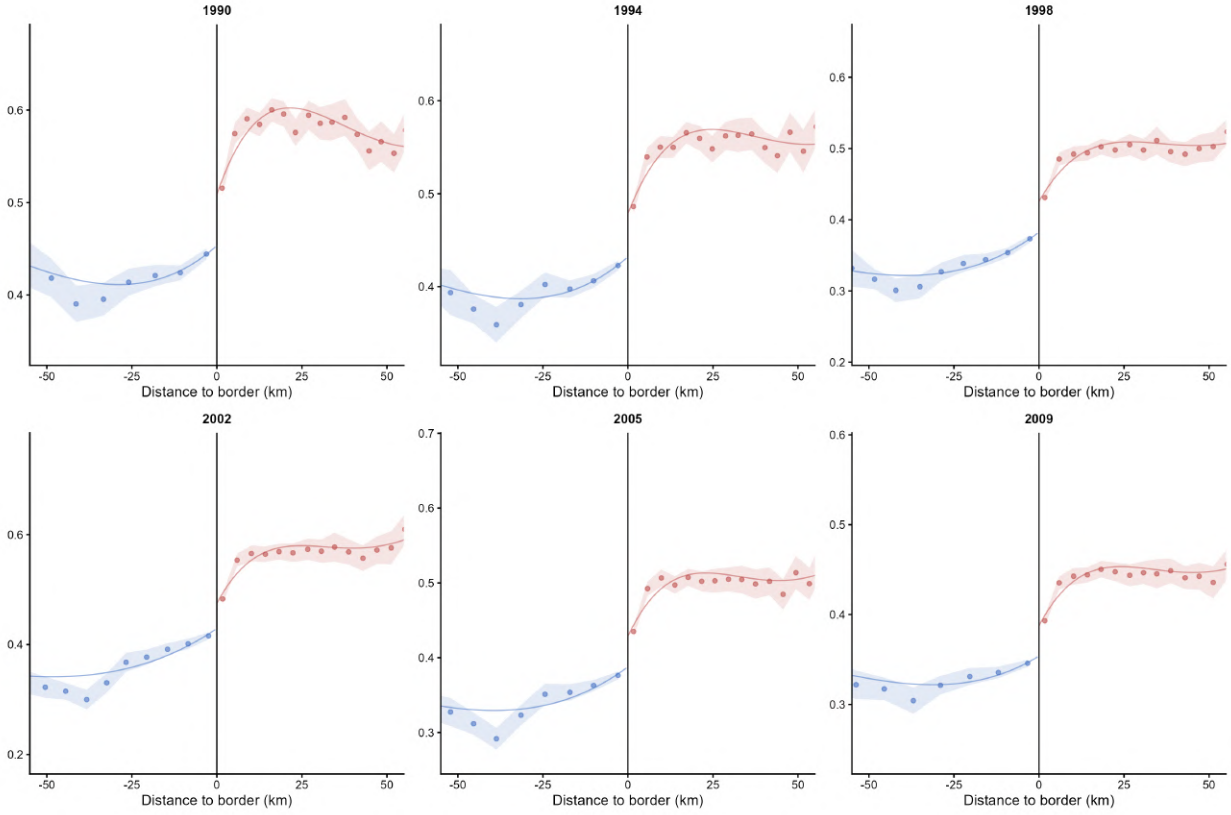

Note: Each dot represents the mean outcome within an evenly spaced bin of the running variable on either side of the cutoff (negative values on the horizontal axis denote historically Protestant municipalities while positive values refer to historically Catholic municipalities). Ribbons indicate 95% confidence intervals. The solid red line shows a fourth-order polynomial fit estimated using a uniform kernel. Bandwidths are selected separately on each side of the threshold using the MSE-optimal two-bandwidth selector.

Figure 8: CDU/CSU Vote Share (2013 - 2025) and Distance to the Confessional Border

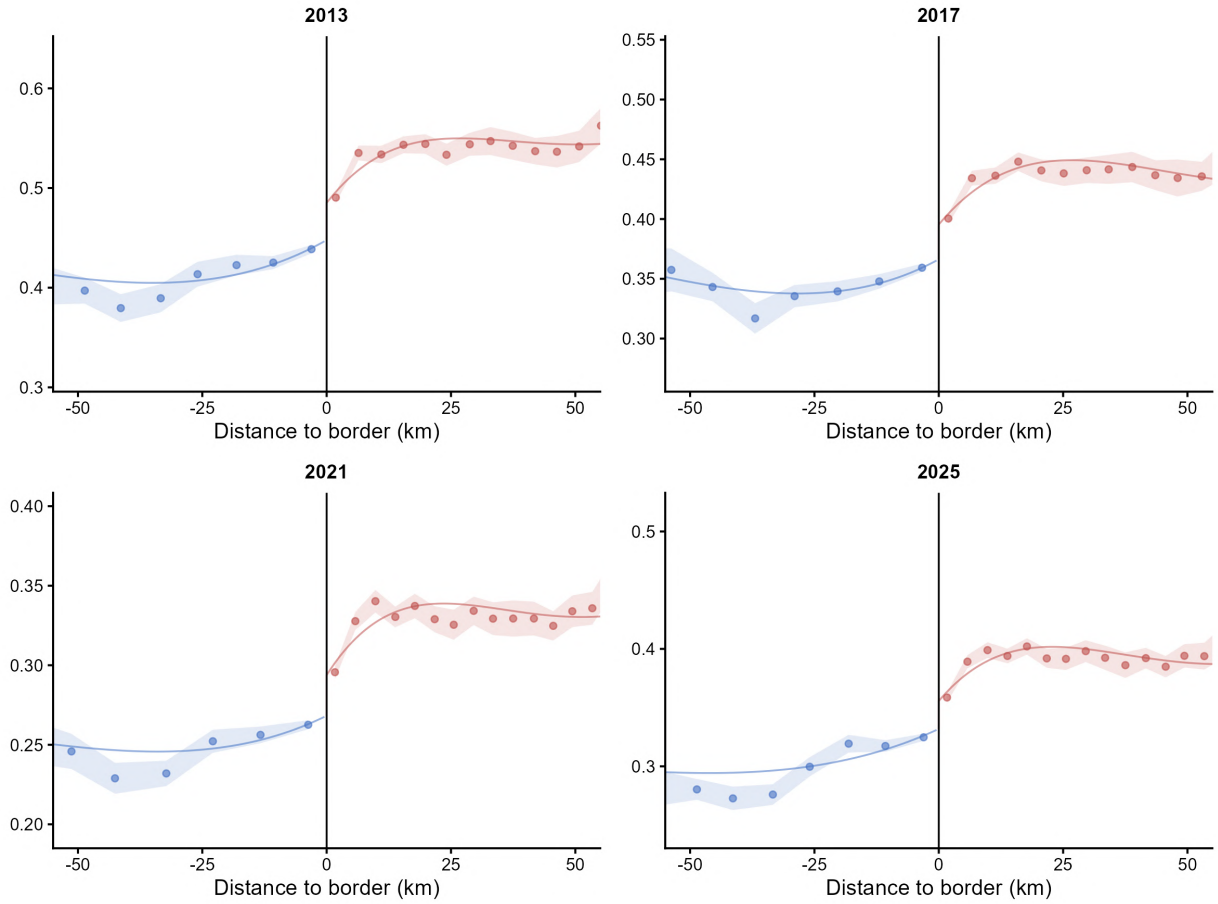

Note: Each dot represents the mean outcome within an evenly spaced bin of the running variable on either side of the cutoff (negative values on the horizontal axis denote historically Protestant municipalities while positive values refer to historically Catholic municipalities). Ribbons indicate 95% confidence intervals. The solid red line shows a fourth-order polynomial fit estimated using a uniform kernel. Bandwidths are selected separately on each side of the threshold using the MSE-optimal two-bandwidth selector.

Figure 9: SPD Vote Share (1990 - 2009) and Distance to the Confessional Border

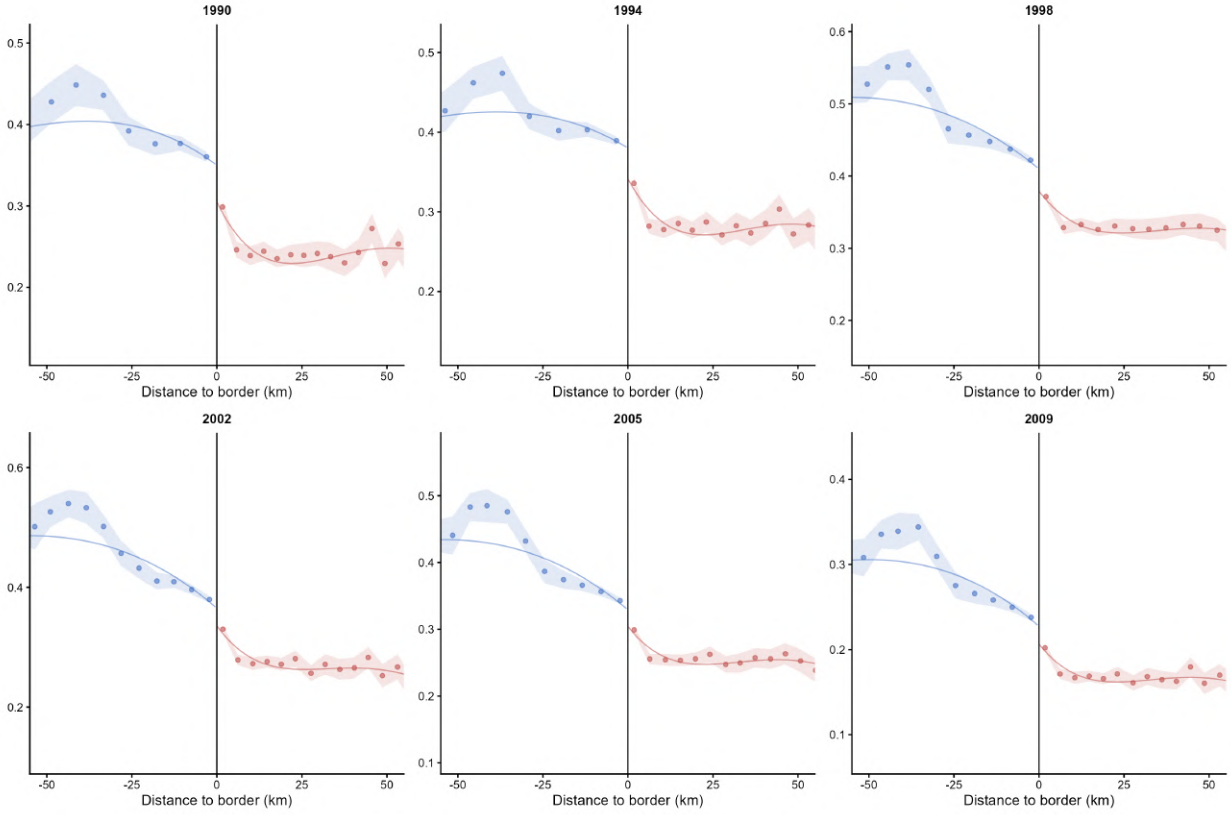

Note: Each dot represents the mean outcome within an evenly spaced bin of the running variable on either side of the cutoff (negative values on the horizontal axis denote historically Protestant municipalities while positive values refer to historically Catholic municipalities). Ribbons indicate 95% confidence intervals. The solid red line shows a fourth-order polynomial fit estimated using a uniform kernel. Bandwidths are selected separately on each side of the threshold using the MSE-optimal two-bandwidth selector.

Figure 10: SPD Vote Share (2013 - 2025) and Distance to the Confessional Border

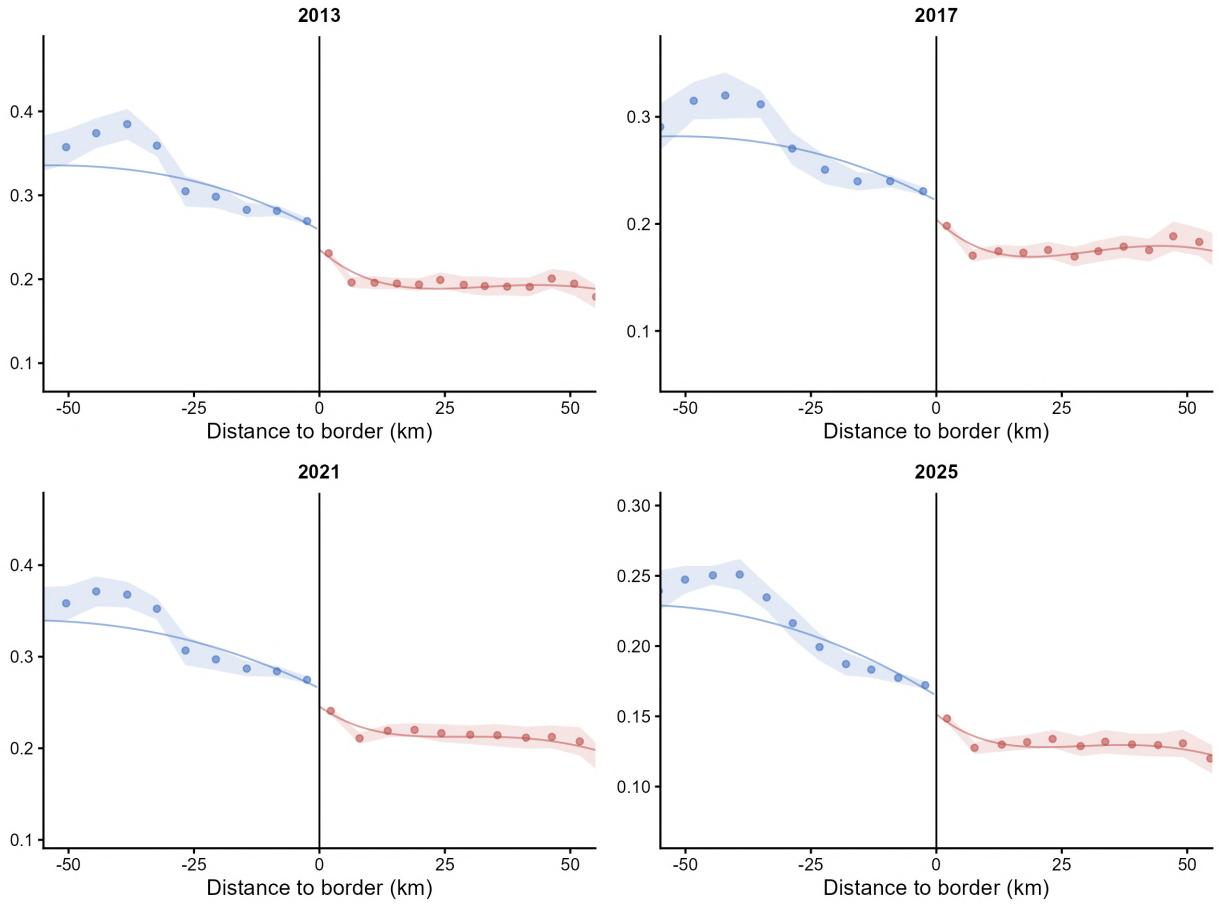

Note: Each dot represents the mean outcome within an evenly spaced bin of the running variable on either side of the cutoff (negative values on the horizontal axis denote historically Protestant municipalities while positive values refer to historically Catholic municipalities). Ribbons indicate 95% confidence intervals. The solid red line shows a fourth-order polynomial fit estimated using a uniform kernel. Bandwidths are selected separately on each side of the threshold using the MSE-optimal two-bandwidth selector.

Figure 11: Far-Left Vote Share (1990 - 2009) and Distance to the Confessional Border

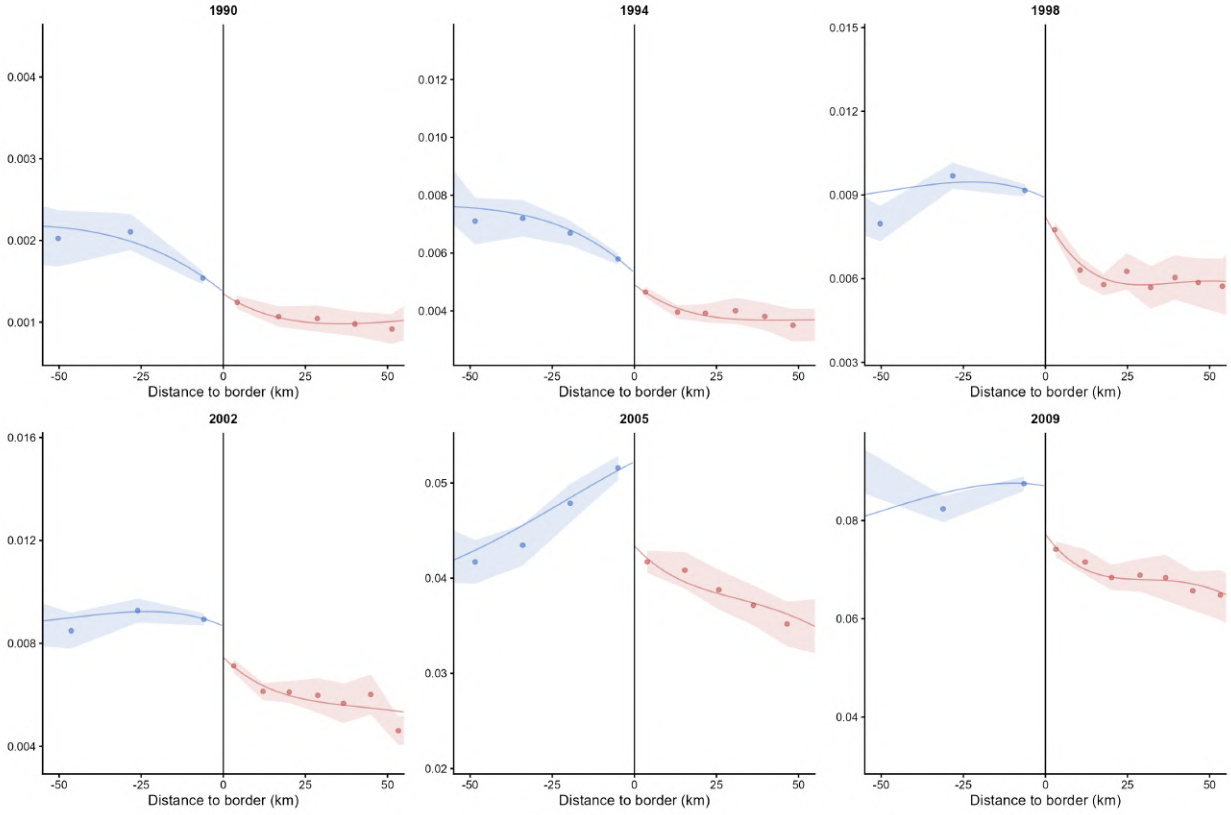

Note: Each dot represents the mean outcome within an evenly spaced bin of the running variable on either side of the cutoff (negative values on the horizontal axis denote historically Protestant municipalities while positive values refer to historically Catholic municipalities). Ribbons indicate 95% confidence intervals. The solid red line shows a fourth-order polynomial fit estimated using a uniform kernel. Bandwidths are selected separately on each side of the threshold using the MSE-optimal two-bandwidth selector.

Figure 12: Far-Left Vote Share (2013 - 2025) and Distance to the Confessional Border

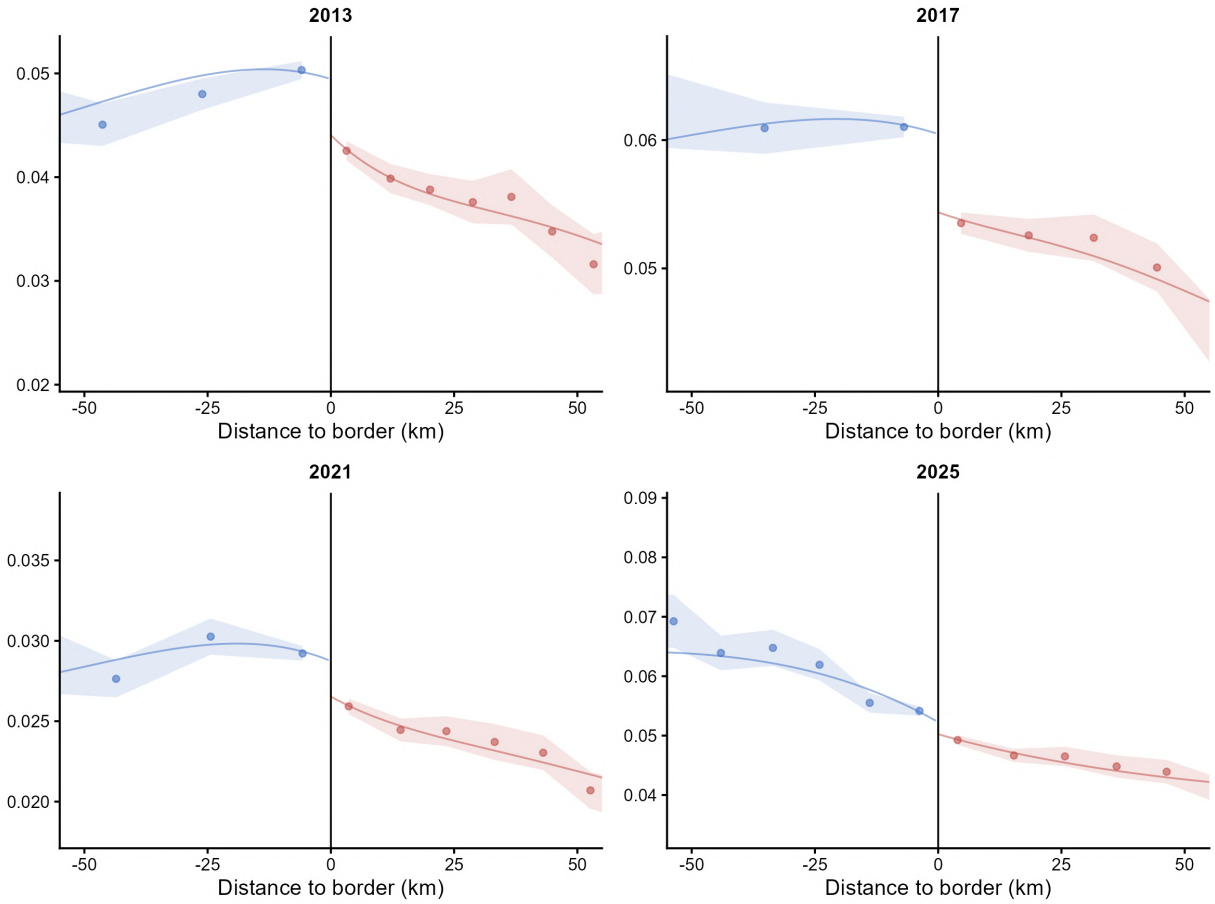

Note: Each dot represents the mean outcome within an evenly spaced bin of the running variable on either side of the cutoff (negative values on the horizontal axis denote historically Protestant municipalities while positive values refer to historically Catholic municipalities). Ribbons indicate 95% confidence intervals. The solid red line shows a fourth-order polynomial fit estimated using a uniform kernel. Bandwidths are selected separately on each side of the threshold using the MSE-optimal two-bandwidth selector.

Figure 13: Far-Right Vote Share (1990 - 2009) and Distance to the Confessional Border

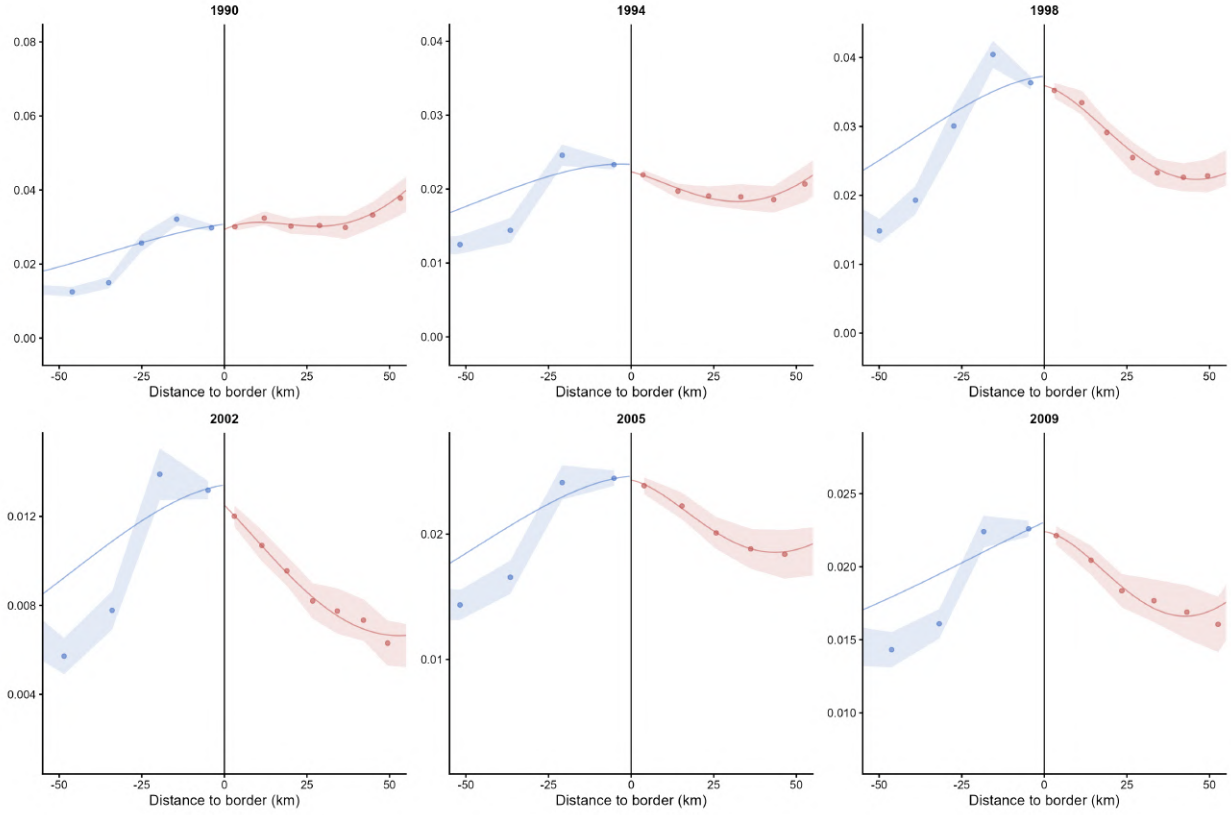

Note: Each dot represents the mean outcome within an evenly spaced bin of the running variable on either side of the cutoff (negative values on the horizontal axis denote historically Protestant municipalities while positive values refer to historically Catholic municipalities). Ribbons indicate 95% confidence intervals. The solid red line shows a fourth-order polynomial fit estimated using a uniform kernel. Bandwidths are selected separately on each side of the threshold using the MSE-optimal two-bandwidth selector.

Figure 14: Far-Right Vote Share (2013 - 2025) and Distance to the Confessional Border

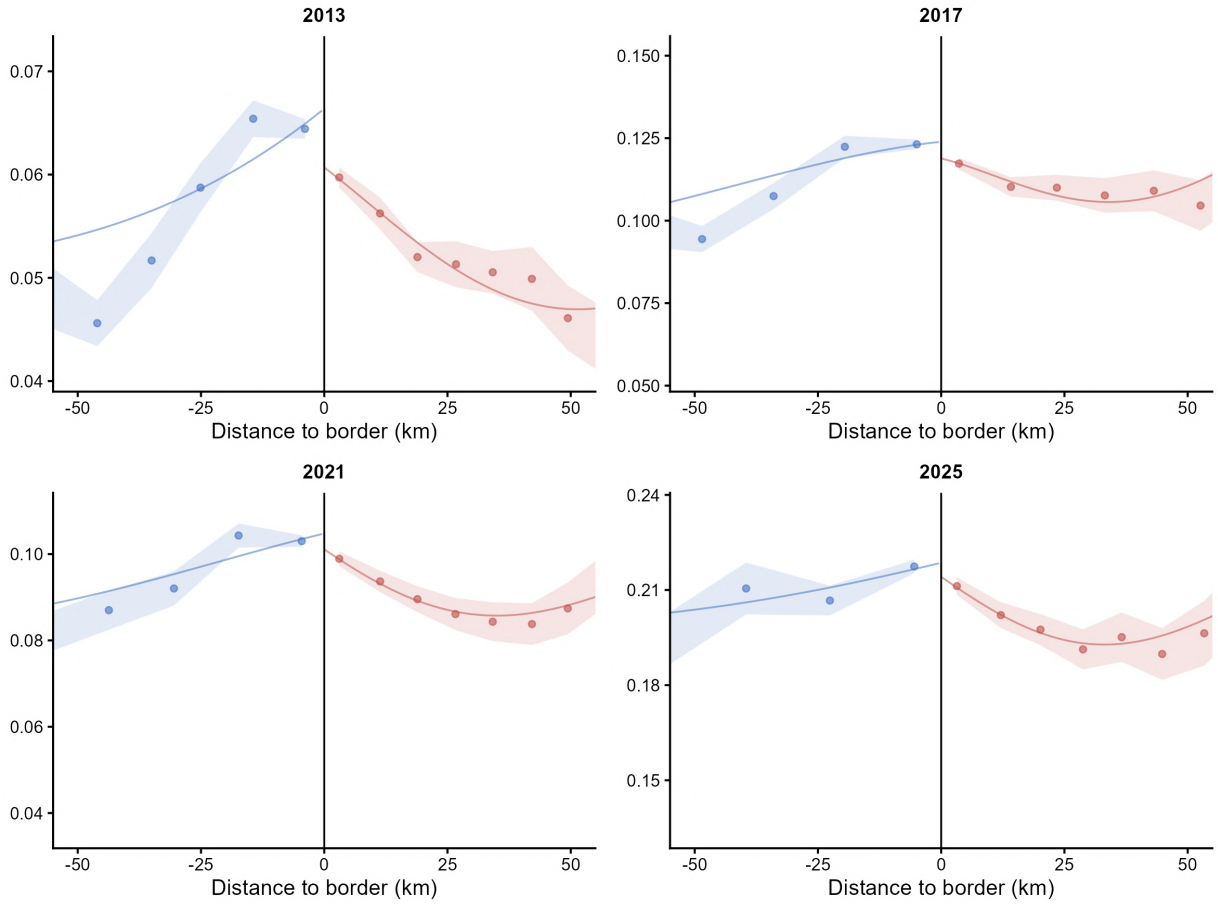

Note: Each dot represents the mean outcome within an evenly spaced bin of the running variable on either side of the cutoff (negative values on the horizontal axis denote historically Protestant municipalities while positive values refer to historically Catholic municipalities). Ribbons indicate 95% confidence intervals. The solid red line shows a fourth-order polynomial fit estimated using a uniform kernel. Bandwidths are selected separately on each side of the threshold using the MSE-optimal two-bandwidth selector.

Figure 15: Greens Vote Share (1990 - 2009) and Distance to the Confessional Border

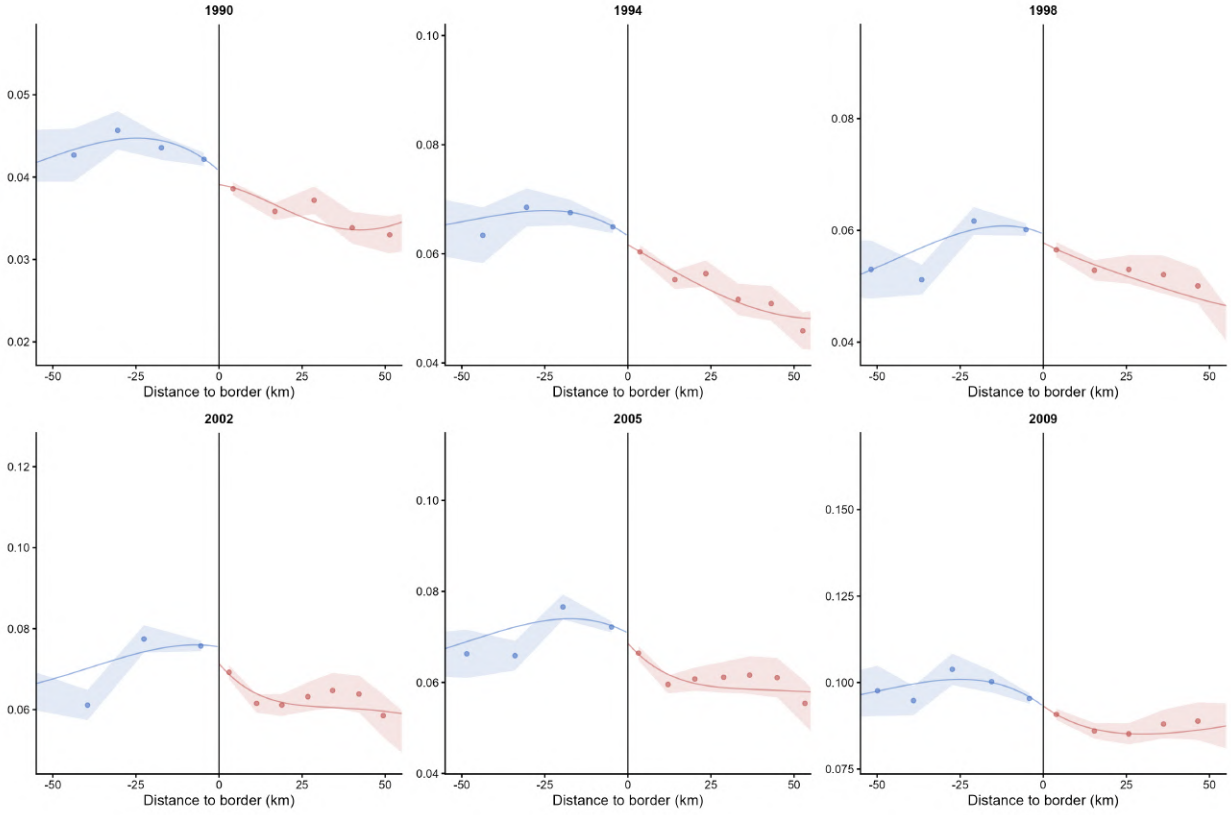

Note: Each dot represents the mean outcome within an evenly spaced bin of the running variable on either side of the cutoff (negative values on the horizontal axis denote historically Protestant municipalities while positive values refer to historically Catholic municipalities). Ribbons indicate 95% confidence intervals. The solid red line shows a fourth-order polynomial fit estimated using a uniform kernel. Bandwidths are selected separately on each side of the threshold using the MSE-optimal two-bandwidth selector.

Figure 16: Greens Vote Share (2013 - 2025) and Distance to the Confessional Border

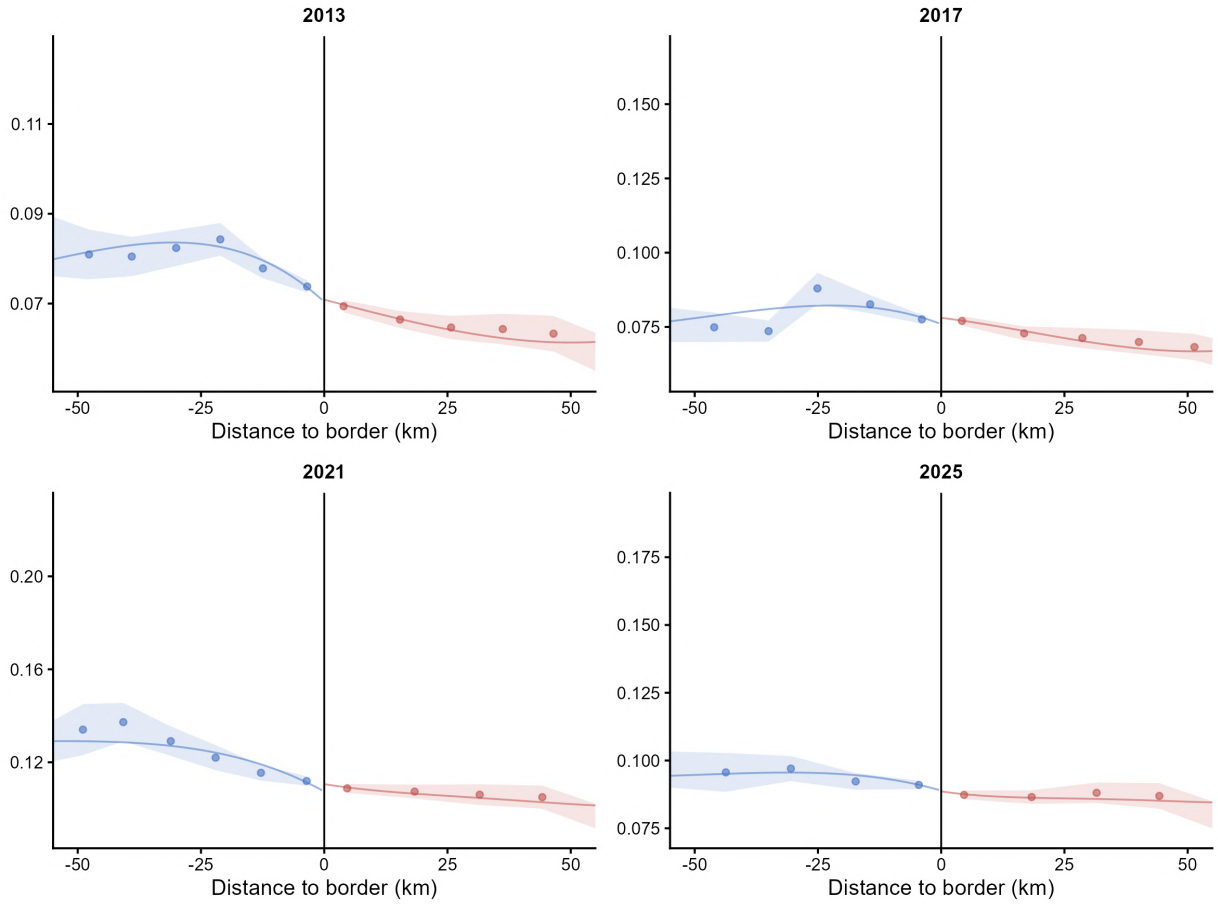

Note: Each dot represents the mean outcome within an evenly spaced bin of the running variable on either side of the cutoff (negative values on the horizontal axis denote historically Protestant municipalities while positive values refer to historically Catholic municipalities). Ribbons indicate 95% confidence intervals. The solid red line shows a fourth-order polynomial fit estimated using a uniform kernel. Bandwidths are selected separately on each side of the threshold using the MSE-optimal two-bandwidth selector.

Figure 17: FDP Vote Share (1990 - 2009) and Distance to the Confessional Border

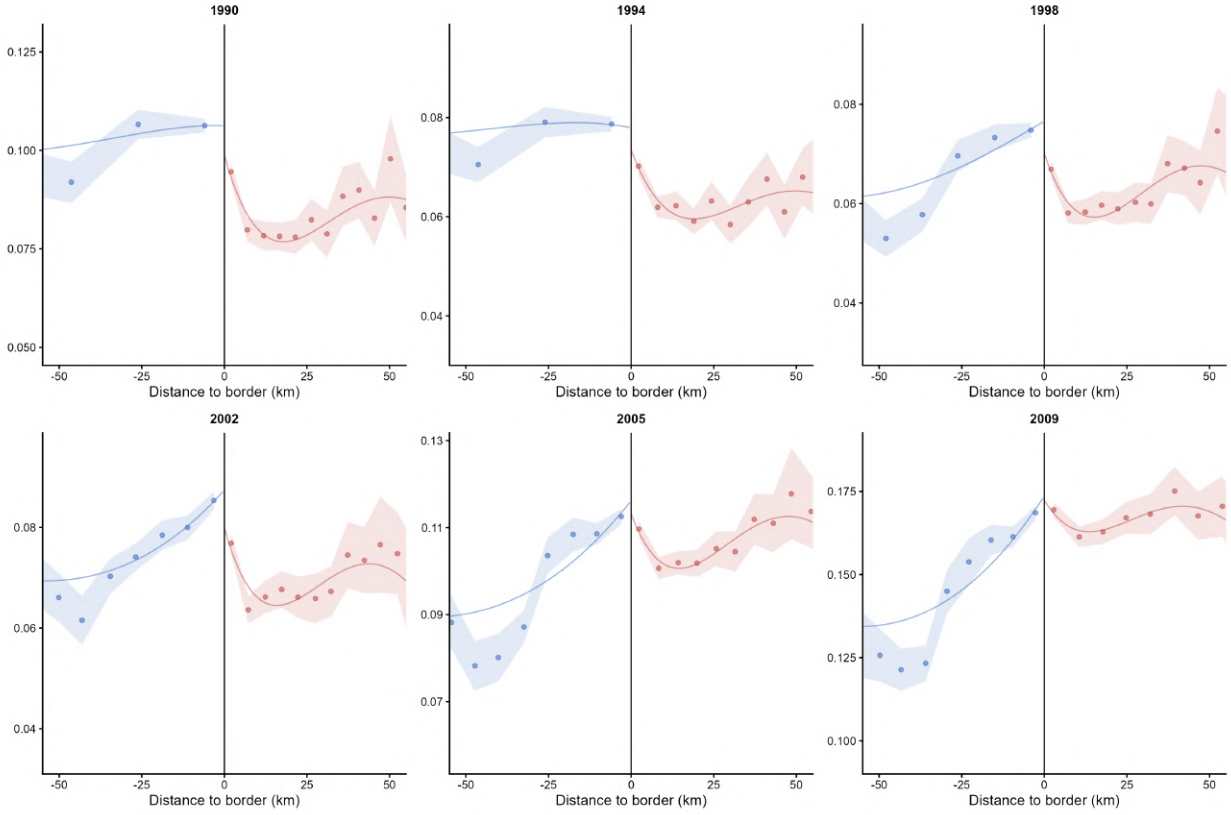

Note: Each dot represents the mean outcome within an evenly spaced bin of the running variable on either side of the cutoff (negative values on the horizontal axis denote historically Protestant municipalities while positive values refer to historically Catholic municipalities). Ribbons indicate 95% confidence intervals. The solid red line shows a fourth-order polynomial fit estimated using a uniform kernel. Bandwidths are selected separately on each side of the threshold using the MSE-optimal two-bandwidth selector.

Figure 18: FDP Vote Share (2013 - 2025) and Distance to the Confessional Border

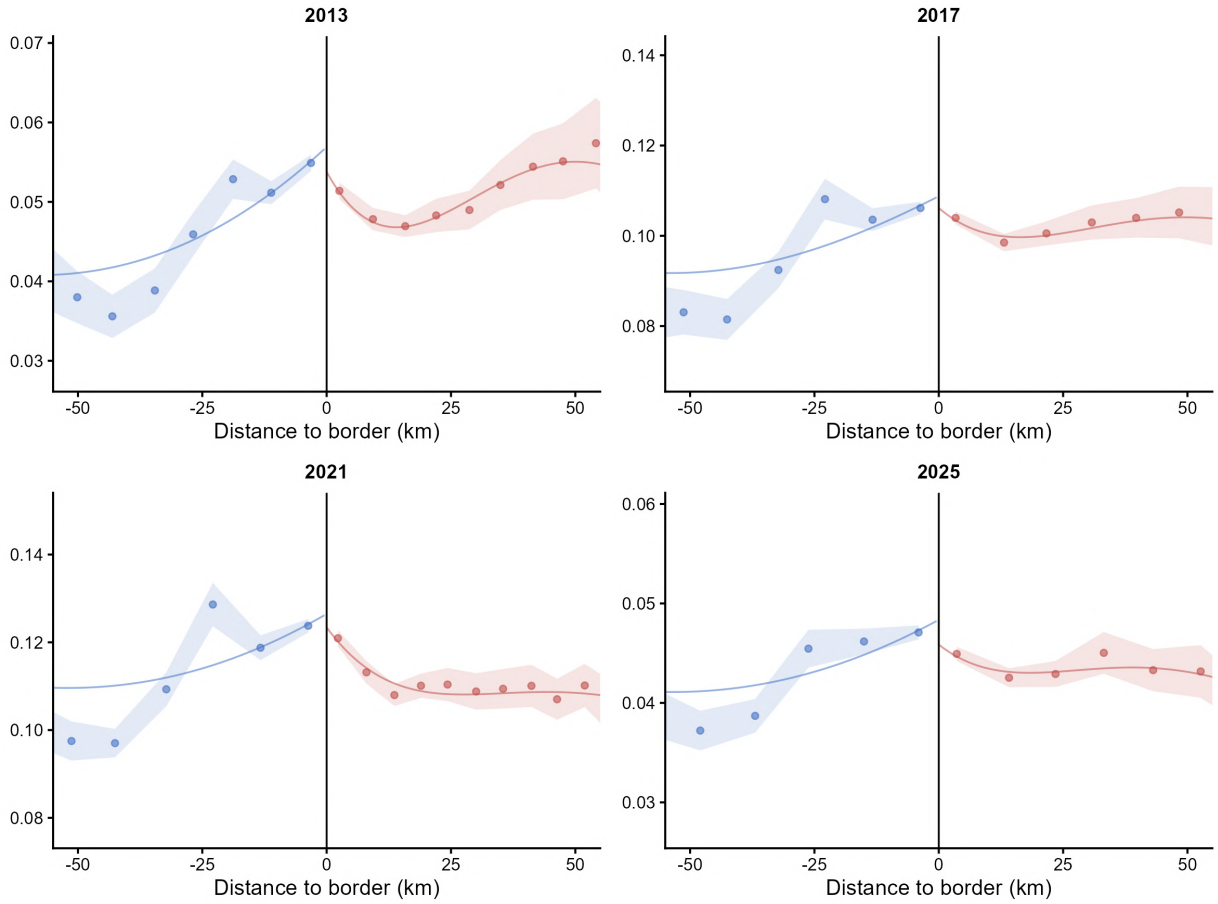

Note: Each dot represents the mean outcome within an evenly spaced bin of the running variable on either side of the cutoff (negative values on the horizontal axis denote historically Protestant municipalities while positive values refer to historically Catholic municipalities). Ribbons indicate 95% confidence intervals. The solid red line shows a fourth-order polynomial fit estimated using a uniform kernel. Bandwidths are selected separately on each side of the threshold using the MSE-optimal two-bandwidth selector.

Figure 19: Average Income (log) (1998 - 2016) and Distance to the Confessional Border

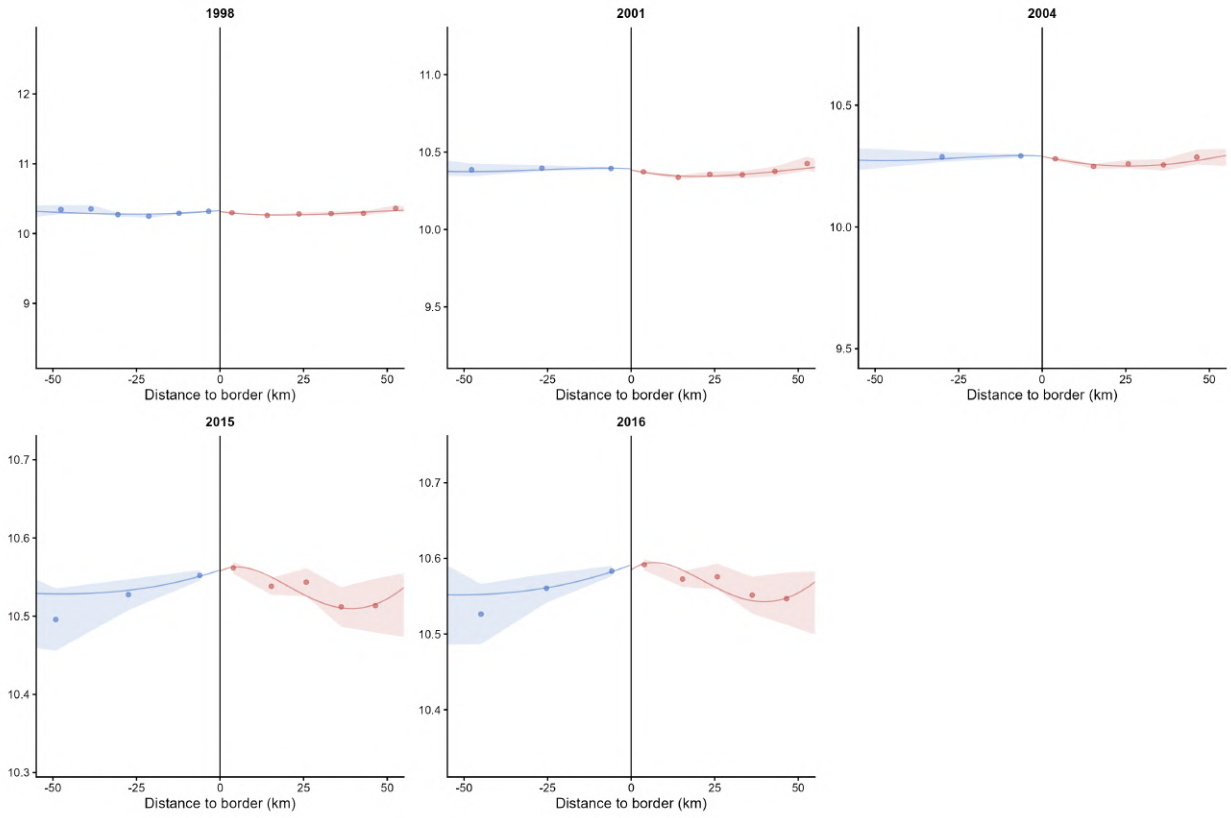

Note: Each dot represents the mean outcome within an evenly spaced bin of the running variable on either side of the cutoff (negative values on the horizontal axis denote historically Protestant municipalities while positive values refer to historically Catholic municipalities). Ribbons indicate 95% confidence intervals. The solid red line shows a fourth-order polynomial fit estimated using a uniform kernel. Bandwidths are selected separately on each side of the threshold using the MSE-optimal two-bandwidth selector.

Figure 20: Capital Tax Adjusted Average Income (log) (1998 - 2016) and Distance to the Confessional Border

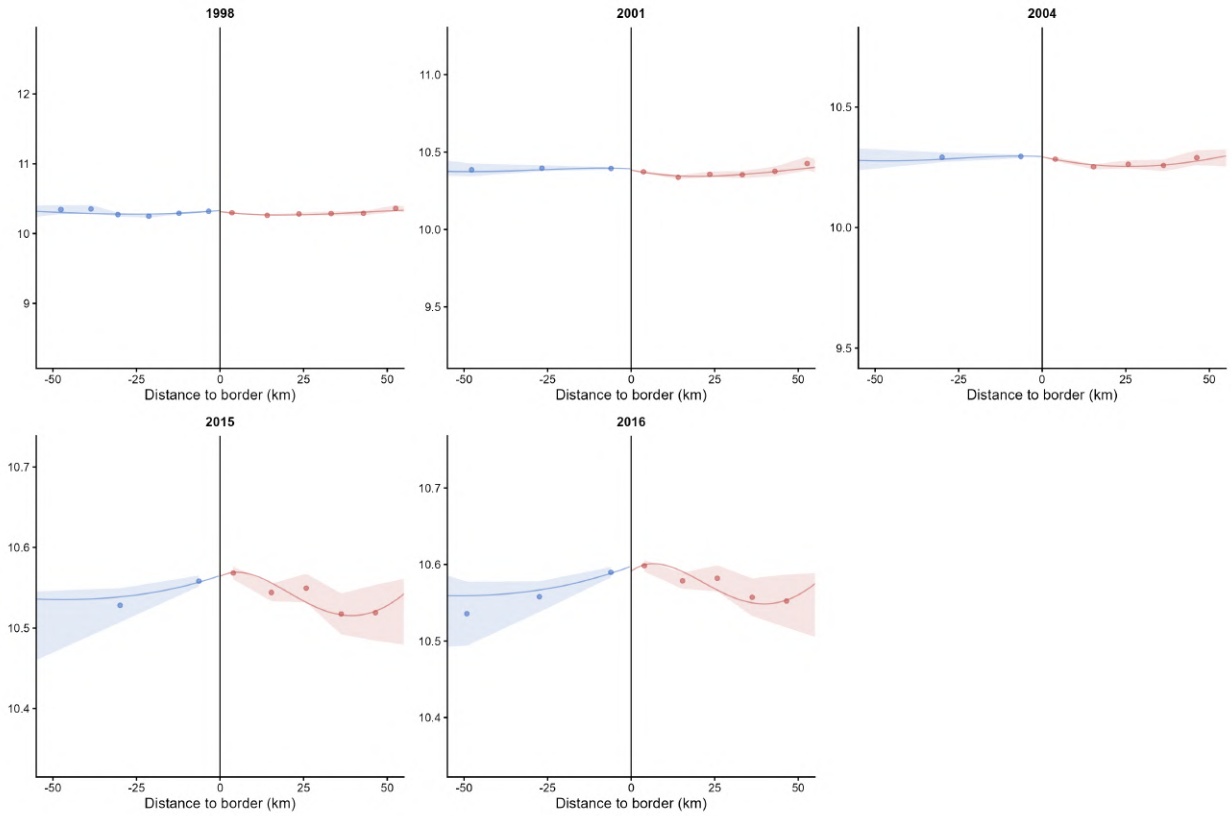

Note: Each dot represents the mean outcome within an evenly spaced bin of the running variable on either side of the cutoff (negative values on the horizontal axis denote historically Protestant municipalities while positive values refer to historically Catholic municipalities). Ribbons indicate 95% confidence intervals. The solid red line shows a fourth-order polynomial fit estimated using a uniform kernel. Bandwidths are selected separately on each side of the threshold using the MSE-optimal two-bandwidth selector.

Figure 21: Gini Index (1998 - 2016) and Distance to the Confessional Border

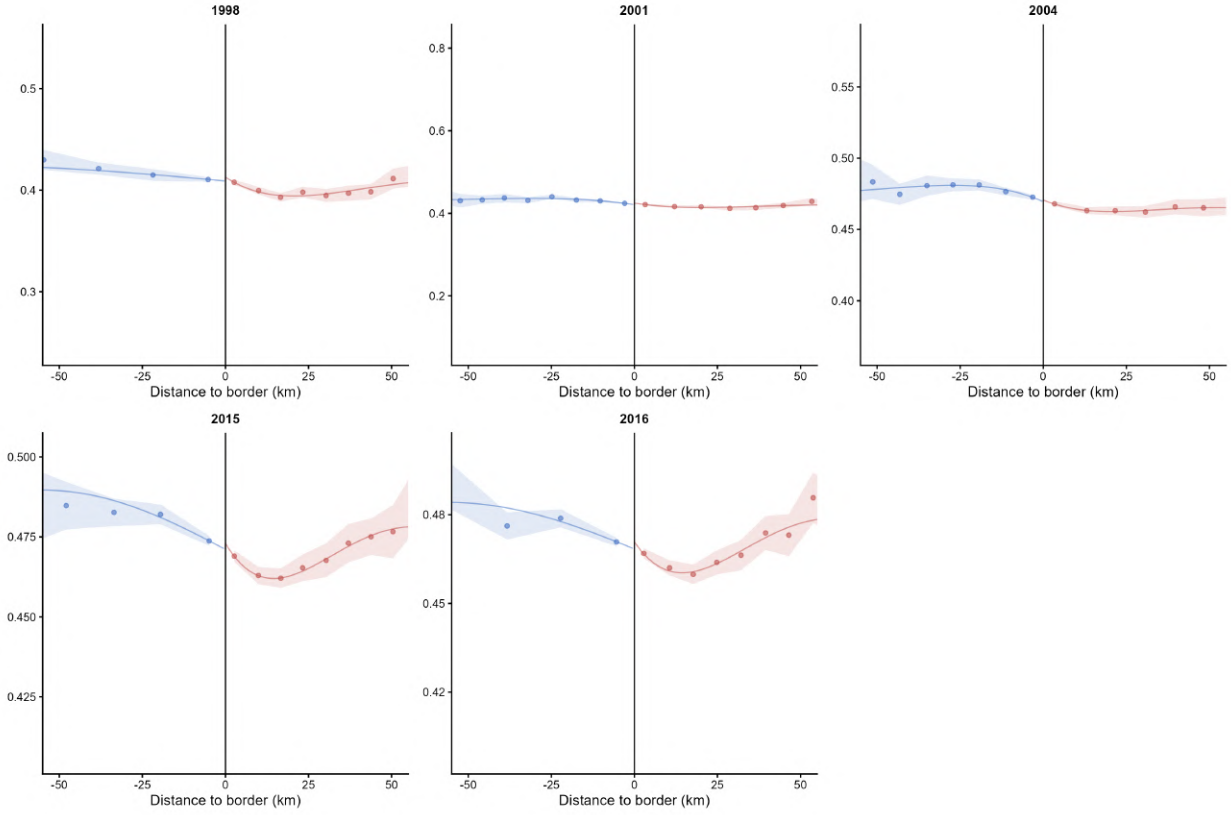

Note: Each dot represents the mean outcome within an evenly spaced bin of the running variable on either side of the cutoff (negative values on the horizontal axis denote historically Protestant municipalities while positive values refer to historically Catholic municipalities). Ribbons indicate 95% confidence intervals. The solid red line shows a fourth-order polynomial fit estimated using a uniform kernel. Bandwidths are selected separately on each side of the threshold using the MSE-optimal two-bandwidth selector.

Figure 22: Theil Index (1998 - 2016) and Distance to the Confessional Border

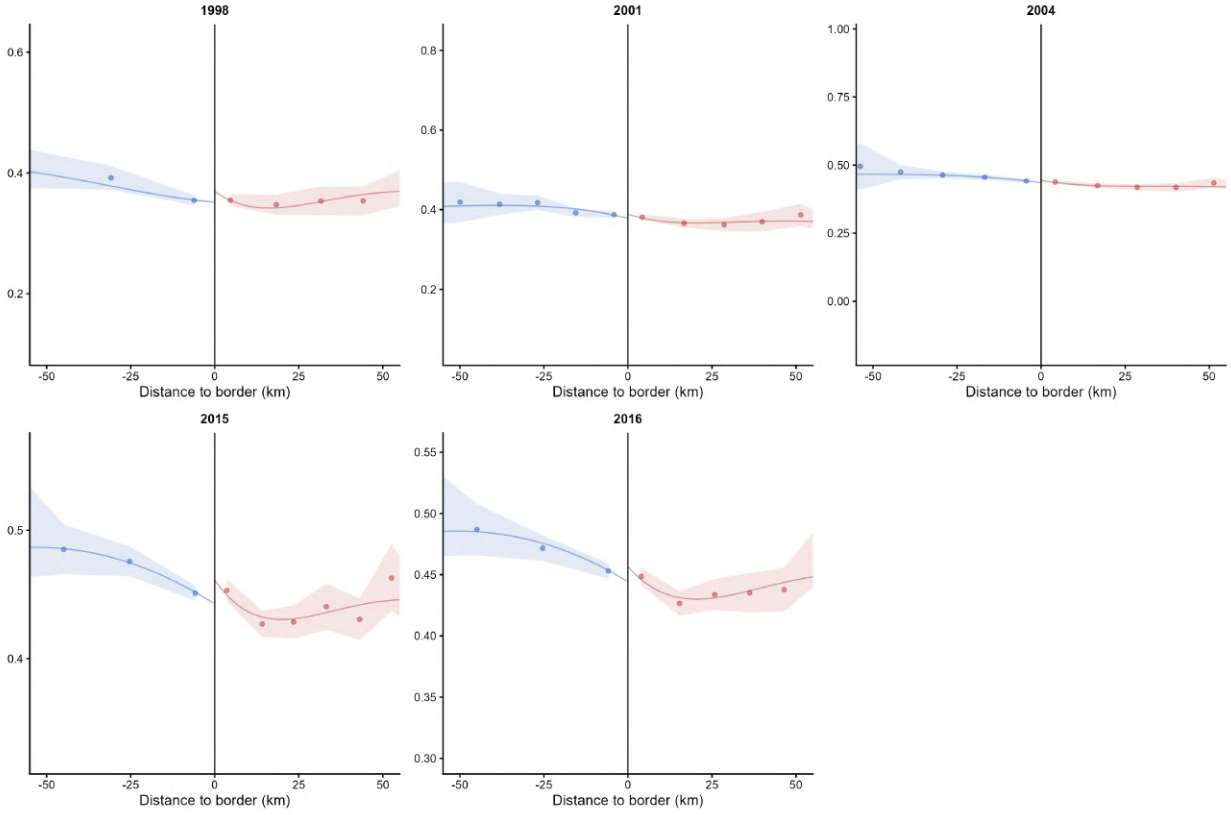

Note: Each dot represents the mean outcome within an evenly spaced bin of the running variable on either side of the cutoff (negative values on the horizontal axis denote historically Protestant municipalities while positive values refer to historically Catholic municipalities). Ribbons indicate 95% confidence intervals. The solid red line shows a fourth-order polynomial fit estimated using a uniform kernel. Bandwidths are selected separately on each side of the threshold using the MSE-optimal two-bandwidth selector.

Figure 23: Included Covariates for the Geographic Regression Discontinuity Design (GRDD) Estimation and Distance to the Confessional Border

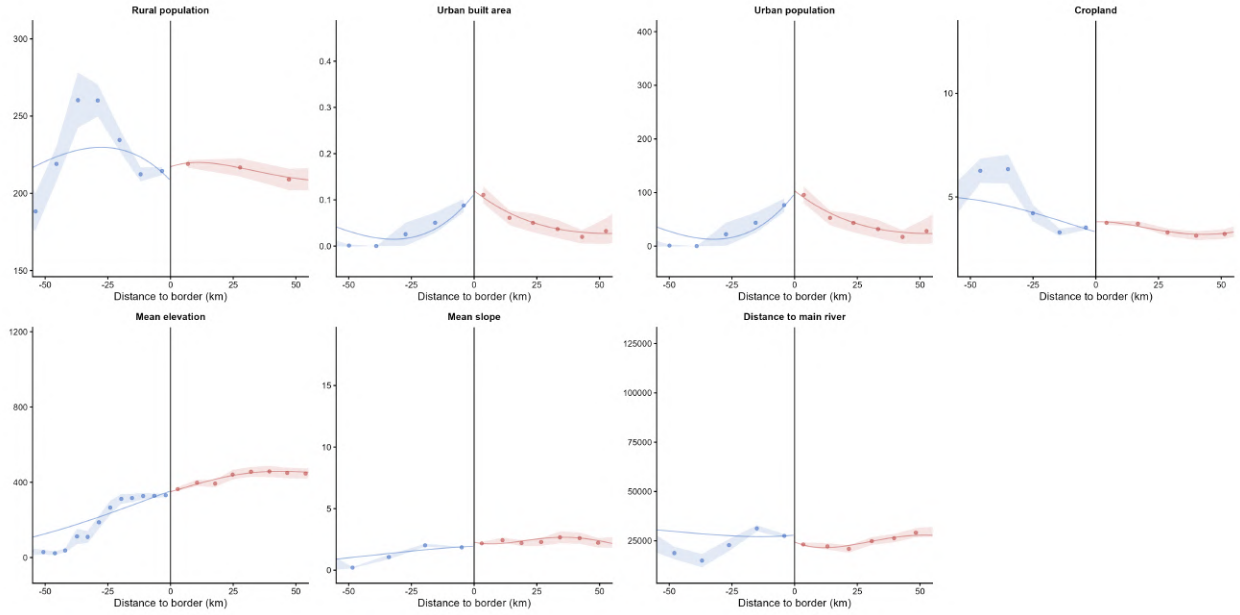

Note: Each dot represents the mean outcome within an evenly spaced bin of the running variable on either side of the cutoff (negative values on the horizontal axis denote historically Protestant municipalities while positive values refer to historically Catholic municipalities). Ribbons indicate 95% confidence intervals. The solid red line shows a fourth-order polynomial fit estimated using a uniform kernel. Bandwidths are selected separately on each side of the threshold using the MSE-optimal two-bandwidth selector.

Figure 24: McCary Density Test for the Geographic Regression Discontinuity Design (GRDD) Estimation

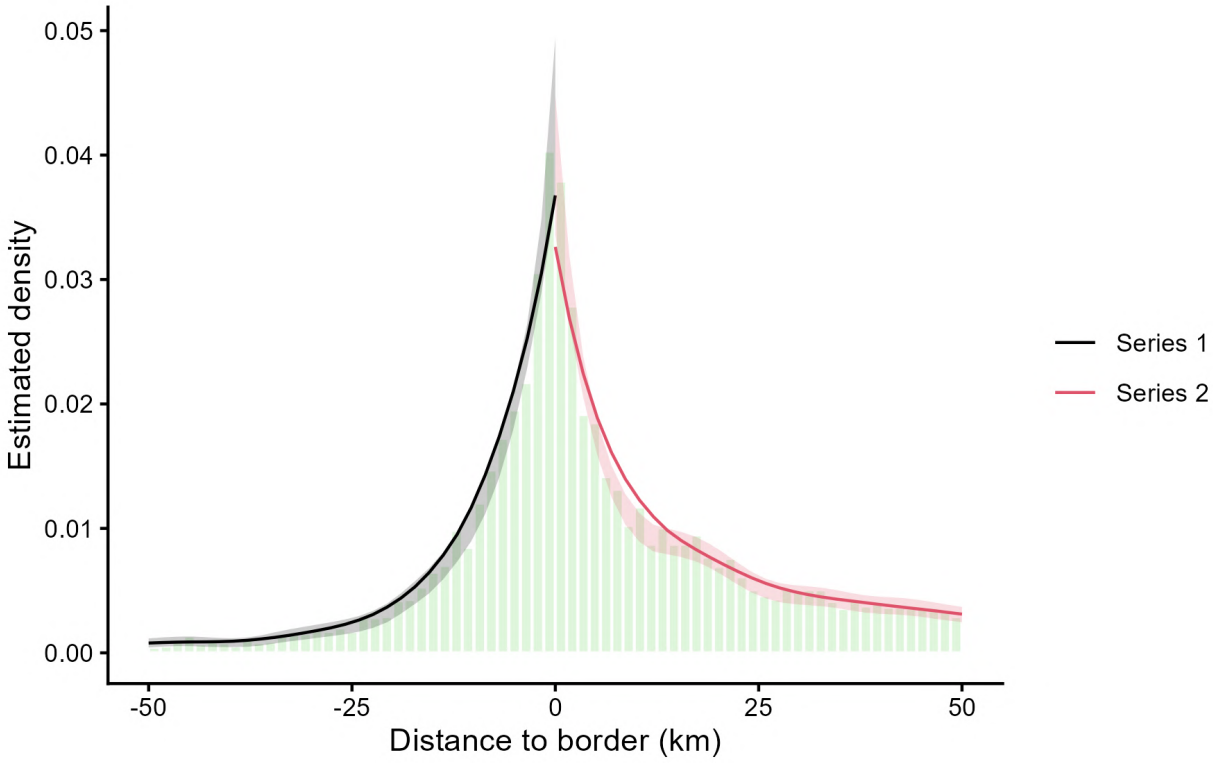

Note: McCrary density continuity test with a triangular kernel and second-order polynomial ($p = 2$). Negative values on the horizontal axis denote historically Protestant municipalities while positive values refer to historically Catholic municipalities.)

Figure 25: Geographic Regression Discontinuity Design Point Estimates for CDU/CSU and SPD by *donut* hole size

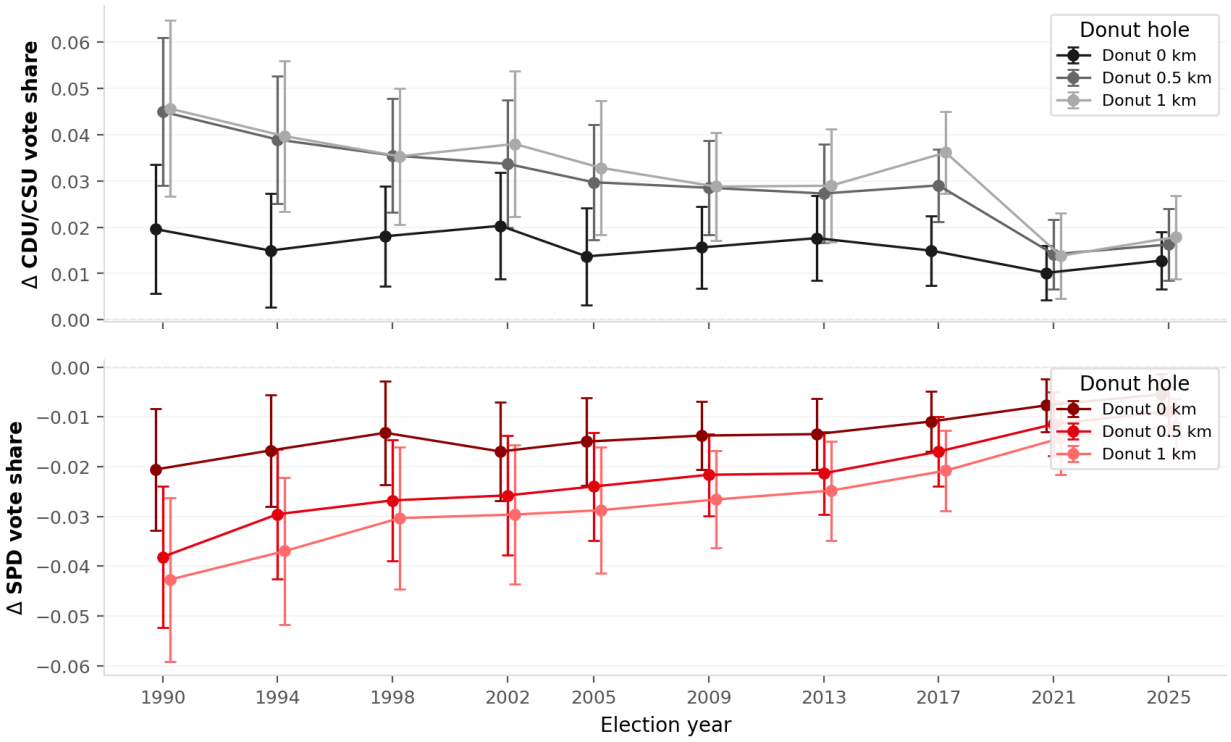

Note: Bias-corrected, covariate-adjusted estimates and heteroskedasticity-robust nearest-neighbour standard errors ($k = 3$). Units are weighted with a uniform kernel. N_l (N_r) and h_l (h_r) denote, respectively, the effective observations and the MSE-optimal bandwidths to the left (right) of the cutoff. Bandwidths are chosen separately on each side of the cutoff with the MSE-optimal two-bandwidth selector.

Figure 26: Spatial Distribution of Catholic Population and CDU Vote Share for the 2017 Federal Election
(North-Western Germany)

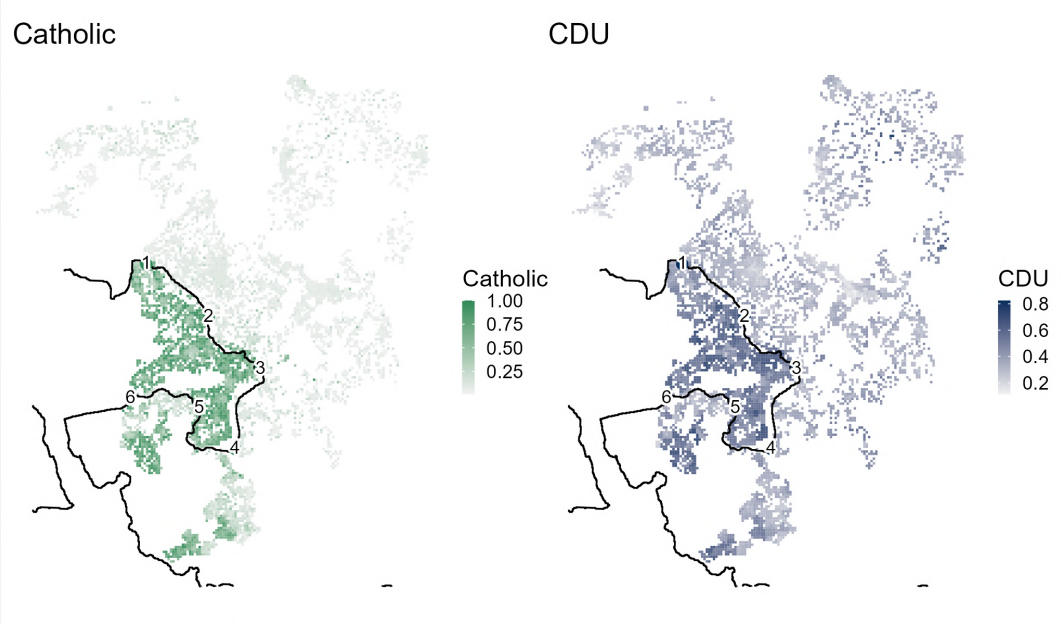

Note: Own elaboration with data from Kunz (2014); Statistisches Bundesamt (2022); Fremerey et al. (2021)

Figure 27: Spatial Distribution of SPD and CDU Vote Shares for the 2017 Federal Election
(North-Western Germany)

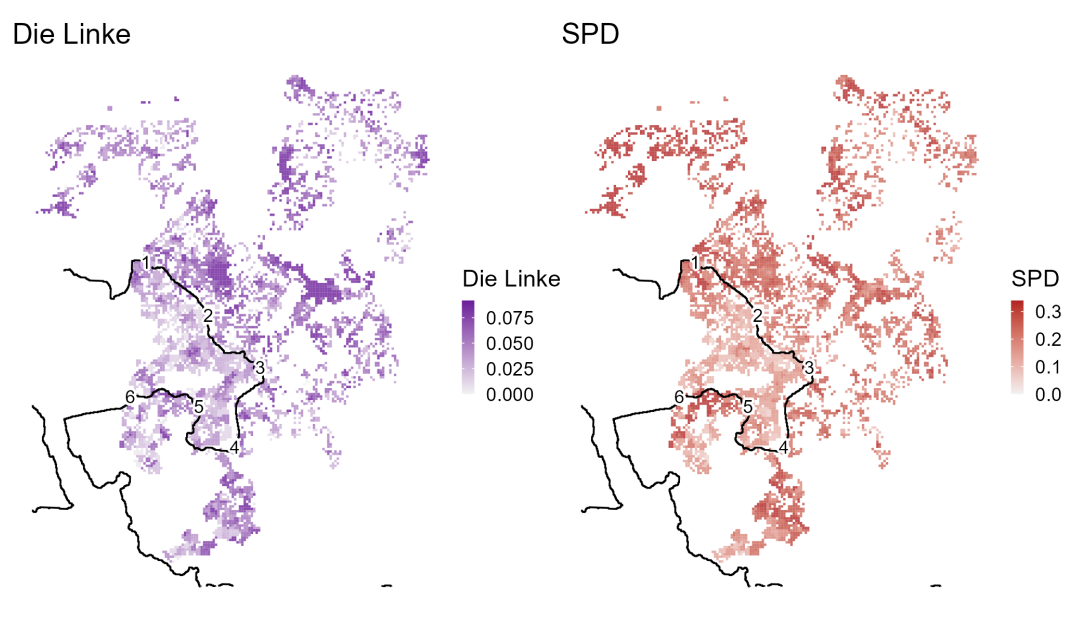

Note: Own elaboration with data from Kunz (2014); Statistisches Bundesamt (2022); Fremerey et al. (2021)

Figure 28: Pairwise Religion-Based Differences in Predicted Vote Probability (2009 -2025)

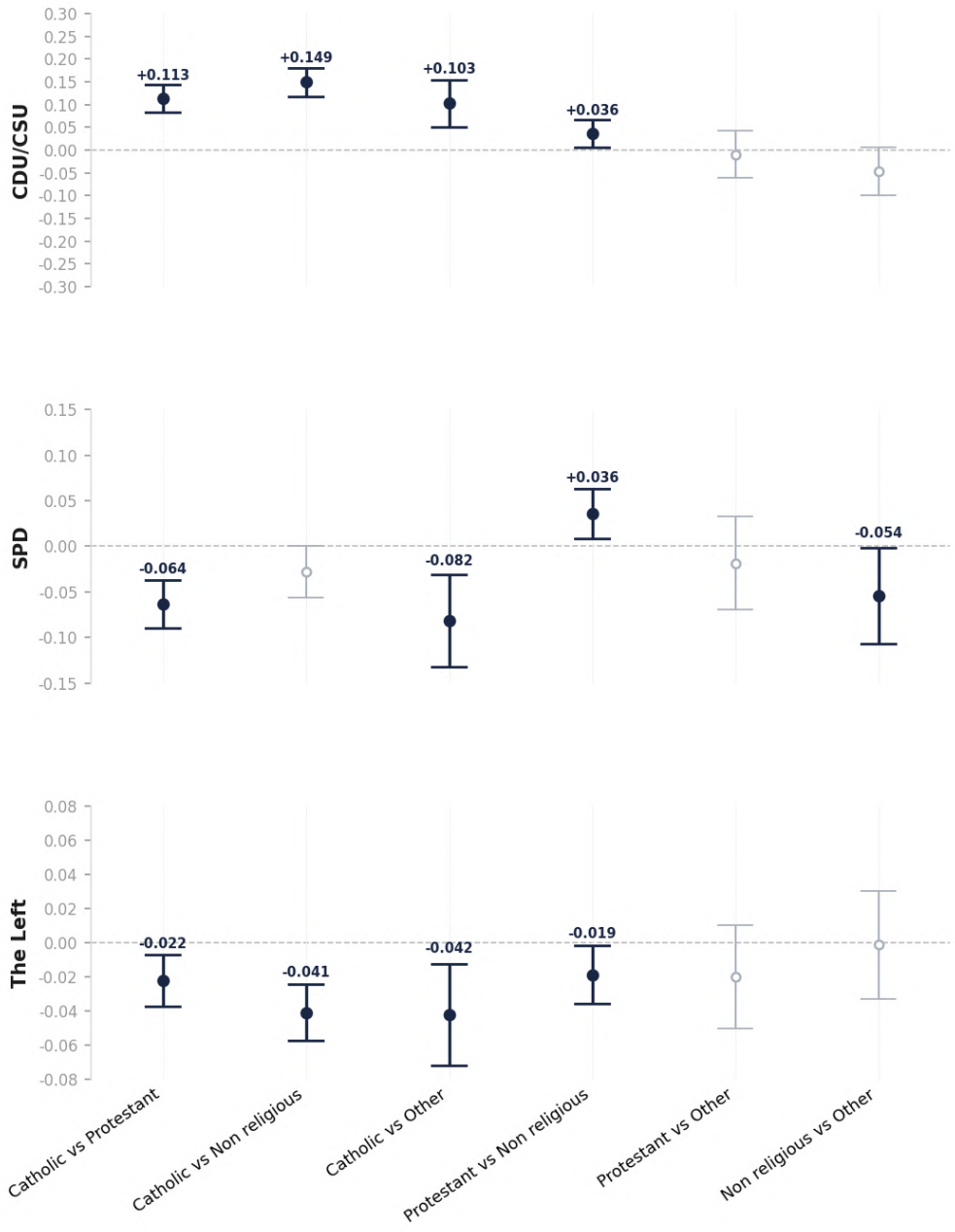

Note: Entries are average marginal differences in the predicted probability of voting for each party obtained from logistic regressions. Heteroskedasticity-robust (HC0) standard errors.

Figure 29: Pairwise Religion-Based Differences in Predicted Vote Probability (1953 - 2005)

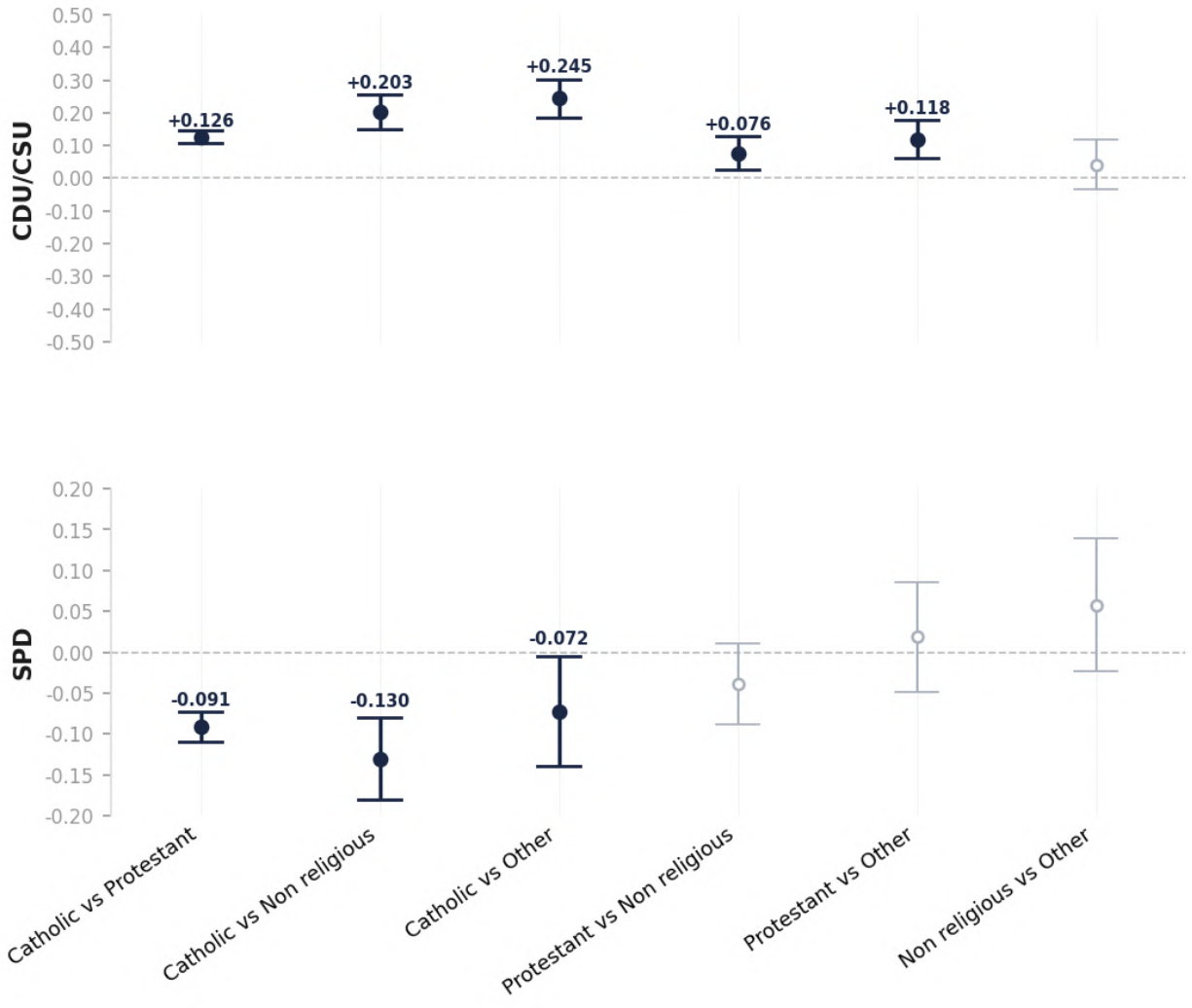

Note: Entries are average marginal differences in the predicted probability of voting for each party obtained from logistic regressions. Heteroskedasticity-robust (HC0) standard errors.

Figure 30: Predicted Voting Probabilities by Confession Over Time (1953–2025)

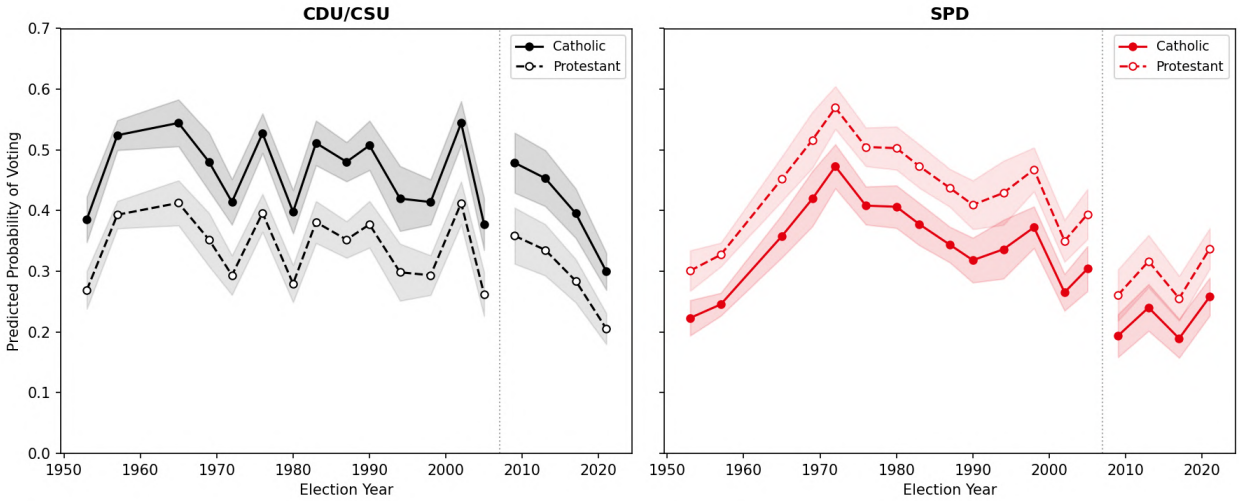

Note: Predicted probabilities of voting for each party, shown separately for Catholic and Protestant respondents at each election year. Shaded areas represent 95% confidence intervals based on heteroskedasticity-robust (HC0) standard errors. The vertical dashed line indicates the transition between the cumulated post-election survey data (1953–2005) and the GLES cross-sections (2009–2025).

Figure 31: Pairwise Religion-Based Differences in Political Attitudes (2009 -2021)

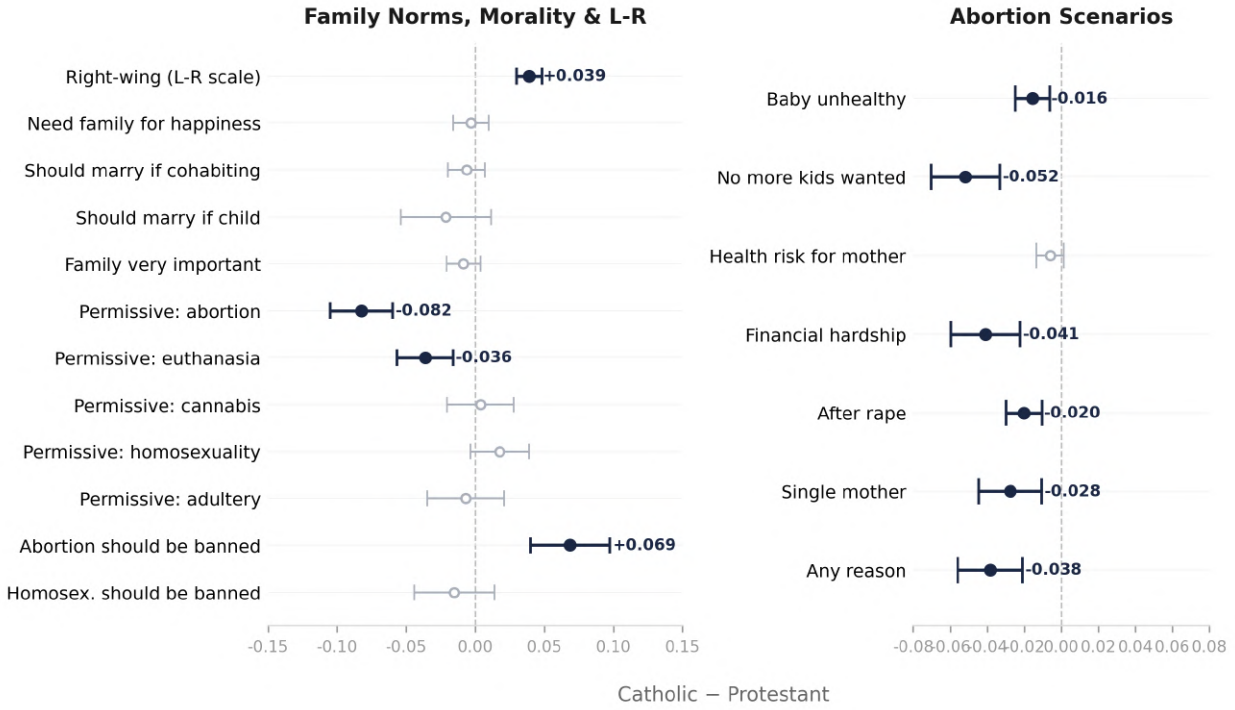

Note: Entries are average marginal differences in the predicted probability of voting for each party obtained from logistic regressions. Heteroskedasticity-robust (HC0) standard errors.

Figure 32: Pairwise Religion-Based Differences in Political Attitudes (2009 -2021)

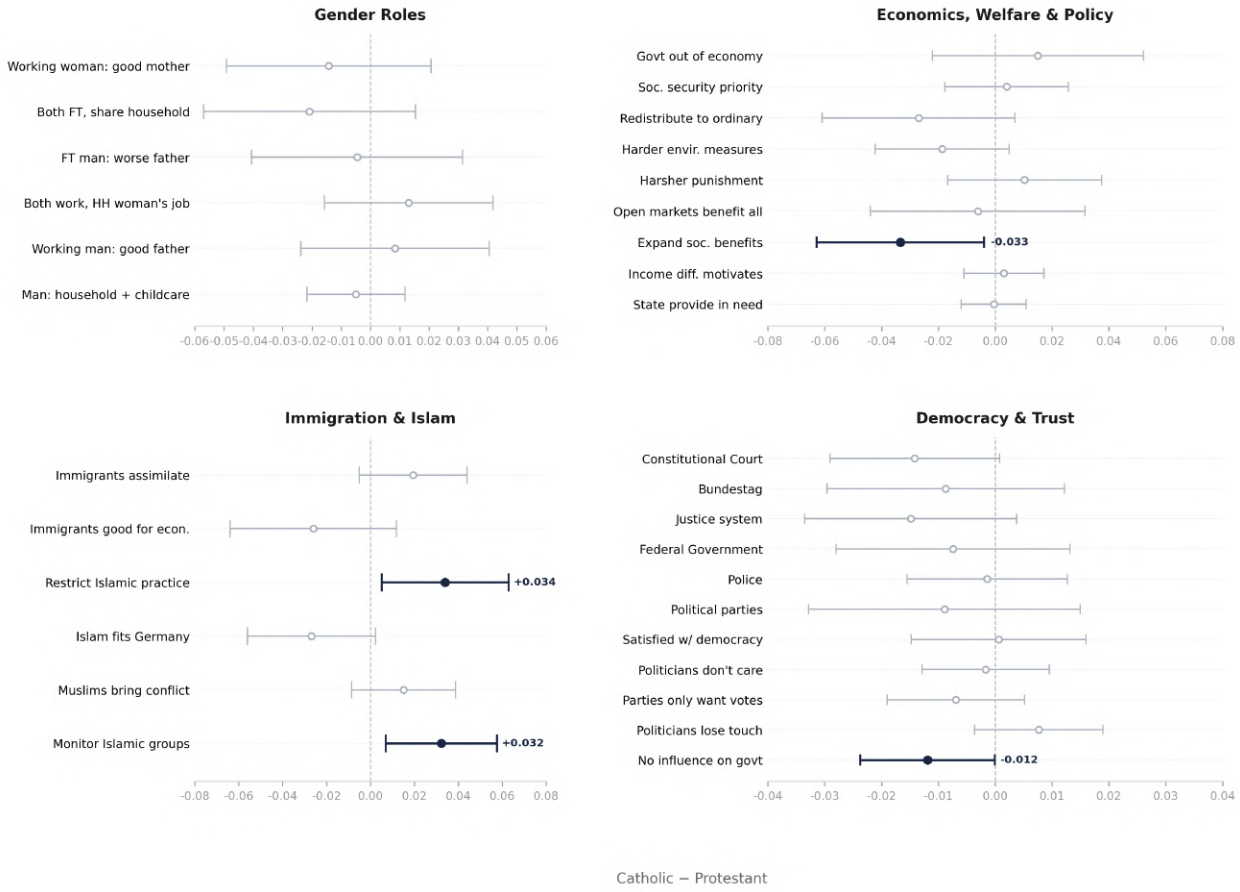

Note: Entries are average marginal differences in the predicted probability of voting for each party obtained from logistic regressions. Heteroskedasticity-robust (HC0) standard errors.

Figure 33: Pairwise Religion-Based Differences in Political Attitudes (2009 -2025)

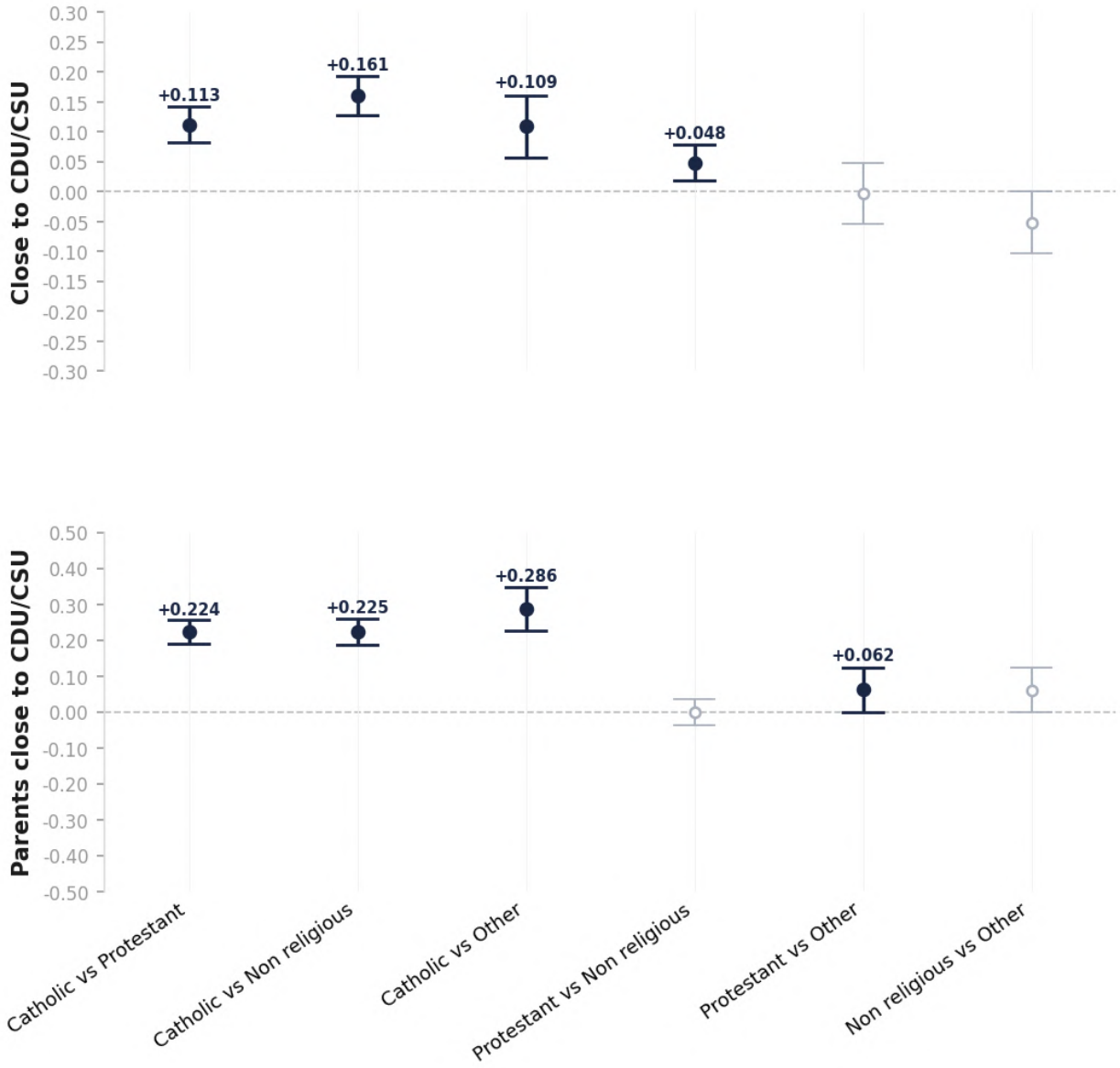

Note: Entries are average marginal differences in the predicted probability of voting for each party obtained from logistic regressions. Heteroskedasticity-robust (HC0) standard errors.

Figure 34: Religious Differences in Party Identification Strength (2009 -2025)

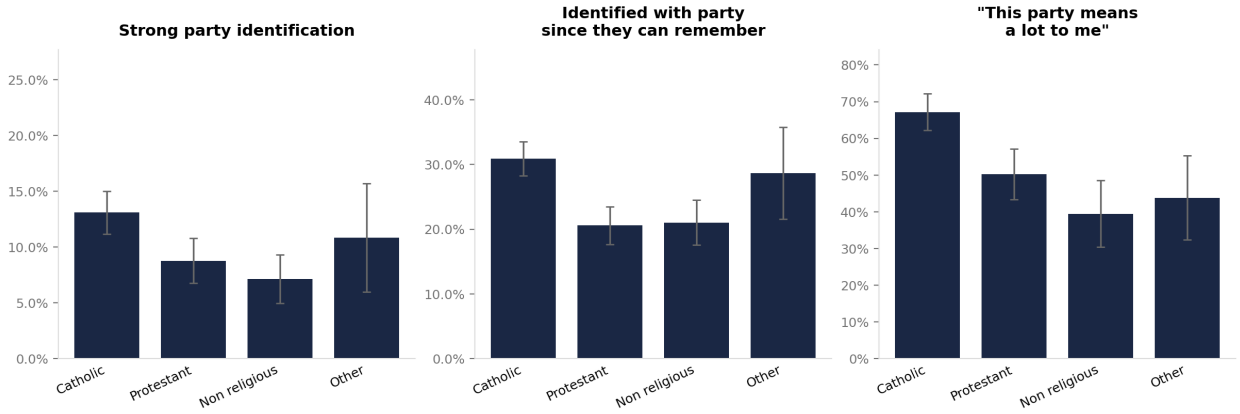

Note: Entries are the share of respondents agreeing with each statement by religious group. Error bars represent 95% confidence intervals based on heteroskedasticity-robust standard errors. Sample restricted to respondents in close union households. The last panel corresponds to data between 2009 - 2021 only.

B Tables

Table 1: Municipality-Level Summary Statistics by Historical Confession

	Total	**Historically Protestant**	**Historically Catholic**
Religious composition			
Catholic share (%)	37	16	57
	(0.30)	(0.24)	(0.28)
Protestant share (%)	29	45	14
	(0.23)	(0.23)	(0.20)
No religion / Other (%)	34	39	29
	(0.14)	(0.18)	(0.16)
Historical (XVI century)			
Rural population (count)	212	207	216
	(0.71)	(0.93)	(1.06)
Urban population (count)	64	69	60
	(2.89)	(4.48)	(3.71)
Urban built-up area	0.07	0.07	0.07
	(0.003)	(0.005)	(0.004)
Cropland area	3.8	3.6	3.8
	(0.02)	(0.03)	(0.02)
Topography			
Mean elevation (m)	320	221	414
	(2.48)	(3.07)	(3.22)
Mean slope (deg)	1.9	1.4	2.3
	(0.03)	(0.02)	(0.05)
Distance to main river (m)	28 218	33 161	23 546
	(246)	(373)	(305)
Socio-economic variables			
Unemployment rate (%)	3	3	3
	(0.02)	(0.03)	(0.04)
Share aged 80+ (%)	7	7	7
	(0.02)	(0.02)	(0.02)
Higher education (%)	18	18	18
	(0.06)	(0.08)	(0.07)
Immigrant share (%)	13	12	13
	(0.05)	(0.06)	(0.06)

Notes: Socio-demographic variables are omitted from the rest of the analysis as they are only available for municipalities with more than 10,000 inhabitants. Standard errors in parentheses.

Table 2: Geographic Regression Discontinuity Design Results for Share of Catholics as of 2022

	Estimate	SE	N_ℓ, N_r	h_l,h_r
Catholic Share	0.033***	(0.012)	(1470, 988)	(8, 5)

Notes: Bias-corrected estimates and heteroskedasticity-robust-nearest-neighbor standard errors ($k = 3$). Units are weighted with a uniform kernel. N_l (N_r) and h_l (h_r) denote, respectively, the effective observations and the MSE-optimal bandwidths to the left (right) of the cutoff. Bandwidths are chosen separately on each side of the cutoff with the MSE-optimal two-bandwidth selector. $^{***}p < 0.01$, $^{**}p < 0.05$, $^{*}p < 0.10$.

Table 3: Baseline means for party vote shares, 1990–2005

	1990			1994			1998			2002			2005		
	Total	Catholic	Protestant	Total	Catholic	Protestant	Total	Catholic	Protestant	Total	Catholic	Protestant	Total	Catholic	Protestant
CDU/CSU	0.511	0.581	0.434	0.486	0.552	0.412	0.486	0.495	0.356	0.429	0.494	0.364	0.413	0.474	0.348
	(0.001)	(0.002)	(0.002)	(0.001)	(0.001)	(0.001)	(0.001)	(0.001)	(0.001)	(0.002)	(0.002)	(0.002)	(0.001)	(0.002)	(0.001)
SPD	0.305	0.242	0.375	0.336	0.281	0.397	0.385	0.332	0.451	0.388	0.338	0.450	0.344	0.291	0.407
	(0.001)	(0.001)	(0.002)	(0.001)	(0.001)	(0.002)	(0.001)	(0.001)	(0.001)	(0.002)	(0.001)	(0.002)	(0.002)	(0.001)	(0.002)
Far-right	0.030	0.034	0.025	0.020	0.022	0.019	0.030	0.031	0.030	0.010	0.010	0.011	0.011	0.011	0.012
	(0.001)	(0.001)	(0.001)	(0.001)	(0.001)	(0.001)	(0.001)	(0.001)	(0.001)	(0.000)	(0.000)	(0.000)	(0.001)	(0.001)	(0.001)
Far-Left	0.001	0.001	0.002	0.005	0.004	0.007	0.005	0.006	0.010	0.008	0.006	0.010	0.050	0.047	0.053
	(0.000)	(0.000)	(0.000)	(0.000)	(0.000)	(0.000)	(0.000)	(0.000)	(0.000)	(0.000)	(0.000)	(0.000)	(0.001)	(0.001)	(0.001)
Greens	0.040	0.037	0.043	0.062	0.055	0.070	0.056	0.055	0.064	0.077	0.071	0.083	0.088	0.082	0.095
	(0.001)	(0.001)	(0.001)	(0.001)	(0.001)	(0.001)	(0.001)	(0.001)	(0.001)	(0.001)	(0.001)	(0.001)	(0.001)	(0.001)	(0.001)
FDP	0.095	0.080	0.110	0.071	0.062	0.080	0.067	0.060	0.075	0.066	0.051	0.082	0.103	0.081	0.127
	(0.001)	(0.001)	(0.001)	(0.001)	(0.001)	(0.001)	(0.001)	(0.001)	(0.001)	(0.001)	(0.001)	(0.001)	(0.001)	(0.001)	(0.001)

Notes: Standard errors in parentheses.

Table 4: Baseline means for party vote shares, 2009–2025

	2009			2013			2017			2021			2025		
	Total	Catholic	Protestant	Total	Catholic	Protestant	Total	Catholic	Protestant	Total	Catholic	Protestant	Total	Catholic	Protestant
CDU/CSU	0.393	0.444	0.337	0.383	0.437	0.323	0.330	0.374	0.279	0.293	0.327	0.255	0.352	0.389	0.311
	(0.001)	(0.001)	(0.001)	(0.001)	(0.001)	(0.001)	(0.001)	(0.001)	(0.001)	(0.001)	(0.001)	(0.001)	(0.001)	(0.001)	(0.001)
SPD	0.211	0.167	0.259	0.310	0.260	0.370	0.214	0.172	0.268	0.249	0.213	0.288	0.156	0.129	0.186
	(0.002)	(0.001)	(0.002)	(0.001)	(0.001)	(0.001)	(0.001)	(0.001)	(0.001)	(0.001)	(0.001)	(0.001)	(0.001)	(0.001)	(0.001)
Far-Right	0.012	0.012	0.012	0.031	0.031	0.030	0.057	0.055	0.060	0.094	0.094	0.095	0.206	0.204	0.208
	(0.001)	(0.001)	(0.001)	(0.001)	(0.001)	(0.001)	(0.001)	(0.001)	(0.001)	(0.001)	(0.001)	(0.001)	(0.001)	(0.001)	(0.001)
Far-Left	0.082	0.080	0.084	0.084	0.083	0.085	0.095	0.094	0.096	0.051	0.050	0.051	0.052	0.047	0.058
	(0.001)	(0.001)	(0.001)	(0.001)	(0.001)	(0.001)	(0.001)	(0.001)	(0.001)	(0.001)	(0.001)	(0.001)	(0.001)	(0.001)	(0.001)
Greens	0.101	0.092	0.111	0.104	0.094	0.115	0.098	0.089	0.109	0.148	0.136	0.162	0.152	0.141	0.164
	(0.001)	(0.001)	(0.001)	(0.001)	(0.001)	(0.001)	(0.001)	(0.001)	(0.001)	(0.001)	(0.001)	(0.001)	(0.001)	(0.001)	(0.001)
FDP	0.093	0.075	0.113	0.054	0.045	0.064	0.094	0.079	0.111	0.114	0.094	0.136	0.072	0.059	0.087
	(0.001)	(0.001)	(0.001)	(0.001)	(0.001)	(0.001)	(0.001)	(0.001)	(0.001)	(0.001)	(0.001)	(0.001)	(0.001)	(0.001)	(0.001)

Notes: Standard errors in parentheses.

Table 5: Baseline Averages for income-related variables

	1998			2001			2004			2015			2016		
	Total	Catholic	Protestant	Total	Catholic	Protestant	Total	Catholic	Protestant	Total	Catholic	Protestant	Total	Catholic	Protestant
Average Income	30 332	30 368	30 284	31 471	31 538	31 389	33 859	33 922	33 786	38 400	38 458	38 325	39 828	39 888	39 753
	(40)	(40)	(41)	(41)	(41)	(42)	(45)	(45)	(46)	(50)	(50)	(50)	(52)	(52)	(52)
Average income (adjusted for capital tax)	30 332	30 368	30 284	32 733	32 603	32 964	29 779	29 760	29 856	39 161	39 530	38 807	40 409	40 836	39 989
	(40)	(40)	(41)	(44)	(44)	(44)	(40)	(40)	(41)	(51)	(51)	(52)	(53)	(53)	(53)
Gini Index	0.407	0.403	0.413	0.414	0.410	0.419	0.430	0.427	0.434	0.439	0.436	0.444	0.445	0.443	0.448
	(0.001)	(0.001)	(0.001)	(0.001)	(0.001)	(0.001)	(0.001)	(0.001)	(0.001)	(0.001)	(0.001)	(0.001)	(0.001)	(0.001)	(0.001)
Theil Index	0.360	0.357	0.365	0.368	0.366	0.370	0.395	0.393	0.398	0.412	0.409	0.415	0.430	0.428	0.433
	(0.001)	(0.001)	(0.001)	(0.001)	(0.001)	(0.001)	(0.001)	(0.001)	(0.001)	(0.001)	(0.001)	(0.001)	(0.001)	(0.001)	(0.001)

Notes: Standard errors in parentheses.

Table 6: Geographic Regression Discontinuity Design results for party vote shares in Federal Elections (1990 -2025)

	1990	**1994**	**1998**	**2002**	**2005**	**2009**	**2013**	**2017**	**2021**	**2025**
CDU / CSU	0.020***	0.015**	0.018***	0.020***	0.014**	0.016***	0.018***	0.015***	0.010***	0.013***
SE	(0.007)	(0.006)	(0.005)	(0.006)	(0.005)	(0.004)	(0.005)	(0.004)	(0.003)	(0.003)
h_l, h_r	(14,7)	(14,7)	(15,7)	(18,7)	(17,6)	(12,8)	(12,7)	(15,8)	(14,7)	(15,8)
N_l, N_r	(1938,1199)	(1910,1180)	(1989,1201)	(2103,1214)	(2039,1163)	(1799,1291)	(1789,1261)	(1949,1306)	(1890,1161)	(1939,1300)
SPD	-0.021***	-0.017***	-0.013**	-0.017***	-0.015***	-0.014***	-0.013***	-0.011***	-0.008***	-0.005***
SE	(0.006)	(0.006)	(0.005)	(0.005)	(0.005)	(0.003)	(0.004)	(0.003)	(0.003)	(0.002)
h_l, h_r	(17,7)	(18,7)	(15,7)	(18,7)	(16,7)	(16,7)	(15,8)	(15,9)	(14,8)	(15,7)
N_l, N_r	(2053,1256)	(2094,1253)	(1971,1254)	(2099,1216)	(2029,1254)	(2037,1268)	(1962,1284)	(1944,1371)	(1860,1282)	(1957,1268)
Far-Right	-0.002**	-0.001	-0.001	-0.000	0.000	-0.000	-0.003***	-0.002	-0.002	-0.000
SE	(0.001)	(0.001)	(0.001)	(0.001)	(0.001)	(0.001)	(0.001)	(0.002)	(0.002)	(0.003)
h_l, h_r	(17,14)	(16,13)	(13,13)	(14,13)	(14,14)	(20,14)	(14,13)	(19,10)	(19,13)	(15,11)
N_l, N_r	(2068,1748)	(2032,1702)	(1875,1675)	(1906,1713)	(1922,1709)	(1759,1644)	(1899,1672)	(2115,1489)	(2076,1656)	(1956,1573)
Far-Left	-0.000	-0.000**	-0.000	-0.001**	-0.003***	-0.002	-0.001	-0.004***	-0.001***	-0.003***
SE	(0.000)	(0.000)	(0.000)	(0.000)	(0.001)	(0.002)	(0.001)	(0.001)	(0.000)	(0.001)
h_l, h_r	(21,17)	(17,20)	(18,12)	(17,14)	(18,12)	(10,12)	(12,13)	(21,15)	(18,17)	(17,17)
N_l, N_r	(2175,1980)	(2051,2173)	(2099,1645)	(2066,1748)	(2165,1766)	(1826,1730)	(2159,1844)	(2055,1928)	(2069,2004)	(1986,2003)
Greens	-0.001	-0.003**	-0.002	-0.001	0.000	-0.001	-0.000	-0.001	-0.001	-0.002
SE	(0.001)	(0.001)	(0.001)	(0.002)	(0.002)	(0.002)	(0.001)	(0.001)	(0.002)	(0.002)
h_l, h_r	(17,9)	(15,15)	(15,16)	(17,9)	(15,8)	(14,9)	(11,10)	(14,9)	(15,9)	(22,9)
N_l, N_r	(2053,1444)	(1946,1870)	(1984,1900)	(2054,1382)	(1964,1402)	(1437,1452)	(1749,1472)	(1929,1428)	(1922,1423)	(2190,1435)
FDP	-0.001	-0.003	-0.002	-0.003*	-0.000	0.001	-0.003***	-0.001	-0.001	-0.001
SE	(0.002)	(0.002)	(0.002)	(0.001)	(0.002)	(0.002)	(0.001)	(0.001)	(0.001)	(0.001)
h_l, h_r	(11,10)	(11,12)	(11,11)	(14,14)	(13,12)	(18,11)	(14,12)	(13,12)	(15,12)	(12,12)
N_l, N_r	(1726,1449)	(1706,1640)	(1718,1574)	(1926,1743)	(1830,1742)	(1532,1581)	(1940,1610)	(1832,1661)	(1901,1591)	(1794,1641)

Notes: Bias-corrected, covariate-adjusted estimates and heteroskedasticity-robust nearest-neighbour standard errors ($k = 3$). Units are weighted with a uniform kernel. N_l (N_r) and h_l (h_r) denote, respectively, the effective observations and the MSE-optimal bandwidths to the left (right) of the cutoff. Bandwidths are chosen separately on each side of the cutoff with the MSE-optimal two-bandwidth selector. $^{***}p < 0.01$, $^{**}p < 0.05$, $^{*}p < 0.10$.

Table 7: Geographic Regression Discontinuity Design results for party vote shares in Federal Elections (1990 -2025)
(0.5 km radius *donut hole*)

	1990	**1994**	**1998**	**2002**	**2005**	**2009**	**2013**	**2017**	**2021**	**2025**
CDU / CSU	0.045***	0.039***	0.036***	0.034***	0.030***	0.029***	0.027***	0.029***	0.014***	0.016***
SE	(0.008)	(0.007)	(0.006)	(0.007)	(0.006)	(0.005)	(0.005)	(0.004)	(0.004)	(0.004)
h_l, h_r	(16,8)	(17,8)	(19,8)	(18,7)	(18,7)	(13,9)	(15,7)	(17,10)	(12,7)	(12,7)
N_l, N_r	(1851,1135)	(1886,1139)	(1933,1141)	(1913,1082)	(1898,1062)	(1693,1200)	(1800,1097)	(1867,1355)	(1605,1009)	(1613,1082)
SPD	-0.038***	-0.030***	-0.027***	-0.026***	-0.024***	-0.022***	-0.021***	-0.017***	-0.011***	-0.009***
SE	(0.007)	(0.007)	(0.006)	(0.006)	(0.006)	(0.004)	(0.004)	(0.004)	(0.003)	(0.002)
h_l, h_r	(16,8)	(16,8)	(16,8)	(16,7)	(13,8)	(14,8)	(13,8)	(14,9)	(14,8)	(14,8)
N_l, N_r	(1825,1130)	(1822,1146)	(1815,1136)	(1839,1084)	(1690,1116)	(1740,1164)	(1707,1161)	(1743,1250)	(1711,1137)	(1752,1133)
Far-Right	-0.003***	-0.001	-0.000	-0.000	0.001	-0.000	-0.004***	-0.002	-0.001	0.001
SE	(0.001)	(0.001)	(0.001)	(0.001)	(0.001)	(0.001)	(0.001)	(0.002)	(0.002)	(0.003)
h_l, h_r	(18,13)	(17,11)	(14,15)	(14,13)	(16,14)	(19,15)	(15,13)	(15,11)	(16,12)	(14,12)
N_l, N_r	(1919,1551)	(1870,1366)	(1731,1612)	(1746,1504)	(1779,1567)	(1554,1554)	(1780,1526)	(1799,1356)	(1787,1425)	(1724,1430)
Far-Left	-0.000	-0.001***	-0.001*	-0.001**	-0.004***	-0.002	-0.001	-0.004***	-0.001*	-0.003***
SE	(0.000)	(0.000)	(0.000)	(0.000)	(0.001)	(0.002)	(0.001)	(0.001)	(0.001)	(0.001)
h_l, h_r	(19,16)	(17,22)	(19,13)	(18,12)	(20,12)	(9,13)	(13,12)	(19,14)	(17,16)	(19,21)
N_l, N_r	(1937,1739)	(1871,2115)	(1938,1528)	(1924,1484)	(1822,1524)	(1554,1638)	(1701,1484)	(1936,1621)	(1831,1719)	(1923,2041)
Greens	-0.003***	-0.004***	-0.002	-0.004**	-0.002	-0.004**	-0.005***	-0.002	-0.002	-0.003
SE	(0.001)	(0.001)	(0.002)	(0.002)	(0.002)	(0.002)	(0.002)	(0.002)	(0.002)	(0.002)
h_l, h_r	(19,11)	(15,19)	(16,11)	(16,10)	(17,8)	(14,10)	(11,16)	(14,9)	(15,9)	(18,9)
N_l, N_r	(1920,1364)	(1774,1938)	(1822,1389)	(1884,1316)	(1713,1314)	(1543,1723)	(1743,1249)	(1765,1201)	(1895,1201)	(1876,1201)
FDP	-0.004	-0.004*	-0.004**	-0.004**	-0.001	0.000	-0.004***	-0.002	-0.001	-0.002**
SE	(0.003)	(0.002)	(0.002)	(0.002)	(0.002)	(0.002)	(0.001)	(0.002)	(0.001)	(0.001)
h_l, h_r	(11,10)	(11,11)	(11,11)	(23,11)	(19,11)	(15,11)	(15,11)	(13,11)	(21,11)	(15,13)
N_l, N_r	(1539,1305)	(1528,1410)	(1562,1356)	(2018,1385)	(1946,1395)	(1793,1391)	(1787,1411)	(1679,1419)	(1960,1361)	(1798,1519)

Notes: Bias-corrected, covariate-adjusted estimates and heteroskedasticity-robust nearest-neighbor standard errors ($k = 3$). Units are weighted with a uniform kernel. N_l (N_r) and h_l (h_r) denote, respectively, the effective observations and the MSE-optimal bandwidths to the left (right) of the cutoff. Bandwidths are chosen separately on each side of the cutoff with the MSE-optimal two-bandwidth selector. $^{***}p < 0.01$, $^{**}p < 0.05$, $^{*}p < 0.10$.

Table 8: Geographic Regression Discontinuity Design results for party vote shares in Federal Elections (1990 -2025)
(1 km radius *donut hole*)

	1990	**1994**	**1998**	**2002**	**2005**	**2009**	**2013**	**2017**	**2021**	**2025**
CDU / CSU	0.046***	0.040***	0.035***	0.038***	0.033***	0.029***	0.029***	0.036***	0.014***	0.018***
SE	(0.010)	(0.008)	(0.007)	(0.008)	(0.007)	(0.006)	(0.006)	(0.004)	(0.005)	(0.005)
h_l, h_r	(14,7)	(16,7)	(16,7)	(16,7)	(16,7)	(17,8)	(16,7)	(14,13)	(11,7)	(12,7)
N_l, N_r	(1609,971)	(1707,973)	(1700,987)	(1685,1011)	(1664,979)	(1470,1028)	(1709,975)	(1604,1393)	(1391,888)	(1479,985)
SPD	-0.043***	-0.037***	-0.030***	-0.030***	-0.029***	-0.027***	-0.025***	-0.021***	-0.014***	-0.012***
SE	(0.008)	(0.008)	(0.007)	(0.007)	(0.006)	(0.005)	(0.005)	(0.004)	(0.004)	(0.003)
h_l, h_r	(14,8)	(13,8)	(13,8)	(13,7)	(12,7)	(11,8)	(11,8)	(12,9)	(13,8)	(14,9)
N_l, N_r	(1606,1009)	(1568,1074)	(1559,1018)	(1579,1006)	(1457,1039)	(1542,1042)	(1433,1020)	(1485,1154)	(1518,1048)	(1596,1076)
Far-Right	-0.004***	-0.002***	-0.000	-0.000	0.001	0.000	-0.004***	-0.004*	-0.002	0.001
SE	(0.001)	(0.001)	(0.001)	(0.001)	(0.001)	(0.001)	(0.001)	(0.002)	(0.002)	(0.004)
h_l, h_r	(18,13)	(17,12)	(13,16)	(12,14)	(13,16)	(18,15)	(15,13)	(20,12)	(18,14)	(14,12)
N_l, N_r	(1777,1424)	(1715,1320)	(1521,1617)	(1617,1453)	(1639,1518)	(1473,1513)	(1643,1409)	(1824,1343)	(1744,1442)	(1570,1352)
Far-Left	-0.000*	-0.001***	-0.001**	-0.000	-0.006***	-0.004*	-0.000	-0.005***	-0.001	-0.003***
SE	(0.000)	(0.000)	(0.000)	(0.000)	(0.001)	(0.002)	(0.001)	(0.001)	(0.001)	(0.001)
h_l, h_r	(18,17)	(20,21)	(19,13)	(17,11)	(21,12)	(13,14)	(15,13)	(19,15)	(19,16)	(18,18)
N_l, N_r	(1770,1670)	(1827,1899)	(1796,1403)	(1778,1458)	(1736,1530)	(1418,1486)	(1635,1418)	(1799,1580)	(1771,1600)	(1773,1734)
Greens	-0.003**	-0.004***	-0.002	-0.006***	-0.003	-0.004*	-0.005***	-0.002	-0.003	-0.002
SE	(0.001)	(0.001)	(0.002)	(0.002)	(0.002)	(0.002)	(0.002)	(0.002)	(0.003)	(0.002)
h_l, h_r	(18,10)	(18,17)	(18,12)	(16,17)	(18,9)	(14,10)	(11,15)	(14,9)	(16,10)	(18,9)
N_l, N_r	(1768,1193)	(1778,1671)	(1751,1355)	(1738,1202)	(1497,1192)	(1401,1577)	(1577,1141)	(1649,1142)	(1755,1126)	(1672,1130)
FDP	-0.006**	-0.006***	-0.008***	-0.004**	-0.001	0.002	-0.004**	-0.000	-0.002	-0.001
SE	(0.003)	(0.002)	(0.002)	(0.002)	(0.002)	(0.003)	(0.001)	(0.002)	(0.002)	(0.001)
h_l, h_r	(21,10)	(20,11)	(26,11)	(17,11)	(15,10)	(15,11)	(21,11)	(20,12)	(17,12)	(23,14)
N_l, N_r	(1840,1159)	(1819,1246)	(1942,1295)	(1745,1276)	(1803,1322)	(1719,1304)	(1854,1255)	(1814,1329)	(1717,1298)	(1876,1517)

Notes: Bias-corrected, covariate-adjusted estimates and heteroskedasticity-robust nearest-neighbor standard errors ($k = 3$). Units are weighted with a uniform kernel. N_l (N_r) and h_l (h_r) denote, respectively, the effective observations and the MSE-optimal bandwidths to the left (right) of the cutoff. Bandwidths are chosen separately on each side of the cutoff with the MSE-optimal two-bandwidth selector. $^{***}p < 0.01$, $^{**}p < 0.05$, $^{*}p < 0.10$.

Table 9: Geographic Regression Discontinuity Design results for income-related variables (1998 - 2016)

	1998	**2001**	**2004**	**2015**	**2016**
Average Income	0.000	-0.010	-0.007	0.001	-0.001
SE	(0.011)	(0.010)	(0.009)	(0.009)	(0.009)
h_l, h_r	(15,10)	(9,11)	(11,13)	(13,11)	(13,12)
N_l, N_r	(1343,995)	(1405,1422)	(1628,1657)	(1777,1563)	(1754,1593)
Average Captax	0.000	-0.010	-0.005	0.001	-0.001
SE	(0.011)	(0.010)	(0.009)	(0.009)	(0.009)
h_l, h_r	(15,10)	(9,11)	(11,13)	(13,11)	(13,12)
N_l, N_r	(1343,995)	(1405,1422)	(1620,1633)	(1792,1564)	(1754,1594)
Gini	0.001	-0.001	-0.002	-0.001	0.000
SE	(0.003)	(0.002)	(0.002)	(0.002)	(0.002)
h_l, h_r	(14,10)	(19,11)	(17,10)	(13,9)	(12,10)
N_l, N_r	(1316,1015)	(1847,1454)	(1910,1444)	(1776,1407)	(1711,1474)
Theil	0.013	-0.006	-0.007	0.006	0.004
SE	(0.012)	(0.009)	(0.008)	(0.008)	(0.007)
h_l, h_r	(16,11)	(20,12)	(17,14)	(17,15)	(17,16)
N_l, N_r	(1358,1056)	(1873,1501)	(1901,1695)	(1956,1823)	(1933,1876)

Notes: Bias-corrected, covariate-adjusted estimates and heteroskedasticity-robust nearest-neighbor standard errors ($k = 3$). Units are weighted with a uniform kernel. N_l (N_r) and h_l (h_r) denote, respectively, the effective observations and the MSE-optimal bandwidths to the left (right) of the cutoff. Bandwidths are chosen separately on each side of the cutoff with the MSE-optimal two-bandwidth selector. $^{***}p < 0.01$, $^{**}p < 0.05$, $^{*}p < 0.10$.

Table 10: Geographic Regression Discontinuity Design results for income-related variables (1998 - 2016)
(0.5 km radius *donut hole*)

	1998	**2001**	**2004**	**2015**	**2016**
Average Income	-0.003	-0.010	-0.008	0.005	-0.002
SE	(0.014)	(0.012)	(0.010)	(0.011)	(0.011)
h_l, h_r	(13,9)	(11,9)	(12,13)	(12,10)	(12,11)
N_l, N_r	(1119,836)	(1351,1186)	(1512,1456)	(1534,1326)	(1547,1348)
Average Captax	-0.003	-0.010	-0.008	0.005	-0.002
SE	(0.014)	(0.012)	(0.010)	(0.011)	(0.011)
h_l, h_r	(13,9)	(11,9)	(12,12)	(12,11)	(12,11)
N_l, N_r	(1119,836)	(1351,1186)	(1512,1415)	(1545,1334)	(1534,1351)
Gini	-0.002	-0.001	-0.003	-0.003	-0.002
SE	(0.003)	(0.003)	(0.002)	(0.002)	(0.002)
h_l, h_r	(15,10)	(13,10)	(12,10)	(11,10)	(11,9)
N_l, N_r	(1201,870)	(1478,1209)	(1533,1246)	(1469,1269)	(1454,1254)
Theil	0.006	0.003	-0.004	0.013	0.004
SE	(0.015)	(0.012)	(0.009)	(0.010)	(0.008)
h_l, h_r	(13,11)	(14,10)	(14,14)	(18,13)	(18,13)
N_l, N_r	(1149,956)	(1513,1207)	(1613,1537)	(1799,1518)	(1799,1497)

Notes: Bias-corrected, covariate-adjusted estimates and heteroskedasticity-robust nearest-neighbor standard errors ($k = 3$). Units are weighted with a uniform kernel. N_l (N_r) and h_l (h_r) denote, respectively, the effective observations and the MSE-optimal bandwidths to the left (right) of the cutoff. Bandwidths are chosen separately on each side of the cutoff with the MSE-optimal two-bandwidth selector. $^{***}p < 0.01$, $^{**}p < 0.05$, $^{*}p < 0.10$.

Table 11: Geographic Regression Discontinuity Design results for income-related variables (1998 - 2016)
(1 km radius *donut hole*)

	1998	**2001**	**2004**	**2015**	**2016**
Average Income	0.002	-0.013	-0.012	0.000	-0.001
SE	(0.016)	(0.014)	(0.011)	(0.012)	(0.012)
h_l, h_r	(13,9)	(13,9)	(13,16)	(14,10)	(14,10)
N_l, N_r	(1048,743)	(1337,1077)	(1423,1578)	(1524,1173)	(1497,1176)
Average Captax	0.002	-0.013	-0.011	-0.002	-0.000
SE	(0.016)	(0.014)	(0.011)	(0.012)	(0.013)
h_l, h_r	(13,9)	(13,9)	(13,17)	(15,10)	(14,10)
N_l, N_r	(1048,743)	(1337,1077)	(1424,1613)	(1537,1165)	(1498,1141)
Gini	-0.002	-0.002	-0.001	0.000	0.002
SE	(0.004)	(0.003)	(0.003)	(0.003)	(0.003)
h_l, h_r	(14,10)	(19,9)	(13,9)	(11,9)	(10,9)
N_l, N_r	(1064,768)	(1556,1046)	(1429,1091)	(1315,1084)	(1300,1103)
Theil	0.007	-0.003	0.001	0.013	0.009
SE	(0.016)	(0.013)	(0.009)	(0.010)	(0.010)
h_l, h_r	(14,11)	(19,10)	(17,14)	(18,13)	(18,13)
N_l, N_r	(1066,872)	(1555,1115)	(1593,1473)	(1664,1390)	(1662,1379)

Notes: Bias-corrected, covariate-adjusted estimates and heteroskedasticity-robust nearest-neighbor standard errors ($k = 3$). Units are weighted with a uniform kernel. N_l (N_r) and h_l (h_r) denote, respectively, the effective observations and the MSE-optimal bandwidths to the left (right) of the cutoff. Bandwidths are chosen separately on each side of the cutoff with the MSE-optimal two-bandwidth selector. $^{***}p < 0.01$, $^{**}p < 0.05$, $^{*}p < 0.10$.

Table 12: Geographic Regression Discontinuity Design Covariate Balance Test Results

	Full Sample	**(0.5 km radius *donut hole*)**	**(1 km radius *donut hole*)**
Rural population	1.329	2.641	2.184
SE	(3.401)	(3.938)	(4.602)
h_l, h_r	(9,12)	(10,12)	(10,12)
N_l, N_r	(1600,1050)	(1400,920)	(1300,875)
Urban built area	0.034**	0.028	0.028
SE	(0.017)	(0.019)	(0.021)
h_l, h_r	(17,27)	(19,23)	(21,21)
N_l, N_r	(1800,1200)	(1550,975)	(1450,950)
Urban population	29.202**	22.337	23.260
SE	(14.549)	(16.032)	(17.826)
h_l, h_r	(17,27)	(19,23)	(21,21)
N_l, N_r	(1750,1250)	(1500,1030)	(1400,1010)
Cropland	0.306**	0.364**	0.191
SE	(0.145)	(0.169)	(0.189)
h_l, h_r	(10,12)	(10,13)	(10,14)
N_l, N_r	(1900,1300)	(1650,1100)	(1520,1080)
Mean elevation	5.676	14.458	27.102*
SE	(10.707)	(13.175)	(15.301)
h_l, h_r	(12,10)	(10,10)	(8,10)
N_l, N_r	(1700,1150)	(1450,1000)	(1350,990)
Mean slope	0.023	0.156	0.165
SE	(0.118)	(0.148)	(0.188)
h_l, h_r	(12,7)	(13,8)	(12,8)
N_l, N_r	(1850,1230)	(1600,1130)	(1500,1000)
Distance to main river	-722.442	-1271.168	-545.092
SE	(1275.349)	(1527.111)	(1811.668)
h_l, h_r	(8,11)	(8,12)	(7,12)
N_l, N_r	(2000,1350)	(1800,1225)	(1650,1180)

Notes: Bias-corrected estimates and heteroskedasticity-robust nearest-neighbour standard errors ($k = 3$). Units are weighted with a uniform kernel. N_l (N_r) and h_l (h_r) denote, respectively, the effective observations and the MSE-optimal bandwidths to the left (right) of the cutoff. Bandwidths are chosen separately on each side of the cutoff with the MSE-optimal two-bandwidth selector. $^{***}p < 0.01$, $^{**}p < 0.05$, $^{*}p < 0.10$.

Table 13: GRDD McCrary Density Test Results

	Statistic
Density difference $(\hat{f}_R - \hat{f}_L)$	-0.0036
SE (jackknife)	(0.0031)
h_l, h_r	$(10.7, 12.6)$
N_l, N_r	$(1\,766, 1\,726)$

Notes: Units are weighted using a triangular kernel. N_l (N_r) and h_l (h_r) denote, respectively, the effective observations and the MSE-optimal bandwidths to the left (right) of the cutoff. Bandwidths are chosen separately on each side of the cutoff with the MSE-optimal two-bandwidth selector. $^{***}p < 0.01$, $^{**}p < 0.05$, $^{*}p < 0.10$.

Table 14: Baseline Averages for the 2017 Federal Election in North-Western Germany (1 km^2 Grid-Cell Resolution)

	Total	**Catholic**	**Protestant**
Catholic share	0.288	0.688	0.174
	(0.004)	(0.006)	(0.003)
CDU	0.422	0.558	0.383
	(0.002)	(0.003)	(0.002)
SPD	0.243	0.174	0.263
	(0.001)	(0.002)	(0.001)
AfD	0.082	0.074	0.084
	(0.000)	(0.001)	(0.000)
The Left	0.057	0.038	0.063
	(0.000)	(0.001)	(0.000)
Greens	0.070	0.044	0.078
	(0.000)	(0.000)	(0.000)
FDP	0.097	0.091	0.098
	(0.000)	(0.001)	(0.000)

Notes: Standard errors in parentheses.

Table 15: 2D Geographic Regression Discontinuity Design Results for the 2017 Federal Election in North-Western Germany (1 km^2 Grid-Cell Resolution)

	b1	**b2**	**b3**	**b4**	**b5**	**b6**
Catholic	0.233***	0.587***	0.100	0.435	0.313***	0.314*
SE	(0.050)	(0.104)	(0.099)	(0.304)	(0.024)	(0.163)
N_l, N_r	(852,208)	(549,173)	(421,151)	(465,121)	(1344,279)	(306,97)
CDU / CSU	0.033**	0.097***	0.091***	0.240**	0.099***	0.204***
SE	(0.015)	(0.030)	(0.034)	(0.098)	(0.024)	(0.043)
N_l, N_r	(1835,113)	(789,77)	(795,267)	(232,265)	(1715,304)	(254,130)
SPD	-0.038***	-0.125***	-0.033	-0.219**	-0.033*	-0.065
SE	(0.010)	(0.012)	(0.024)	(0.111)	(0.018)	(0.051)
N_l, N_r	(1688,153)	(804,56)	(441,236)	(199,113)	(1672,233)	(200,185)
Far-Right	0.014***	-0.011**	0.005	-0.037	0.006	-0.031***
SE	(0.003)	(0.006)	(0.030)	(0.036)	(0.005)	(0.006)
N_l, N_r	(846,153)	(955,56)	(656,52)	(484,54)	(1039,250)	(246,54)
Far-Left	-0.005	-0.048***	-0.014*	-0.067*	-0.016***	-0.024**
SE	(0.004)	(0.006)	(0.008)	(0.035)	(0.005)	(0.011)
N_l, N_r	(1318,113)	(369,213)	(584,52)	(226,148)	(1012,304)	(254,185)
Greens	-	0.008	-0.033***	-0.048***	-0.017***	-0.022***
SE	-	(0.007)	(0.009)	(0.013)	(0.006)	(0.007)
N_l, N_r	-	(384,114)	(309,233)	(108,290)	(1455,304)	(94,137)
FDP	-0.012***	0.053***	0.009	0.046**	-0.015**	0.000
SE	(0.004)	(0.018)	(0.009)	(0.021)	(0.007)	(0.036)
N_l, N_r	(153,340)	(447,104)	(261,402)	(435,103)	(2400,114)	(398,83)

Notes: $N = 5,730$. Bias-corrected estimates. Vote share per party regressions are clustered at the electoral district level. Units are weighted with a uniform kernel. N_l (N_r) denote, respectively, the effective observations and the *rule-of-thumb* bandwidths to the left (right) of the cutoff. Bandwidths are chosen separately on each side of the cutoff with the *rule-of-thumb* two-bandwidth selector. Results for Greens in $b1$ are not identifiable due to a lack of enough observations/variability. $^{***}p < 0.01$, $^{**}p < 0.05$, $^{*}p < 0.10$.

Table 16: Distribution of Religious Affiliation in the GLES Sample (2009 - 2025)

	N	**Percent**
Catholic	3 321	32.78
Protestant	3 058	30.18
Non-religious	3 065	30.25
Other	687	6.78
Total	10 131	100.00

Notes: Sample includes only eligible voters residing in West Germany.

Table 17: Distribution of Religious Affiliation in the Post Election Survey Sample (1953 - 2005)

	N	**Percent**
Catholic	19 131	43.43
Protestant	21 633	49.11
Non-religious	2 551	5.79
Other	739	1.68
Total	44 054	100.00

Notes: Sample includes only eligible voters residing in West Germany.

Table 18: Pairwise Religion-Based Differences in Predicted Vote Probability (2009 - 2025)

	Catholic vs Protestant	Catholic vs Non-religious	Catholic vs Other	Non-religious vs Protestant	Other vs Protestant	Other vs Non-religious
CDU / CSU	0.113***	0.149***	0.103***	-0.036**	0.010	0.046*
	(0.015)	(0.016)	(0.026)	(0.015)	(0.026)	(0.027)
SPD	-0.064***	-0.028*	-0.082***	-0.036**	0.018	0.054**
	(0.013)	(0.014)	(0.026)	(0.014)	(0.026)	(0.027)
AFD	0.006	-0.020**	0.011	0.026***	-0.005	-0.031**
	(0.009)	(0.010)	(0.015)	(0.009)	(0.014)	(0.015)
The Left	-0.022***	-0.041***	-0.042***	0.019**	0.020	0.001
	(0.008)	(0.008)	(0.015)	(0.009)	(0.015)	(0.016)
Greens	-0.040***	-0.039***	0.022	-0.001	-0.061***	-0.061***
	(0.013)	(0.013)	(0.022)	(0.013)	(0.022)	(0.023)
FDP	-0.010	-0.018*	-0.008	0.008	-0.002	-0.010
	(0.008)	(0.009)	(0.015)	(0.009)	(0.016)	(0.016)

Notes: $N = 6,319$ for the *Union* and SPD samples, $N = 6,284$ for the FDP and Left samples, and $N = 5,811$ for the AfD sample. Entries are average marginal differences in the predicted probability of voting for each party obtained from logistic regressions. Heteroskedasticity-robust (HC0) standard errors are in parentheses. $^{***}p < 0.01$, $^{**}p < 0.05$, $^{*}p < 0.10$.

Table 19: Pairwise Religion-Based Differences in Predicted Vote Probability (1953 -2005)

	Catholic vs Protestant	Catholic vs Non-religious	Catholic vs Other	Non-religious vs Protestant	Other vs Protestant	Other vs Non-religious
CDU/CSU	0.126***	0.203***	0.245***	-0.076***	-0.118***	-0.042
	(0.010)	(0.027)	(0.030)	(0.026)	(0.030)	(0.039)
SPD	-0.091***	-0.130***	-0.072**	0.039	-0.019	-0.058
	(0.009)	(0.026)	(0.034)	(0.025)	(0.034)	(0.042)
Greens	-0.013*	-0.027	-0.023	0.014	0.010	-0.004
	(0.007)	(0.016)	(0.025)	(0.016)	(0.025)	(0.029)
FDP	-0.026***	0.000	-0.052**	-0.026*	0.026	0.052**
	(0.005)	(0.014)	(0.023)	(0.014)	(0.023)	(0.026)

Notes: $N = 11,957$ for all parties but the Greens with $N = 5,610$. Entries are average marginal differences in the predicted probability of voting for each party obtained from logistic regressions. Heteroskedasticity-robust (HC0) standard errors are in parentheses. $^{***}p < 0.01$, $^{**}p < 0.05$, $^{*}p < 0.10$.

Table 20: Pairwise Religion-Based Differences in Political Attitudes (2009 - 2025)

	Catholic vs Protestant	Catholic vs Non-religious	Catholic vs Other	Non-religious vs Protestant	Other vs Protestant	Other vs Non-religious
Close to Union	0.113***	0.161***	0.109***	-0.048***	0.003	0.052*
	(0.016)	(0.017)	(0.026)	(0.015)	(0.026)	(0.027)
Parent Close to Union	0.224***	0.225***	0.286***	-0.001	-0.062**	-0.062*
	(0.017)	(0.019)	(0.031)	(0.018)	(0.031)	(0.032)
Right-wing Orientation	0.049***	0.047***	0.104***	0.003	-0.055**	-0.058**
	(0.014)	(0.015)	(0.023)	(0.015)	(0.023)	(0.023)

Notes: $N = 6,112$ for the Close to Union sample, $N = 5,327$ for the Parent Close to Union Sample and $N = 6,688$ for the Right-wing orientation sample. Entries are average marginal differences in the predicted probability of voting for each party obtained from logistic regressions. Heteroskedasticity-robust (HC0) standard errors are in parentheses. $^{***}p < 0.01$, $^{**}p < 0.05$, $^{*}p < 0.10$.